Development of an ‘artificial human’ for clothing research

presented by

Agnieszka Psikuta

A thesis submitted in partial fulfillment of the requirements of
De Montfort University for the degree of Doctor of Philosophy

Institute of Energy and Sustainable Development
at De Montfort University Leicester

Empa - Swiss Federal Laboratories for Materials Testing and Research
in St. Gallen

Sponsors of research:
Swiss National Science Foundation
W. L. Gore & Associates

January 2009

Abstract

The clothing is the closest envelope of the human body, and hence, has the primary impact on thermal comfort, physiological response of the human body and environmental strain. On the other hand, the clothing microenvironment is affected by physiological reactions (sweating, temperature distribution, body movement).

Nowadays, thermal sweating manikins used to study the interactions of the body-clothing-environment system are unable to simulate adequately the spatial and transient thermal behaviour of the human body. Ideally, a human simulator should ‘feel’ and respond dynamically to the thermal environment as real humans do.

In this work thermal sweating devices were coupled with the iesd-Fiala multi-node model of human physiology and thermal comfort. The coupling procedure was first developed for the iesd-Fiala model and a single-sector cylinder Torso. A new single-sector thermophysiological human simulator reproduced adequately the overall physiological response of the average human, which was proved by comparison with results of human subject tests for a wide range of environmental conditions.

In the next step, the elaborated coupling method was applied to the multi-sector, anatomically-shaped thermal sweating manikin SAM. The multi-sector thermophysiological human simulator with homogenous surface temperature distribution reproduced the thermal behaviour observed in human subject tests with good accuracy. However, an attempt to advance this human simulator to one with a heterogeneously distributed surface temperature was unsuccessful, as the results predicted by the simulator differed greatly from those obtained from human subject tests.

The single-sector physiological simulator has been shown to perform well in the validation tests with use of clothing ensembles. Time saving testing, repeatability of the measurement of the physiological response of an average individual and the ability of testing in conditions unsafe for humans are major advantages of this human simulator.

Acknowledgments

It would not have been possible to write this doctoral thesis without the help and support of the kind people around me, to only some of whom it is possible to give particular mention here.

This thesis would not have been possible without the help, support and patience of my supervisor **Dr. Mark Richards**, who is mostly responsible for helping me complete the writing of this dissertation as well as the challenging research that lies behind it. Mark has been a friend and mentor. He taught me how to write academic papers, made me a better programmer, and brought out the good ideas in me. He was always there to meet and talk about my ideas, to proofread and mark up my papers and chapters, and to ask me good questions to help me think through my problems (whether philosophical or analytical).

I would like to register sincere gratitude to my principal supervisor **Dr. Dusan Fiala** for his good advice, support and friendship that has been invaluable on both an academic and a personal level. I have really appreciated his well chosen observations as well as eager discussions on contentious subjects, which allowed me to improve this and other writings.

I would like to acknowledge the financial, academic and technical support of the Swiss Federal Laboratories for Materials Testing and Research – **Empa.** I have been given opportunity to attend many training courses and international conferences, which greatly enhanced my personal and professional development. I would like to thank the members of Laboratory for Physiology and Protection: **Dr. René Rossi**, who gave insightful comments and reviewed my work at a very short notice, **Nick Mattle**, who always gave time and attention for my technical questions, **Prof. Paul Brühwiler, Dr. Corinne Keiser, Markus Weder and Niels Bogerd**, who kindly reviewed pieces of my writing and asked me thought-challenging questions.

During the course of this work, at Empa SG and Institute of Energy and Sustainable Development at De Montfort University Leicester (2005-2008), I was supported by Empa internal research funds, W. L. Gore & Associates, Ltd., and a grant from Swiss State Secretariat for Education and Research as part of COST action 730 under project C06.0023.

I would like to thank participants of the COST Action 730, especially members of Working Group 1, for providing me with the data, samples and instructive comments that enhanced the quality of this work.

I would like to acknowledge and extend my heartfelt gratitude to the lecturers and participants of the EuroAcademy on Ventilation and Indoor Climate, so-called Climacademy, supported by the European Commission through Marie Curie funds, for relevant comments to the pieces of my work presented and interesting discussions during Climacademy conventions.

Much gratefulness goes to my dear friend **Dr. Desislava Stoitseva** for help with PID control simulations, interesting discussions, constructive observations and a lot of patience during this stressful time, especially as she also had a busy schedule.

Last, but not least, great and sincere thanks go to my brother **Marcin Psikuta** for the extraordinary assistance in the process of learning Delphi language and programming the software.

Table of content

Table of tables

Table of figures

Variables and units

Variable	Description	Unit
T_{sk}	average body skin temperature	°C
m_{sw}	average body sweat rate	g/min
q_{sk}	average body heat flux	W/m^2
T_{core}	core temperature	°C
T_a	ambient air temperature	°C
T_r	radiant temperature	°C
RH	relative humidity	%
v_{air}	average air velocity	m/s
MR	metabolic rate; 1 met = 58.1 W/m^2	met
n	number of human subjects participating in the experiment	-
rep	number of repetitions carried out per human subject	-
T_{K50}	temperature measured by sensor K50	°C
T_{Ni}	temperature measured by sensor Ni	°C
R_{Torso}	thermal resistance of the layers between sensors K50 and Ni	m^2°C/W
clothing	intrinsic thermal resistance of garment; 1 clo = 0.155 W/Km^2	clo

1. Introduction

As technology has advanced, the requirements posed on clothing and the indoor microclimate have magnified. In order to provide better clothing and indoor thermal environment, a thorough understanding of human thermoregulation is necessary. The interest in mammals physiology was manifested already in XVIII century (Jessen 2001). However only the second half of XX century has brought significant knowledge on human physiology and new developments in clothing, comfort and microclimate research (Parsons 2003). During this time the first thermal manikins were manufactured (Wyon 1989; Holmer 2004) and first mathematical models of human physiology and comfort were developed and subsequently improved (Lotens 1988). These two achievements were true milestones, especially for clothing research.

Current manikins are more sophisticated, however, limited by their passiveness. That means that they are mostly used with evenly heated skin and homogenous sweating for comparative measurements under steady-state conditions. The mathematical models also became more complex. Over recent years significant advances have been made in their development allowing simulation of human thermal and perceptual behaviours over a wide range of environmental and personal conditions.

Nevertheless, very few attempts have been undertaken to bring these two technologies together to enable the development of an 'artificial human' that thermally behaves and 'feels' as human beings do. Present-day advances in knowledge, computational technique and hardware are sufficient to establish advanced thermal manikins capable of simulating the dynamic human thermal and perceptual responses and the release of heat and moisture from the human body to the environment. In a coupled system, the computer model provides the physiological intelligence, and the hardware measures the required calorimetric states relevant to the human heat exchange with the actual environment, provided that the manikin is sufficiently responsive.

Thanks to research collaboration between the Institute of Energy & Sustainable Development at De Montfort University Leicester and the Swiss Federal Laboratories for Materials Testing and Research (Empa) in St. Gallen, the two most advanced

systems are available for such coupling: the iesd-Fiala model, which is a multi-node mathematical model of human thermal physiology and thermal sensation (Fiala 1998; Fiala, Lomas et al. 1999), and the Sweating Agile thermal Manikin (SAM), which is a versatile manikin with a fine body resolution, the ability of sweating and realistic repetitive limb movement (Richards and Mattle 2001).

Aims and objectives

The aims of this PhD work were as follows:

- To provide a tool for real-life assessment of clothing, which is a human-like manikin that 'feels' and responds to the thermal environment as real humans do;

- To demonstrate the applicability and emerging merits and limitations of the newly developed human simulator and to illustrate a method that shall help to determine the characteristics of a clothing ensemble and their effect on physiological response of the wearer.

The individual objectives of this PhD work were as follows:

(1) To provide a literature review on the components of the human simulator and methods for clothing evaluation, namely:

    - existing mathematical models of human thermal physiology, their structure, complexity and reliability;

    - various types of thermal manikins, their attributes and limitations;

    - methods and standards used for evaluation of thermal and evaporative properties of clothing and their interpretation with regards to human thermophysiological response.

    The literature survey is provided in chapter 2. In the course of reviewing the existing mathematical models, the iesd-Fiala model was evaluated for its predictive accuracy and subsequently additional validation work has been done to increase its credibility. These validation results are described in chapter 3.

(2) To elaborate a method of coupling the iesd-Fiala model of the human thermoregulatory system with the control software of a sweating thermal cylinder named Torso. The individual stages of work included:

- evaluation of the sweating thermal cylinder for its accuracy and its consequence for convergence and precision of the coupled system;
- evaluation of the performance of the iesd-Fiala model when coupled to the single-sector device representing the entire human body;
- development of the data exchange software with the user interface and coupling it with adjusted software of the iesd-Fiala model and Torso;
- optimisation of the performance of the human simulator and estimation of its limitations when simulating transient environmental conditions;
- validation of the human simulator by comparison of the simulation results with the human subject data for various environmental conditions.

The details of this work are described in chapter 4.

(3) To develop an 'artificial human' consisting of the advanced multi-segmental sweating manikin SAM coupled with the iesd-Fiala model based on the method developed for Torso. The individual stages of work included:

- evaluation of the sweating thermal manikin for its accuracy and its consequence for convergence and precision of the coupled system;
- amendment of the data exchange software for a multi-segmental device and coupling it with the adjusted control software of the thermal manikin;
- optimisation of the performance of the whole-body human simulator and estimation of its limitations;

- validation of the whole-body human simulator by comparison of the simulation results with the human subject data for various environmental conditions.

The details of this work are described in chapter 5.

(4) To develop a database of clothing systems based on measurements using actual clothing. The individual stages of work were as follows:

- creating the database of the human subject experiments with the detailed physiological data and corresponding original clothing available;

- validation of human simulator by comparing the physiological responses of human and results obtained using the human simulator dressed in the actual clothing used in subject test.

The details of this work are described in chapter 6.

Chapter 7 includes summarising conclusions and recommendations for future work and further development of the human simulator.

2. Literature survey

2.1. Present situation in environmental ergonomics

2.1.1. Basics of human thermoregulation

Humans are warm-blooded and their body core and brain temperatures are maintained at an almost constant level of around 37°C over a wide range of environmental temperatures (Shitzer and Eberhart 1985). The human thermoregulation system aims at maintaining the thermal equilibrium of the body by both behavioural and physiological means, e.g. choice of clothing, liquid intake, vasomotion, sweating, shivering thermogenesis. For this purpose, temperature sensors located throughout the body continuously detect the thermal state by the way of the temperature and its rate of change (Hensel 1981). These signals are processed in a complex neural network located primarily in the hypothalamus and used to initiate the behavioural and physiological responses (Gagge, Stolwijk et al. 1967; Parsons 2003).

Blood flow to the skin plays a crucial role in body temperature regulation. By changing cutaneous blood flow and blood volume, the effective insulation of the body shell can be reduced or increased (Shitzer and Eberhart 1985). In warm environments, the first reaction against the body temperature rising too much, which is termed heat stress, is to increase skin blood flow to help the transfer heat from the body core to the skin. If the core temperature continues to rise, sweating begins. If this sweat evaporates, it cools the skin surface and consequently, the blood in the skin. A typical human is capable of sweating at a maximum rate of about 1500-1800g/h (Sharpiro, Pandolf et al. 1982; Sawka and Pandolf 1990) or about 10-15% more when trained and heat acclimatised (Gisolfi and Mora 2000). In cold environments, the skin cools, and thereby, stimulates cold receptors, which results in superficial vasoconstriction, piloerection (or ‘goose pimples’) and subsequently shivering. During vasoconstriction the superficial veins and blood vessels constrict and blood returns from the limbs to the central body parts via deeper veins. This can cause up to a six-fold increase in the effective tissue insulation, which is equivalent to putting on a light wool business suit (Gisolfi and Mora 2000). Shivering is an involuntary contraction of skeletal muscles that can increase heat

production by 3- to 4-fold and thereby, rise core temperature by more than 0.5°C (Gisolfi and Mora 2000; Parsons 2003).

When the thermoregulatory actions cannot maintain the body core temperature within a sufficiently narrow range, thermal stress may occur. Heat stress may result from a combination of factors, which include excessive heat production of the body when performing exercise, exposure to external heat from the environment (high ambient temperature and humidity, direct exposure to sunlight or another radiant heat source), limited air movement and reduced or prohibited evaporation of sweat. When the body is unable to cool itself, heat-induced illness such as heat stress and heat exhaustion may result. The symptoms show as a reduction in work capacity and efficiency, tiredness, irritability, inattention and even muscular cramps (Graveling, Morris et al. 1988; Wexler 2002; Bethea and Powell 2005). A more severe effect is a heat stroke with body core temperatures exceeding 40°C, which could even result in death (Wexler 2002). Hypothermia (literally "low-heat") is a condition marked by an abnormally low internal body temperature below 35°C. Hypothermia can cause illness and consequently, when not recognized, death (Powell, Davies et al. 2005).

2.1.2. Clothing

Putting on clothing with a suitable thermal insulation is one of the most important behavioural actions, which help humans survive in most of climates available on the Earth. Clothing usually covers most of the skin surface for most of the human life, and can serve as a heat and moisture barrier in both directions. The protective performance of clothing depends on a number of parameters, such as the structure of the textile, its moisture permeability, absorption and wicking capability as well as on the course of thermal and mass transfer processes within the clothing system (condensation, evaporation and wicking on the individual layers of clothing) (Lotens 1993).

For physically active person the heat and mass transfer within the clothing system is a complex and dynamic phenomena. The thermal properties of clothing depend not only on the properties of the textiles used for the garment but also on the properties of the layers of air trapped between the skin and clothing, and clothing layers, and on the air layer adjacent to the outer surface of clothing. The major physical processes occurring

in the textile are: dry heat exchange (conduction, convection, and radiation), evaporation and condensation, sorption, and vapour and liquid water transfer. In addition, factors associated with construction of the garment, such as clothing fit, subject posture, compression (e.g. caused by wind), pumping effects (e.g. caused by body movement), and air penetration (e.g. through fabric, vents and openings) have great influence on the thermal behaviour of the clothing (Havenith, Heus et al. 1990; Bouskill, Havenith et al. 2002; Ghaddar, Ghali et al. 2003; Havenith and Nilsson 2004).

Most of single processes of heat and mass transfer have been analysed and described in more depth (Havenith, Heus et al. 1990; Havenith, Holmer et al. 1999; Holmer, Nilsson et al. 1999; Parsons, Havenith et al. 1999), whereas there is still incomplete knowledge on interactions between them, e.g. effects of moisture absorption and eventual freezing on thermal and vapour resistance (Lotens and Havenith 1995), distribution of moisture through clothing layers (Ueda, Inoue et al. 2006; Keiser 2007; Takada, Hokoi et al. 2007), latent heat dissipation by alternate condensation and evaporation at subsequent layers of a clothing (Lotens, Vandelinde et al. 1995; Havenith, Richards et al. 2008; Richards, Rossi et al. 2008). Although, some interactions have already been characterised empirically (influence of wind, movement and posture on thermal insulation) (Holmer, Nilsson et al. 1999), further research is required.

2.1.3. Measurement methods

The understanding of clothing systems has benefited from widespread use of thermal sweating devices such as guarded hot plates (McCullough, Kwon et al. 2003; Cheng and Fan 2004; Kothari and Bal 2005; Huang 2006; Kar, Fan et al. 2007), cylinders (Zimmerli and Weder 1996) and thermal manikins (Tanabe, Arens et al. 1994; Richards and Mattle 2001; Fan and Chen 2002; Holmer 2004). However, these devices are usually used for steady-state measurements (Richards, Psikuta et al. 2006) with either constant homogenous surface temperature or constant power being delivered and suitable for comparison. The need for more advanced systems able to simulate actual physiological responses was demonstrated by attempts to construct manikins with non-homogenous skin temperatures over the body, for example manikin with cooler hands and feet (McCullough, Jones et al. 1985; McCullough 2002), manikin with dynamically controlled homogenous skin temperature (Tanabe, Arens et al. 1994) or advanced

automotive manikin (ADAM) controlled by a computational fluid dynamics (CFD) implementation of a human thermoregulatory model (Farrington, Rugh et al. 2004; Rugh and Lustbader 2006). All of those manikins are designed for use in thermal environments close to comfortable.

Human subject tests are used when physiological responses play an essential role for the performance of the measured clothing, e.g. when the onset or the amount of sweating, vasomotor reactions or perceptual responses are of particular interest. Nowadays, such tests are frequently used when developing clothing for special purposes, including cooling garments, functional garments with improved heat and/or moisture management or impermeable garments. Nonetheless, such tests are associated with a number of deficiencies. Despite standards providing guidelines on how to conduct human subject tests (ISO9886 2004), planning, executing (including scrutiny of the experimental protocol and pilot studies) and analysing are a time-consuming process. Reliability of instrumentation and motivation of subjects is also an important issue. The use of human tests is furthermore limited to conditions, in which health safety of the test subjects is ensured which must also be confirmed by the approval of an ethical committee. In order to get representative results, a great number of test subjects is usually required adding to the cost of the experiment. Finally, the results are often difficult to interpret and insensitive to smaller differences in clothing properties, due to intra- and inter-subject variability.

2.1.4. Standards

The international, American and European standards in the domain of environmental ergonomics describe in detail the conditions and protocols of measuring clothing thermal and evaporative properties using various thermal devices (EN13537 2002; ISO15831 2004; ASTMF1291-05 2005; ASTMF2370-05 2005; ISO9920 2007). Other standards were designed to test thermal properties of textiles alone using sweating guarded-hot-plate at steady state (ISO11092 1993; ASTMF1868-02 2002; ASTME96/E96M-05 2005) and, to some extend, dynamic conditions (ASTMF2298-03 2003; ASTMD7024-04 2004). These standards (see table 2.1), however, are insufficient to evaluate the dynamic properties of ensembles when worn by humans and to predict their physiological effects on the wearer.

Table 2.1. Standards relating to measurement methods of thermal and evaporative resistance of fabrics, clothing and sleeping bags.

No	Standard number	Standard title
1	ISO 15831:2004	Clothing - Physiological effects - Measurement of thermal insulation by means of a thermal manikin
2	ASTM F1291 - 05	Standard Test Method for Measuring the Thermal Insulation of Clothing Using a Heated Manikin
3	ASTM F2370 - 05	Standard Test Method for Measuring the Evaporative Resistance of Clothing Using a Sweating Manikin
4	EN 13537:2002	Requirements for sleeping bags
5	ISO 9920:2007	Ergonomics of the thermal environment -- Estimation of thermal insulation and water vapour resistance of a clothing ensemble
6	ASTM E96/E96M - 05	Standard test methods for water vapor transmission of materials
7	ASTM F1868 - 02	Standard test method for thermal and evaporative resistance of clothing materials using a sweating hot plate
8	ISO 11092:1993	Textiles - Physiological effects - Measurement of thermal and water-vapour resistance under steady-state conditions (sweating guarded-hotplate test)
9	ASTM D7024 - 04	Standard test method for steady state and dynamic thermal performance of textile materials
10	ASTM F2298 - 03	Standard test methods for water vapor diffusion resistance and air flow resistance of clothing materials using the dynamic moisture permeation cell

Another group of standards (table 2.2) and simulation tools is dedicated prevention of the physiological strain at the working place through proper clothing, hydration level and limiting the working time (ISO15831 2004; Malchaire 2006; ISO11079 2007) and were developed based on a large number of physiological experiments. However, these do not account for human responses when wearing modern functional garments. Effectively, another approach of assessing their properties is required by mean of human subject tests.

Table 2.2. Standards relating to interpretation of physiological effects under physiological stress while wearing clothing at defined activity and environmental conditions.

No	Standard number	Standard title
1	ISO 15265:2004	Ergonomics of the thermal environment - Risk assessment strategy for the prevention of stress or discomfort in thermal working conditions
2	ISO 11079:2007	Ergonomics of the thermal environment - Determination and interpretation of cold stress when using required clothing insulation (IREQ) and local cooling effects

2.2. Thermal manikins

The thermal manikins are the most advanced devices for clothing measurements due to their anatomic shape and their ability to sweat and move. The interest in using thermal manikins in research and product development has increased continuously over the past 20 years as indicated by the number of manikins being developed and manufactured (Wyon 1989; Holmer 2004). In addition, the level of advancement has also increased either for improved precision of the device or for reduced costs. Furthermore, these versatile evaluation instruments are implemented nowadays in a wide range of disciplines including clothing research and manufacturing, automobile industry, environmental engineering of artificial microclimates for human occupancy. These developments have become so important that an international meeting on thermal manikin research, applications and virtual modelling is held every two to three years (the last 7th International Thermal Manikin and Modelling Meeting on 3-5 Sept 2008 was organised by University of Coimbra in Portugal).

2.2.1. History of the development of thermal manikins

There are over a hundred different manikins in use worldwide. The first one was a one-segment copper analogue device made for the US Army in the early fourties (Wyon 1989). Subsequently the need for more detailed measurements forced the construction

of manikins with several, independently-controlled segments. Almost all contemporary manikins available today consist of at least 15 such segments. Additionally, a significant step forward was taken by the introduction of digital control and measurement techniques to improve the measurement accuracy. A further step forward was the development of a manikin equipped with a cooling device, which enabled measurements of heat gains and losses detecting surface temperature during exposure to intensive convective and radiative heat (Behenke, Geshury et al. 1990). However, static and standing manikins provided test activities of limited relevance to actual, typical user conditions. Therefore, the construction of the manikins was enriched with joints so that they could be seated or simulate walking, running or climbing with the aid of mechanical drives (Richards and Mattle 2001). Recently, a few manikins have been constructed with the ability of sweating, which enables more realistic study of the human heat exchange by evaporation (Dozen, Adachi et al. 1989; Burke, O'Neil et al. 1994; Meinander 1994). Addition of a breathing system was implemented for indoor climate researchers (Melikov 2004). Simultaneously to the adult-man-shape trend, the female manikins (Kuklane, Sandsund et al. 2004) and baby manikins (Elabbassi, Beighazi et al. 2004; Kuklane, Sandsund et al. 2004) were developed to represent different groups of the human population and their needs.

In general, recent development of thermal manikins went in two directions. One is a complex sophisticated, multi-functional approach for research and advanced testing. One example this approach is the Swiss manikin SAM that has fine segmental division of the body, is able to sweat and perform realistic walking movements (Richards and Mattle 2001). Another example is the American sweating manikin ADAM, which is completely self-contained (carries in the body all necessary equipment including water reservoir, batteries and circuitry needed for control, regulation and data acquisition) and primarily intended for vehicle climate testing (Farrington, Rugh et al. 2004). The other direction of development aimed for relatively simple, yet accurate and reliable manikins that are inexpensive (Fan and Chen 2002; Dukes-Dobos and Reischl 2003). They are meant to satisfy the needs of occupational hygienists, smaller clothing manufacturers, etc.

2.2.2. Attributes of modern manikins

Manikins tend to be complex, fragile and expensive instruments. Nevertheless, those constraints are balanced by high performance and adequacy to real user conditions tests. Human shaped thermal (sweating) manikins measure all sorts of heat losses in all directions over the whole body and over defined local surface areas providing realistic simulations of the three-dimensional human body heat exchange and allowing an objective measurement of clothing insulation (McCullough 2002). The method is usually quick, repeatable and accurate which makes thermal manikins cost-effective instruments for comparative measurements and product development.

Thermal manikins vary in many aspects: size, shape, number of segments, regulation modes, measurement and calculation methodologies (Elabbassi, Beighazi et al. 2004; Kuklane, Sandsund et al. 2004; Melikov 2004). The diversity of manikins, their relevance, accuracy and reliability has been described in international standards (ISO15831 2004; ASTMF2370-05 2005). The reproducibility of the results obtained on manikins in interlaboratory tests varies widely up to 50% for thermal insulation and over 100% for vapour resistance measurements (Holmer 2004; Richards and McCullough 2004).

Despite various advances, thermal manikins are not capable of adequately simulating the human thermophysiological response. The limiting factor is their passivity. Presently, manikins are usually operated at uniform steady-state surface temperatures and homogenous sweat rates in comparative measurements, for example according to standards, such as ASTM F 1291-05 (2005), ASTM F 1868-02 (2005), ISO 15831 (2004) and ISO 9920 (2007). Nevertheless, various attempts have been undertaken to mimic the thermal response of human more realistically, for example, by setting uniform heat fluxes to simulate different work loads, or non-uniform surface temperatures over the body, such as cooler hands and feet (McCullough, Jones et al. 1985; McCullough 2002), or uniform surface temperature change over time (Tanabe, Arens et al. 1994). These attempts indicate the growing interest in using manikins to adequately simulate the human thermal behaviour, e.g. effects of vasomotion. This can only be achieved by combining manikins with a mathematical model of human thermoregulatory system.

A forerunner of such a new generation of manikins was developed in American National Renewable Energy Laboratory for comfort testing. Their advanced automotive manikin (ADAM) consists of a multi-segmental sweating thermal manikin controlled by a computational fluid dynamics (CFD) implementation of a human thermoregulatory model (Farrington, Rugh et al. 2004). ADAM was primarily intended to test comfort in vehicles and has been validated for steady-state conditions within the range of comfort-related temperatures (23.2–38.0°C). In the course of validation, ADAM showed a human-like distribution of skin temperatures under the conditions analysed. However, compared to human subject results, deviations in predicted core temperature of up to 0.6°C and in predicted local skin temperatures of up to 4.2°C have been reported under steady-state conditions (Rugh and Bharathan 2005) with even larger increasing discrepancies in core temperature under transient conditions (Rugh and Lustbader 2006).

2.3. Mathematical models

2.3.1. Types and structure of models

In modern world, humans might be exposed to a variety of harsh or dangerous environments and the consequences of temperature strain may be serious and irreversible. Therefore, risks of temperature strain became a concern of medical doctors, physiologists, ergonomists and environmental engineers. Research has been carried out on the prevention of, protection against and treatment of temperature strain. The development of the models of human thermal physiology has been a desirable aid ever since. Perhaps the first one was developed and published by Burton in 1934. Models of human physiology have evolved from a time when a clear understanding of human thermoregulation and computers were not available. The development of both of these disciplines enabled significant improvement in modelling so the subsequent models differed in the details provided, the advancement of the controller and also the use of model.

Physiological models usually consist of a controlled part (passive system) which is a model of physical body. The second part is a controller (active system) which simulates the responses of the human thermoregulatory system. These two systems interact with

each other as a feedback system. The simulation of the passive system evolved from one homogenous cylinder into multi-layered cylinders of various sizes for separate body parts with applied blood circulation. The layers reflect the typical division of body tissues: skin, fat, muscle and core or bone. However, the development of both the single-homogenous-cylinder approach and the advanced-multi-layer-structure approach was continued independently as so-called one or two-node models (Fanger 1970; Gagge, Stolwijk et al. 1971; Osczevski 1995) and multi-node models (Stolwijk, Nadel et al. 1973; Fiala, Lomas et al. 1999; Fiala, Lomas et al. 2001; Huizenga, Hui et al. 2001; Tanabe, Kobayashi et al. 2002).

Another classification of predictive thermal models could be done according to the level of versatility that the model represents. The calculation steps included in the model can not only account for physiological parameters an average person at simulated environments but also for heat and mass processes occurring in clothing and/or for psychological effects of the physiological state of the body. Figure 2.1 shows the general scheme by Lotens (1988), who summarised various elements, such as environment, skin heat transfer, physiological strain, and performance as the most relevant issues considered in physiological models.

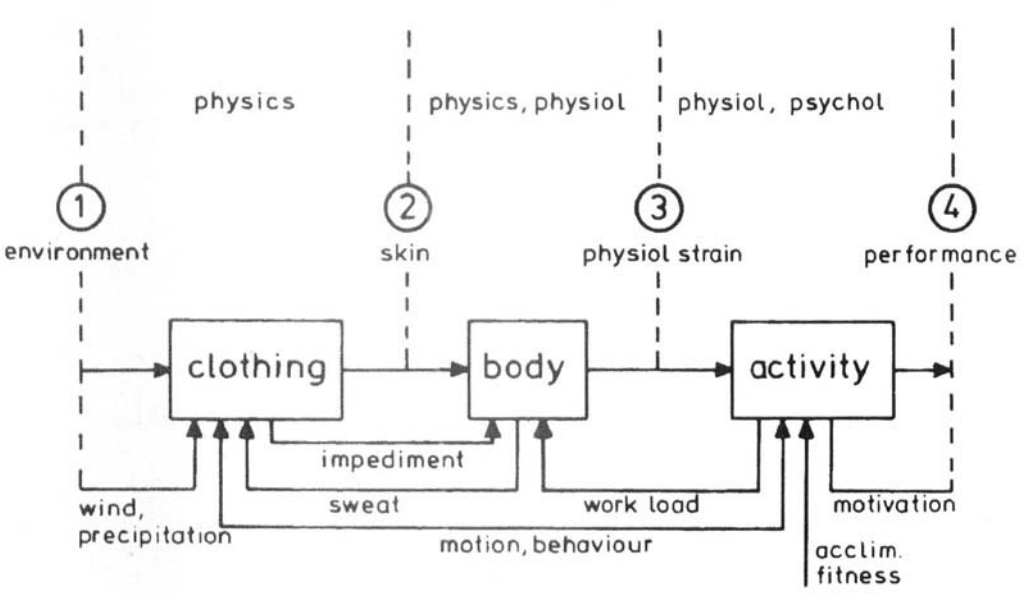

Figure 2.1. A general scheme of calculation steps in relation of the environmental conditions to the operational performance (Lotens 1988).

2.3.2. Significant models

The most influential example of the two-node model is the model of Gagge (Gagge, Stolwijk et al. 1971). Its passive system consists of only a core and a shell as tissue layers (two nodes) connected to a simplified controller. This model, however, aimed at simulation of comfort states of the body rather than for detailed simulation of physiological response. It was adopted by ASHRAE for predicting the standard operative humid temperature (ASHRAE-55 2004). Later on, it has been subjected to further improvements (Hoppe 1993; Pickup and De Dear 1999; Ghaddar, Ghali et al. 2003).

The thermal sensation model of Fanger is also one of the well-known and widely propagated in this field (Fanger 1970; Charles 2003). Fanger investigated the body's physiological processes of individuals exposed to moderate environmental conditions and found that the only physiological processes influencing the human heat balance in this context were the sweat rate and the mean skin temperature, both depending on activity level. Thus, his PMV model, which is based on a general heat balance consideration of the human body, combines the effect of four environmental variables (air temperature, air velocity, mean radiant temperature, and relative humidity) and two personal variables (clothing insulation and activity level) into an index that is used to predict thermal sensation of an average individual in conditions where thermal state of comfort would occur.

Another example of a simple one-compartment model is a model of the human face exposed to wind chill (Osczevski 1995; Bluestein and Zecher 1999). It calculates wind chill factor, which is the air temperature without wind, which would result in the same heat loss rate from bare skin, as that due to the combination of actual temperature and wind.

An interesting initiative was undertaken by physiologists to incorporate differences between individuals such as acclimatization, fitness, hydration, anthropometrical measures, time of the day and secondary variables of sex and age (Havenith 1985; Havenith 2001; Zhang, Huizenga et al. 2001; Lichtenbelt, Frijns et al. 2004).

The first advanced model of the human thermoregulatory system was developed by Wissler, who after several improvements came up with a very detailed model (250 nodes) with physiological control requiring great computation capacity (Wissler 1985). For this reason it was not widely used at later time.

The Stolwijk model developed for NASA (Stolwijk, Nadel et al. 1973) is probably the most popular amongst the multi-node models. It stood out due to its original approach to input signals from the skin and the core for the controller, which were defined as differences between the actual and a set-point temperatures. This controller was connected to a six-sector passive system model of the human body (head, trunk, arms, hands, legs, feet) with four tissue layers each (skin, fat, muscles, core) and with a central blood pool. The Stolwijk model became an inspiration to the great number of presently used simulation tools, for which it got improved with regards to the precision and number of details (Hwang and Konz 1977; Wissler 1985; Huizenga, Hui et al. 2001). Recently the interest in mathematical modelling of human models has blossomed again as availability of computing power and mathematical modelling software has increased. The most recently available models provide a high resolution and sophisticated calculation of the environmental heat exchange (Huizenga, Hui et al. 2001; Tanabe, Kobayashi et al. 2002; Sanders 2003; Yi, Li et al. 2004). These models provide a wide range of physiological data including temperatures and blood perfusion rates in all tissue nodes, local heat fluxes and sweat rates, cardiac output, basal and activity induced metabolic rates, core temperatures, respiration losses and comfort sensation factors.

One of the most recent models, which is becomeing widely used is the iesd-Fiala model. Although it was also inspired by Stolwijk work, its originally developed active system (controller) and incorporated thermal sensation model set it ahead of others (Fiala, Lomas et al. 1999; Fiala, Lomas et al. 2001). Its advancement and precision was appreciated by the members of the European project COST 730 and used for development of the universal climate index (UTCI) to be disseminated for the general public.

2.4. Need for a thermo-physiological human simulator

Over recent years, significant advances have been made in the development of mathematical models of the human thermoregulatory system. Ideally, these models should reliably predict human thermal and perceptual responses over a wide range of environmental and personal conditions, including the clothing worn. Several current computer models simulate human thermophysiological responses in detail. Nevertheless, detailed simulation of the human–environment interactions remains technically a complex task and various situations still cannot be analysed with sufficient detail by means of numerical simulation. Ambient air turbulences, local fluctuations in air, temperature and humidity, asymmetries of radiation from surrounding surfaces at inhomogeneous temperatures, and the non-uniform heat and mass transfer within multi-layered clothing systems are some examples of such phenomena. In many situations experimental analysis is, therefore, required.

Mathematical models of human thermoregulation usually include simplified clothing models, which do not account for the complexity of the heat and mass transport between the surrounding environment and the human skin surface. These models are used to provide input values of boundary conditions to the physiological model rather than realistic simulation of the physical processes occurring within clothing. More advanced clothing models should, in principle, simulate the complexity of heat exchange through multiple clothing layers (Lotens and Havenith 1995; Li and Holcombe 1998; Yi, Li et al. 2004; Cheng and Fan 2005) and offer a potential solution as inputs to physiological models. Nonetheless, the combined effects of the inhomogeneous dynamic heat and mass transfer processes in clothing are either difficult to characterize or not yet well understood, e.g. evaporation, condensation and moisture migration processes in multi-layer clothing systems (Chen, Fan et al. 2003; Fan and Cheng 2005; Keiser 2007; Takada, Hokoi et al. 2007; Havenith, Richards et al. 2008).

On the experimental side, the understanding of clothing systems has benefited from widespread use of thermal sweating devices (guarded hot plate, cylinders, and manikins) capable of only artificial steady-state measurements. Over recent years, the attempts to build advanced manikins with physiological components demonstrated the growing interest for devices, which would adequately simulate the thermal behaviour of

the human being. Thus, combining the strengths of an advanced mathematical model of human physiology and a thermal manikin is a new paradigm for simulating thermal behaviour of humans. By coupling the control system of a thermal manikin with such a mathematical model, the manikin should supply the model with the required calorimetric variables relevant to the human heat exchange with the real environment directly (figure 2.2). The role of the computer model is to provide the manikin with physiological intelligence, so that the 'physiological' conditions at the manikin's surface are adjusted corresponding to the actual exposure, provided that the manikin is sufficiently responsive.

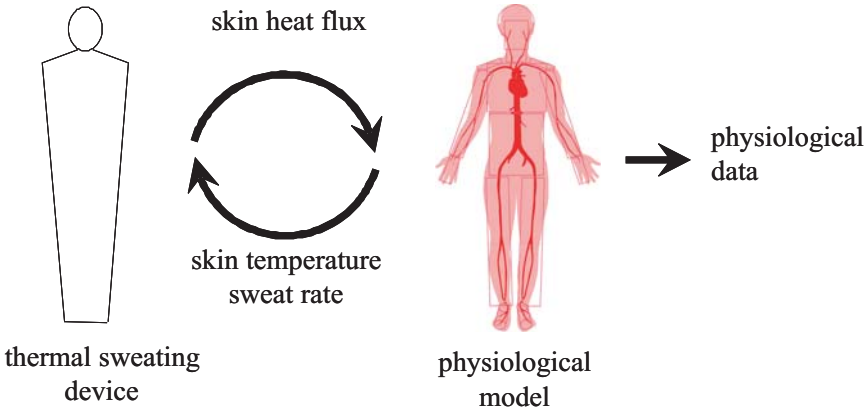

Figure 2.2. A scheme of the information flow in the coupled thermal device and physiological model.

3. The iesd-Fiala model – extended validation

3.1. The iesd-Fiala model of human physiology and thermal comfort

The iesd-Fiala model, used in this project, consists of two interacting systems: the passive system representing the human body with tissue discrimination (Fiala, Lomas et al. 1999) and the active system simulating the thermoregulatory responses of the central nervous system (Fiala, Lomas et al. 2001). Furthermore, the model also includes a physiological thermal comfort model for predicting human perceptual responses under transient conditions based on simulated physiological states (Fiala, Lomas et al. 2003).

The passive system is a three-dimensional representation of the human body with spatial subdivisions of 59 sectors and up to 7 different tissue layers in the radial direction with specific thermo-physical properties (see figure 3.1). In addition, each body part is divided axially into three or four lateral sectors: posterior, anterior, exterior and interior, if body parts are very close, e.g. the inner sectors of legs. Physiological body parameters are provided not only for each sector but also for each node out of 7 spread through tissues (see figure 3.1, cross-section). This high nodal resolution is supplemented with heat transport mechanisms occurring in the living tissue (blood circulation, metabolic heat generation, conduction and accumulation) (Pennes, 1948). At the body surface, the model accounts for free and forced convection, long- and short-wave radiation, skin moisture evaporation, diffusion and accumulation. The presence of clothing and its parameters is considered in the model in the form of static inputs (Fiala et al. 1999). That means that the resultant thermal and evaporative insulation, the emissivity and the clothing area factor are requested as input data but the physical processes occurring within clothing are not simulated by the model.

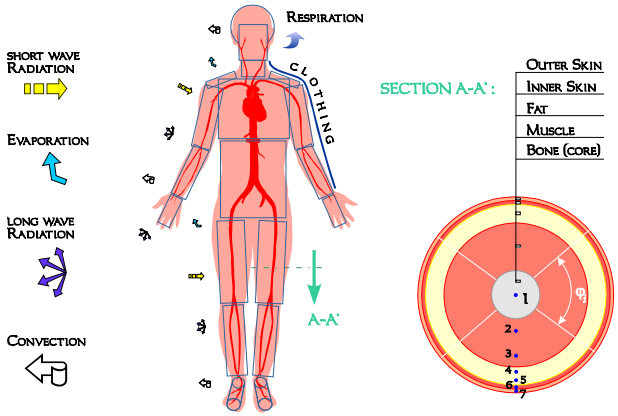

Figure 3.1. The scheme of the passive system of the iesd-Fiala model (Fiala et al. 1999)

The active system represents actions of the human thermoregulatory system, such as cutaneous vasomotion, sweat excretion and shivering thermogenesis (see figure 3.2). The algorithms for those actions were derived by non-linear regression analysis based on 27 experimental scenarios by different authors involving a total of 279 human subjects, each of whom was exposed repeatedly (8 experiments under steady-state conditions involving 163 subjects, and 19 experiments under transient conditions involving 116 subjects) (Fiala, Lomas et al. 2001). The model is able to simulate human thermal responses under both steady-state and transient conditions including any drink intakes and the thermal history prior to an experiment for a wide range of environmental (ambient temperature of 5 - 48°C) and personal conditions (metabolic rate of 0.8- 7 met).

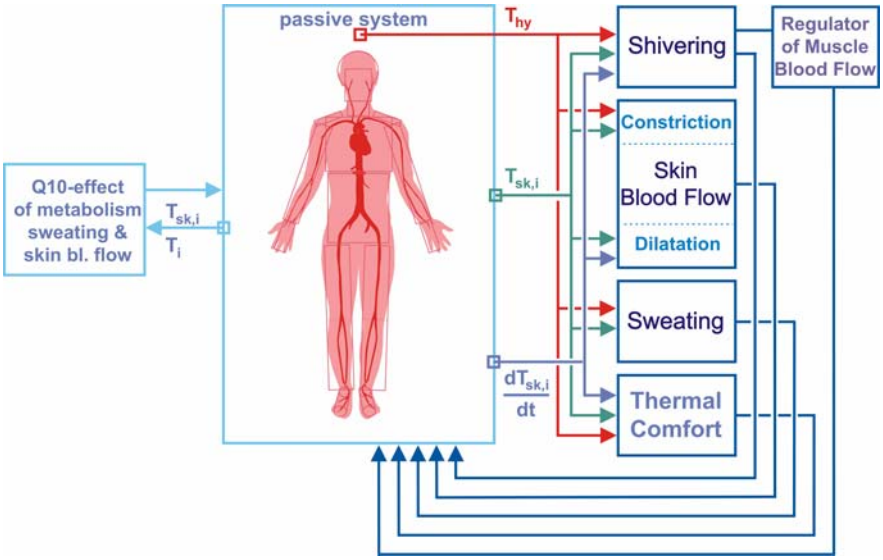

Figure 3.2. Block-diagram of the iesd-Fiala model of human physiology (Fiala et al. 2001)

The thermal comfort model predicts human perceptual responses related to the physiological states of the body. Over 300 different exposures and over 1600 human subjects formed the basis for the development of the predicting algorithm. Data analysis showed that the best predictors of thermal sensation are the weighted influence of the skin temperature (all conditions), hypothalamus temperature (warm conditions) and the rate of change in skin temperature (all conditions) (Fiala et al. 2003).

3.1.1. Application of the iesd-Fiala model

The iesd-Fiala model is a fairly complex simulation tool. It operates using the configured input data, simulates the physiological states of the body for every time step and provides a detailed output matrix. The model requires a set of parameters to be defined in the configuration file, such as environmental conditions (ambient and radiative temperatures, relative humidity, air velocity, solar radiation intensity and direction), activity level, clothing type, time step of the simulation progress, definition of the drink intake and history of the exposure prior to the actual simulation. The output data, representing the simulated physiological response is provided for each time step and at every node of the passive system. The most relevant parameters include skin and core temperatures, sweat rates, skin wettedness, skin blood flows, dry and latent heat fluxes, thermal sensation indices and heat generated by shivering.

A clear understanding of the operating principle and the human thermal physiology output data is of great importance for interpretation of the output data. Thus, the exercise of simulation procedure and understanding the results was an intermediate goal of this PhD project. In this exercise, the human thermophysiological responses were analysed in relation to time of exposure, relative humidity, clothing worn and activity levels for the entire body and for body parts. Every case study was based on altering one parameter and reading physiological parameters for either time steps or different exposure temperatures, while other parameters remained fixed.

3.1.2. Examples of simulations performed using the iesd-Fiala model

The following example of the analysis for different levels of activity illustrates the interrelations between physiological parameters and the complexity of interpreting the results. Parameters of simulation exercise are listed in table 3.1 and the results are plotted in figure 3.3.

Table 3.1. Settings used in the simulation exercise demonstrating dependence of physiological parameters on activity level of the individual.

activity level	0.8 met	1.1 met	2.6 met	5.2 met
	reclining	sedentary	walking	running
ambient and radiative temp. ($t_r = t_a$)	0 – 40 °C			
relative humidity	50 %			
relative air velocity evoked by activity	0.1 m/s	0.1 m/s	1.2 m/s	2.5 m/s
exposure time	60 min			
clothing system	0.8 clo			

Generally, dry heat loss from the human body (figure 3.3a) decreases with an increase of ambient air temperature. Furthermore, it differs noticeably with regards to various activity types. This variation is due to different metabolic heat production levels as well as the convective heat exchange rate evoked by body movement. The latter prevails in cold to moderate ambient temperatures (0-~20°C). Although the skin surface of the runner remains cooler than that of the person with a lower activity level, the speed of movement makes the heat exchange more efficient and results in higher heat losses

during running. This trend reverses for higher ambient temperatures, probably due to the decrease of dry heat exchange efficiency by high skin wettedness (above 50%). Reclining and sedentary positions represent the same level of dry heat loss due to insignificant differences in energy expense and thereby, in skin temperatures.

Low activity levels entail constant evaporative heat loss rate (figure 3.3b) by diffusion in cold and moderate environments and it rises for warm and hot conditions when regulatory sweating occurs. Higher metabolic rates imply a greater heat exchange by evaporation. At these activity levels, sweat excretion starts at lower temperatures and evaporative heat loss plays a greater role in the overall heat exchange through the skin. Evaporative heat losses correspond closely to the sweat rate and skin wettedness levels apart from the one for a person running at high environmental temperatures. In this case, the entire amount of sweat excreted cannot be retained on or evaporate from the skin surface, but some sweat drips off, without contributing to evaporative heat loss.

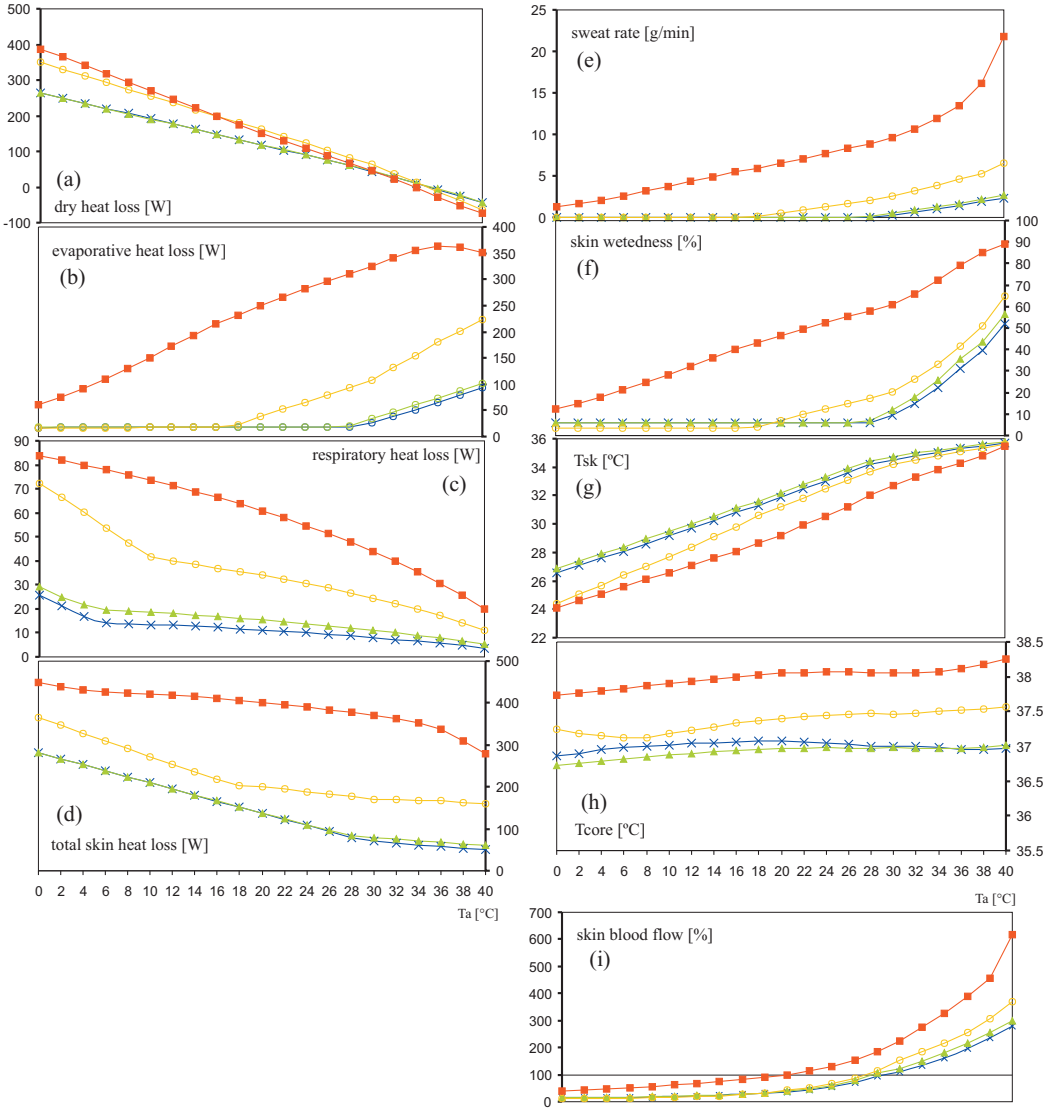

Figure 3.3. Results of the simulation exercise demonstrating dependence of physiological parameters on activity levels such as reclining (blue crosses), sedentary (green triangles), walking at 1.2m/s (yellow circles) and running at 2.5m/s (red squares) of the individual.

A respiratory heat loss (figure 3.3c) generally constitutes only a minor part of the overall heat loss. However, it does play an appreciable role (up to ~20%) at higher metabolic rates, which involve increased ventilation rate. Subjects at low activity levels maintain an almost constant respiratory heat loss over a wide range of ambient temperatures. The noticeable increase in respiratory heat loss at lower temperatures is due to shivering thermogenesis, which is accompanied by a higher ventilation rate. Interestingly, a walking person also shivers also at higher ambient temperatures (~10°C)

due to the higher efficiency of cooling during walking (by increased convective heat exchange).

Generally, the higher activity level, the higher the resultant core temperature (e.g. 37°C±0.2 for low activity levels, 37.4°C±0.2 for walkers, 38.0°C±0.2 for runner in figure 3.3h). However, the core temperature declines slightly with an increase in evaporative cooling. Finally, this trend is reversed by shivering thermogenesis at low ambient temperatures. Reversely, the higher the activity level, the lower the mean skin temperature (figure 3.3g). This is a combined result of regulatory sweating and convective cooling by body movement.

The model also outputs the skin blood flow levels as the percentage of the blood flow under thermoneutral conditions, when no vasomotor action is required (100%) (figure 3.3i). Values below 100% indicate vasoconstriction and above 100% vasodilatation. The higher the activity level, the lower the ambient temperature for which the thermoneutral state is reached. However, the dependency seems to be highly non linear as activities of 0.8-2.6met result in nearly the same ambient temperature required for the thermoneutral state, whereas 5.2met requires a temperature 8 degrees lower.

The simulation exercise was done also to compare physiological responses to different transient conditions under fixed clothing, activity level and environmental conditions. In the experiment, subjects were exposed initially to either warm (31°C) or thermoneutral (24°C) conditions for half an hour and then moved to cold or cool environments. Parameters of simulation exercise are listed in table 3.2 and the results are plotted in figure 3.4.

Table 3.2. Settings used in the simulation exercise demonstrating physiological response in transient conditions.

	before	after		
activity level	2.0 met	2.0 met		
ambient and radiative temp. ($t_r = t_a$)	24°C or 31°C	0°C	10°C	20°C
relative humidity	50 %			
time step	1 min			
time exposure	30 min			
air velocity	0.9 m/s			
clothing system	0.8 clo			

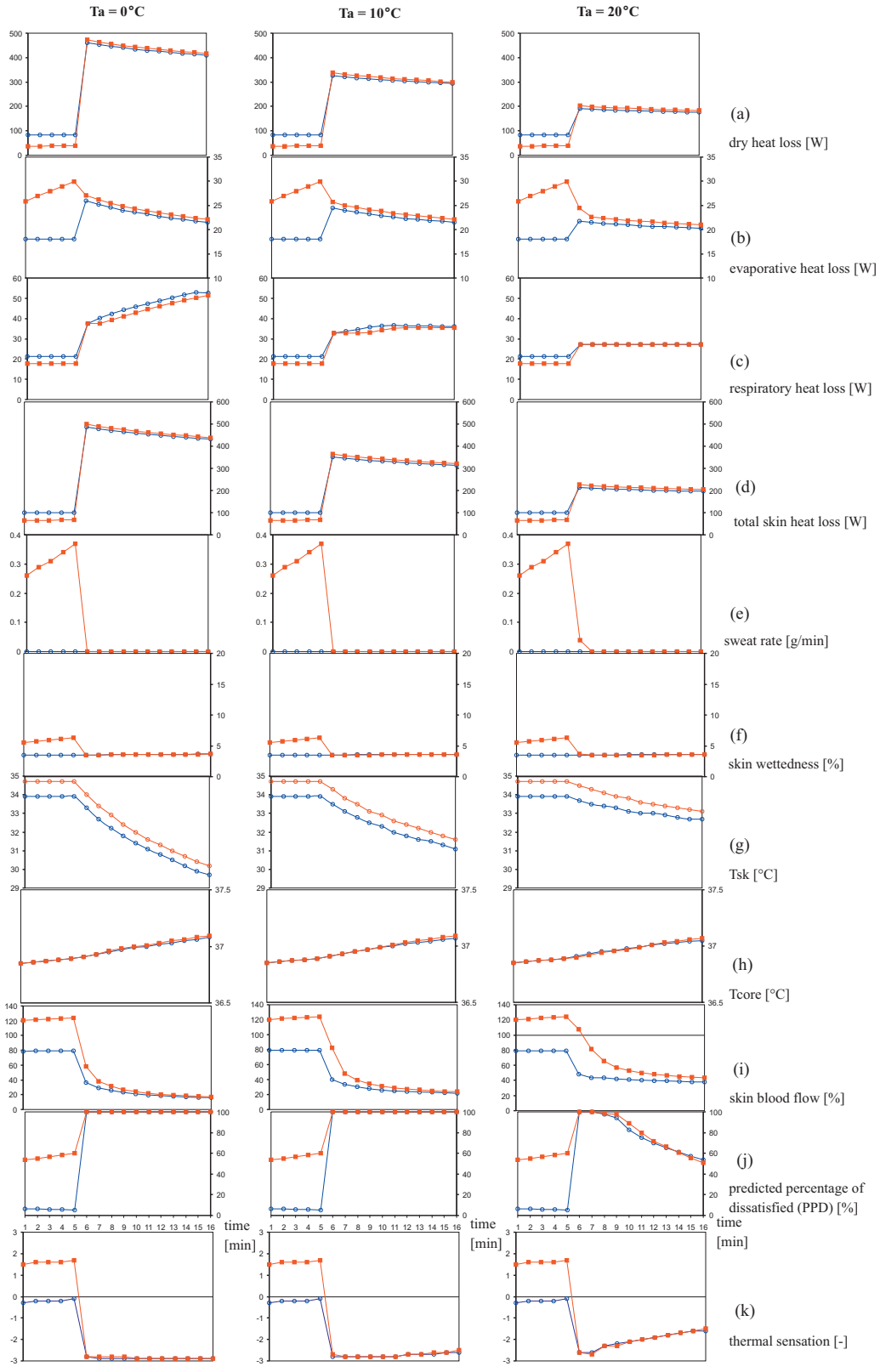

Figure 3.4. Results of the simulation exercise demonstrating physiological response in transient conditions beginning from neutral initial state (blue circles) or pre-warmed one (red squares).

Sudden change of ambient temperature is reflected in a quick change of dry heat loss through the skin (figure 3.4a), as it depends mainly on the temperature difference between the skin surface and ambient air. Thus, dry heat loss increased with increase in the temperature gradient and subsequently, followed the trend of change of the mean skin temperature. The evaporative heat loss is directly linked with the sweat rate. The pre-warmed subjects stopped sweating with a milder transition in moderate environments (20°C).

Respiration heat loss (figure 3.4b) also changes sharply since it depends on the temperature gradient between ambient air and body temperature. Furthermore, the shivering thermogenesis in cold environments (0°C and 10°C) causes further increase in respiration heat loss (figure 3.4c), which occurs later when the subject was initially pre-warmed.

Skin temperature (figure 3.4g) declines with time during exposure to the colder conditions. It initiates the vasoconstriction process, which is more gently introduced when the human system was pre-warmed at the beginning. The core temperature (figure 3.4h) increases slightly due to relatively high metabolic rate (2 met) over time and is undisturbed by changes in environmental temperature.

The thermal sensation (figure 3.4k) is significantly affected by a sudden change in ambient temperature. Both the pre-warmed subject and the one at the thermoneutral state became dissatisfied (PPD 100%) and shortly after transition their thermal sensation adapted to the ambient conditions. An overestimation of discomfort (figure 3.4j) was observed for a smaller temperature gradient shortly following the transition, whereas in cool and cold environments a person, once exposed, remained feeling cold.

3.1.3. Reliability of the iesd-Fiala model

The complete model was validated over a range of environmental conditions between 5°C and 48°C and activity levels between 0.8 met and 7met (Fiala, Lomas et al. 2001; Richards and Fiala 2004). The non-linear model of the active system was based on coefficients in the control equations obtained by regression analysis on all data used for the development of the model. However, these coefficients might not match the data of the individual experiments exactly. An initial validation determined the accuracy of the

model in reproducing the physiological responses observed for individual exposures from the database used for development of the model. In addition, the complete iesd-Fiala model was validated using additional independent experiments, which were not included in the database used for development. Both steady-state exposures and transient conditions (sudden changes of activity or climatic conditions) were used in the validation process. A good general performance of the model for the whole range of climatic conditions and types of exposure with regards to mean and local skin temperatures, body core temperature, sweating and shivering was found. The accuracies of prediction of these parameters were as follows (Fiala 1998):

- the mean and local skin temperatures predicted within the range of the measurement error observed in different experiments was typically ±1°C (with larger differences observed when sweating in the cold),

- the predicted body core temperature deviated from corresponding measurements by less than ±0.5°C,

- the predicted increase in metabolism due to shivering differed from experimental observations generally by less than the assumed measurement error of the experimental data of 50W,

- the prediction of sweating during alternating periods of heavy work and recovery was in poorer agreement with experimental results than predictions for environmentally induced sweating of non-exercising subjects, for which the error was usually less than 50W.

Fiala also reported that some further modelling and data mining would be necessary to refine the sweating algorithm, especially for cool environments.

In order to develop reliable measurement systems controlled by the iesd-Fiala model, extensive validation of this model and possible refinement of the regression coefficients is certainly advantageous. The iesd-Fiala model was accepted by members of the European project COST 730 entitled: ‘Towards a Universal Thermal Climate Index UTCI for Assessing the Thermal Environment of the Human Being’ as the best model of human physiology presently available and was chosen to be used in the development

of the UTCI. As part of the project, the model was validated extensively, and based on results of error analysis, was amended when necessary. Joining this initiative gave access to a large database of detailed experimental results collected from several leading European physiological laboratories and facilitated the desired extensive validation as a part of this PhD work.

3.2. The COST 730 database of physiological experiments

The database of experimental results collected within the COST 730 action accounted for 58 exposures with full descriptions of experimental protocol, environmental conditions and parameters of clothing. The ranges of the experimental parameters of all exposures in the database are given in table 3.3 in form of the maximum and minimum values.

Table 3.3. Maximum and minimum values of parameters in the database of COST 730.

	Ta	RH	v_a	Solar radiation	MR	R_{cl}
	°C	%	m/s	W/m^2	met	clo
max	50	98	21.2	600	12.1	1.91
min	-13	20	0.1	0	0.8	0.10

One third of the total number of exposures (16 experiments) was conducted outdoors and the remaining two third (42 experiments) were carried out in climatic chambers. In addition, almost all experiments concerned transient conditions (52 out of 58 exposures). The distribution of the exposures in the database in relation to two of the most influential parameters on the physiological response of the body, namely ambient temperature and metabolic rate, is plotted in figure 3.5.

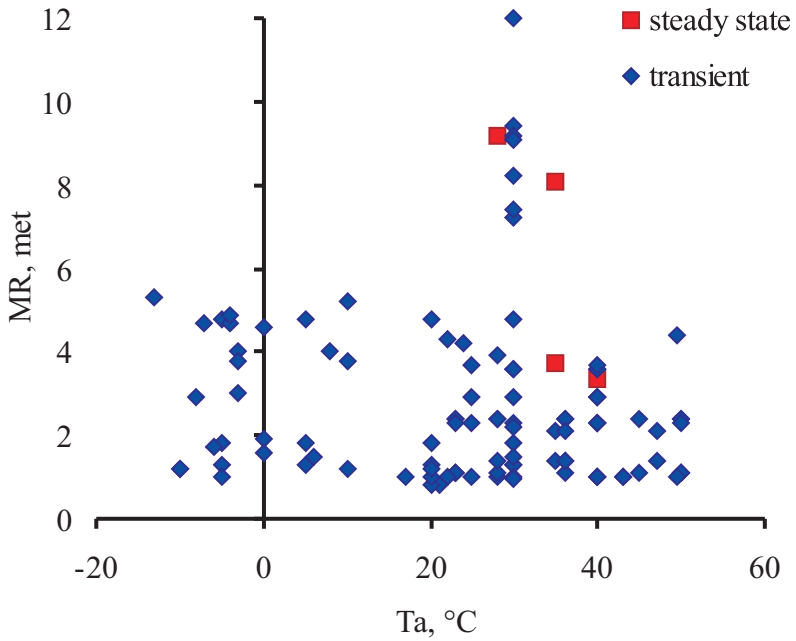

Figure 3.5. Distribution of the exposures in the database in relation to the ambient temperature and the metabolic rate used.

The total number of subjects participating in validation exposures amounted to 274 persons including 18 women and 256 men. A detailed description of the environmental conditions, number of subjects and number of repetitions for all exposures simulated is given in table 3.4.

Table 3.4. General description and root-mean-square deviations of all experiments simulated for COST 730

No.	Source of data	Experiment name	Exposure	Environmental parameters						Subjects				Clothing			rmsd	
			Length	Type	Ta	Tr	RH	va	Solar radiation	Activity type	Metabolic rate	External work	Number	Avaliability	Rcl/Rt	Recl	Tsk	Tcore
			min	field/ chamber	°C	°C	%	m/s	W/m^2	-	met	met	males/ females	measured/ estimated	clo	m^{2}kPa/W	°C	°C
1	Prof. Igor Mekjavic, Josef Stefan Institute in Ljubljana, Slovenia	Pokljuka1	180	field	8	-	48	0.10	48	hiking	4.0	0.01	0/6	estimated	1.40/1.83	0.037	0.644	0.313
2					0	-	64	0.16	134		4.6	-0.04	9/1				0.811	0.379
3					-4	-	77	0.17	138		4.9	-0.02	1/2				0.734	0.519
4		Pokljuka1			6	-	61	0.09	67	walk/stand	1.5	-	0/9	estimated	1.40/1.83	0.037	0.530	0.303
5					0	-	63	0.18	140		1.9	-	10/0				0.502	0.185
6					-6	-	88	0.30	149		1.7	-	2/0				0.915	0.382
7		Pokljuka2			-13	-	61	21.1	55	hiking	5.3 (2.5)	-0.07	1/0	measured	1.40/1.83	0.037	1.470	0.753
8					-3	-	77	21.2	65		3.8	-0.08	6/0				2.227	0.282
9		Pokljuka2			0	-	82	18.0	11	walk/stand	1.6	-	4/0	measured	1.91/2.31	0.064	0.432	0.257
10					-8	-	54	20.4	14		2.9	-	4/0				0.797	0.281
11		Ankaran			22	-	71	0.30	57	hiking	4.3	-0.01	6/0	measured	0.84/1.28	0.024-0.006	2.580	0.848
12					24	-	57	0.41	109		4.2	-0.01	3/0				2.235	0.521
13	Prof. Hannu Rintamaki, Finnish Institute of Occupational Health, Oulu, Finland	cold wind	60/30	chamber	20/-10	~=Ta	-	0.2/0.2	-	recl/stand	1.0/1.2	-	8/0	measured	1.2/1.88	0.02	0.391	0.169
14							-	0.2/1.0	-			-	8/0				0.528	0.103
15							-	0.2/5.0	-			-	8/0				0.660	0.143
16					-5/-10		-	0.2/0.2	-	recl/stand	1.0/1.2	-	8/0	measured	1.88	0.02	0.783	0.145
17							-	0.2/1.0	-			-	8/0				0.532	0.105
18							-	0.2/5.0	-			-	8/0				0.722	0.214
19	Chappuis, Pittet et al (1976) Heat storage regulation in exercise during		50/50/30	chamber	30	~=Ta	30	0.1	-	bicycle ergometer	2.21/3.59/0.98	-	11/0	semi-nude	0.1	0.013	1.592	0.067
20	Kobayashi, Horvath et al (1980) Thermoregulation during rest and		45/45	chamber	49.5	~=Ta	32	0.1	-	bicycle ergometer	1.0/4.42	-	5/0	semi-nude	0.1	0.013	0.683	0.229
21	Hardy and Stolwijk (1966): Partitional		60/120/60	chamber	43/17/43	~=Ta	30	0.12	-	sitting	1.0	-	3/0	semi-nude	0.1	0.013	0.505	0.165
22	Gonzalez, McLellan et al (1997) Heat strain models applicable for protective clothing systems: comparison of core temperature		100	chamber	35	~=Ta	50	1.0	-	walking	3.75	-	10/0	impearm. measured at wind condition	1.69 0.82	0.100	-	0.130 0.088
23	Moran, Shitzer et al (1998) A		120	chamber	40	~=Ta	40	0.2	-	walking	3.35	-	100/0	semi-nude	0.1	0.013	-	0.117
24	Biomed	CCR	170	chamber	28	~=Ta	50%	0.1	-	work/rest	1.0/3.9	0.0/0.9	6/0	semi-nude	0.1	0.013	-	0.104
25		CTE	180	chamber	28/45	~=Ta	2kPa	0.1	-	work	1.1/2.4	0.0/0.5	6/0	semi-nude	0.1	0.013	1.202	0.192
26					23/50	~=Ta	2kPa	0.1	-				6/0				1.552	0.204
27					36	~=Ta	4/2kPa	0.1	-		1.1/2.4	0.0/0.5	6/0				0.933	0.206
28					23/50	~=Ta	2kPa	0.1	-				6/0				1.468	0.194
29		Gile	165	chamber	40/40	~=Ta	65%	0.1	-	work/rest	1.0/2.3/ 2.9/3.6	0.0/0.5/ 0.7/0.9	8/0	semi-nude	0.1	0.013	-	0.150
30			180		23/50	~=Ta	2kPa	0.1	-	work	1.1/2.3	0.0/0.5	8/0				1.339	0.325
31			165		40/30	~=Ta	65%	0.1	-	work/rest	1.0/2.3/ 2.9/3.6	0.0/0.5/ 0.7/0.9	8/0				-	0.201
32			166		40/25	~=Ta	5/2kPa	0.1	-	work/rest	1.0/2.3/ 2.9/3.7	0.0/0.5/ 0.7/0.10	8/0				-	0.294

No.	Source of data	Experiment name	Exposure	Environmental parameters						Subjects				Clothing			rmsd	
			Length	Type	Ta	Tr	RH	va	Solar radiation	Activity type	Metabolic rate	External work	Number	Avaliability	Rcl/Rt	Recl	Tsk	Tcore
			min	field/ chamber	°C	℃	%	m/s	W/m^2	-	met	met	males/ females	measured/ estimated	clo	m^{2}kPa/W	℃	℃
33	Biomed	HCANNEU	160	chamber	28/36	28/36	6kPa	0.5	-	work/rest	2.4/1.4	0.5/0.0	5/0x6	semi-nude/ clothed	0.1-0.6	0.013	0.356	0.171
34		HCANFCO	160	chamber	47	36	0.9kPa	0.5	-	work/rest	2.1/1.4	0.5/0.0	5/0x6		0.1-0.6	0.013	1.089	0.363
35		HCANBRA	160	chamber	35	14	0.9kPa	0.5	-	work/rest	2.1/1.4	0.5/0.0	5/0x6		0.1-0.6	0.013	1.089	0.116
36		HCANFRA	160	chamber	36	57	0.9kPa	0.5	-	work/rest	2.1/1.4	0.5/0.0	5/0x6		0.1-0.6	0.013	0.758	0.361
					min/max	min/max	min/max	min/max	min/max		min/max	min/max			in;out	in;out		
37	Prof. Krzysztof Blazejczyk, PAN, Warsaw, Poland	winter	430	field	-3/22	-11/22	60/98%	0.2/2.6	0/128	hiking	1.0/3.0	-0.7/1.6	1/0	measur./ estim.	0.87/1.37; 1.25/1.43	0.02;0.04	1.754	0.252
38			407		-4/21	-11/21	60/71%	0.2/10.5	0/362		0.8/4.7	-2.3/0.5	1/0		0.94/1.49; 1.07/1.21	0.02;0.04	2.777	0.227
39			347		-3/20	-12/20	60/96%	0.2/2.4	0/55		0.8/4.0	-1.3/1.3	1/0		0.92/1.46; 1.22/1.40	0.02;0.04	2.050	0.182
40			460		-7/20	-11/22	42/60%	0.2/2.8	0/411		1.0/4.7	-2.6/0.7	1/0		0.92/1.45; 1.24/1.41	0.02;0.04	1.441	0.203
41	Andreas Jack (Mark Richards), EMPA, St. Gallen, Switzerland	body mapping	40	chamber	28	28	50%	3.28	-	running	12.1	-	6/0	semi-nude	0.04/0.74	0.001	2.316	0.898
42											9.2		7/0	semi-nude	0.04/0.74		0.857	0.225
43		0 insulation	40	chamber	35	35	40%	2.85	-	running	8.1	-	7/0	semi-nude	0.04/0.74	0.001	1.166	0.724
44	Daanen et al.(2005) Heat strain and		70	chamber	30	~=Ta	70%	0.3/0.7	-	ergometer	1.5/8.2	0.0/	8	semi-nude	0.1	0.013	2.589	0.236
45	Emiel den Hartog, TNO Defence, Security and Safety, Netherlands	VU2001	120	chamber	30	~=Ta	20	0.3	-	work/rest	~1.3/~4.8	1.4	1/1	estimated	0.23	0.01	0.546	0.440
46											~1.3/~1.8	0.5	1/1				0.597	0.461
47					30	~=Ta	80				~1.3/~4.8	1.4	1/1				0.881	0.459
48											~1.3/~1.8	0.5	1/1				1.230	0.802
49					20	~=Ta	50				~1.3/~4.8	1.4	1/1	estimated	0.73	0.02	1.130	0.682
50											~1.3/~1.8	0.5	1/1				2.020	0.568
51					5	~=Ta	50				~1.3/~4.8	1.4	2/0				0.835	0.637
52											~1.3/~1.8	0.5	1/1				1.908	0.759
53					-5	~=Ta	50				~1.3/~4.8	1.4	2/0				1.277	0.642
54											~1.3/~1.8	0.5	2/0				1.002	0.292
55		UW	75	chamber	10	~=Ta	60	0.3/1.0	-	work/rest	3.8/5.2/1.2	0.9/1.3	12/0x3	estimated	1.0	0.02	0.577	0.284
56		Rowers	56	chamber	30	~=Ta	80	0.3	600	work/rest	1.3/7.4/9.4	1.5/1.9	0/1	estimated	0.12	0.01	5.223	0.411
57			56								1.3/7.2/9.2	1.4/1.9	0/1				2.096	0.409
58			90								1.3/9.1/12	1.8/2.6/2.6	1/0				1.741	0.305

Each exposure was simulated using the iesd-Fiala model with detailed reconstruction of the clothing worn, environmental conditions and activity level. The simulation and experimental results were compared in figures and using statistical tools.

3.2.1. Statistical method of evaluation

Root-mean-square deviations (rmsd) of mean skin temperature and local skin temperatures and core temperatures were calculated for all experiments simulated for COST 730. The root-mean-square deviation quantifies the average difference between a prediction and a measurement for an exposure (Barlow 1989). It is defined as:

$$rmsd = \sqrt{\frac{\sum \left(x_{measured} - x_{predicted} \right)^2}{n}}, \qquad (3.1)$$

where:

$x_{measured}$ – measured data point,

$x_{predicted}$ – corresponding predicted data point,

n – number of data points.

The goodness of fit of the simulation results and the experimental data can be practically assessed by comparing the rmsd value to the average standard deviation of the experimental data.

3.2.2. Results

The validation results are shown in the form of the root-mean-square deviation calculated for each exposure. The mean rmsd, its standard deviation and median for mean skin and core temperatures for the entire COST 730 database of experiments are given in table 3.5 and plotted in figure 3.6. Exposures 41, 43 and 56-58 in table 3.4. involving well-trained sportsmen were excluded from the database for statistical analysis as the iesd-Fiala model was designed to simulate average human. The detailed data of each exposure and the individual rmsds for mean skin and core temperatures are listed in table 3.4.

Table 3.5. Mean, standard deviation and median of root-mean-square deviations for the mean skin and core temperatures of validations done for COST 730.

	rmsd T_{skin} [°C]	rmsd T_{core} [°C]
mean	1.14	0.32
standard deviation	0.64	0.20
median	0.92	0.26

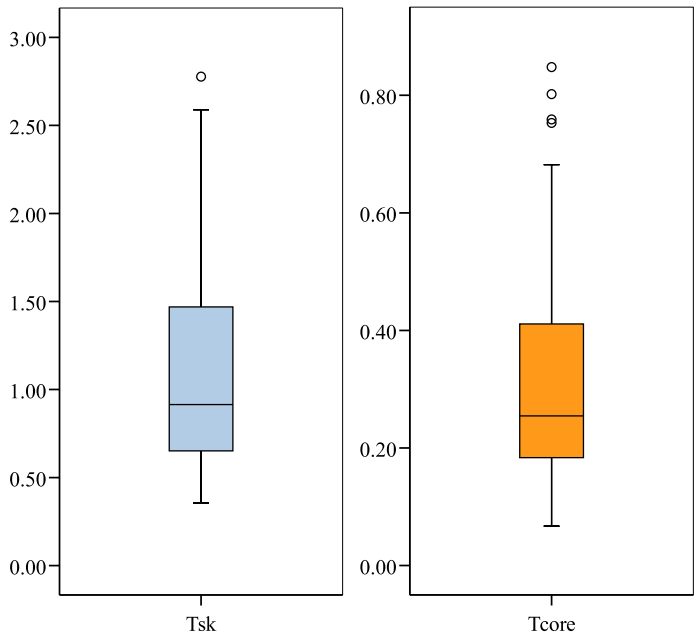

Figure 3.6. Box plots of rmsd for mean skin and core temperatures of validations done for COST 730.

Although the model was successfully validated by comparing the simulation results with those available from the human subject studies, for many cases, only the mean skin and the core temperatures were available. Although other physiological parameters could not be directly validated for most of the COST database, their plausibility can be deduced from the parameters validated. For example, the skin blood flow and the sweat rate should result in the adequate skin temperature or the overall thermal sensation is calculated based on the mean skin and the core temperatures.

3.2.3. Discussion

During simulation work, each exposure had to be individually investigated with regards to proper reproduction of experimental protocol, body coverage by the clothing and environmental conditions around the body of a human subject. In some cases, the analysis of individual exposures was hindered by the lack of detailed information such as the activity of subjects prior to exposure, local thermal and evaporative resistances of clothing worn (when these differences were significant), the exact locations of measurements of skin temperatures, detailed weather data at the location of the subject in field experiments, and sometimes indication of departure from the experimental protocol. In each of these cases, the most probable scenario was chosen, simulated and evaluated statistically.

Furthermore, for a few exposures, some details of the experiment could not be simulated by the iesd-Fiala model. For example, in exposures 33-36 in table 3.4, radiant surfaces were only located in front of the subjects, while in the iesd-Fiala model, the radiation is simulated evenly from all directions. Moreover, the iesd-Fiala model also simplifies the exposure to solar radiation. The amount of heat absorbed from the sun by the human body when standing still is calculated for an unknown orientation from the beam-intensity and the elevation of the sun. The amount of direct radiation absorbed by a person in postures other than the standing position or in motion in relation to the sun differs from that of a standing person. The local effect of the direct radiation on the body would also be different, since, normally, the energy of direct radiation is delivered only to exposed body parts, and not uniformly over the body as assumed in the iesd-Fiala model. This simplification hindered analysis of exposures 56-58 in table 3.4, as a high intensity radiation source of 600kW/m^2 was applied to the rowing person in this experiment.

Another simplification is the clothing model included in the iesd-Fiala model. This model does not enable dynamic changes of clothing properties due to body and air movements, which changed during several field exposures, i.e. 1-6, 11-12, 37-40 in table 3.4. The correction coefficients to thermal and evaporative resistances of clothing were calculated for the average walking and wind speeds during the exposure, which might have differed significantly from that, based on momentary values of wind and

walking speed on climbs and descents. By such averaging, the details of exposure were lost, which was especially pronounced during the experiments with high variability of wind and walking speeds such as in studies 37-40 in table 3.4.

A further adverse interference between the clothing model and the iesd-Fiala model was observed in exposure 55 in table 3.4, which is depicted in figure 3.7. During the first phase of this exposure (first 40 minutes), subjects exercised at a relatively high metabolic rate, which, subsequently, induced high sweating. In the second phase of the experiment, subjects rested after exercise in the wind wearing moist clothing from the preceding workout session. During this time, the mean skin temperature was predicted to be too high by the iesd-Fiala model. The most plausible explanation of this effect could be moisture retention within the clothing layers during the first phase of the human subject test and its evaporation with a certain delay in the second phase. However, the iesd-Fiala model does not account for the complex dynamic heat and mass transfer processes in the clothing as it uses only the static clothing parameters as inputs. Thus, the phenomena of moisture retention and delayed evaporation could not be simulated properly.

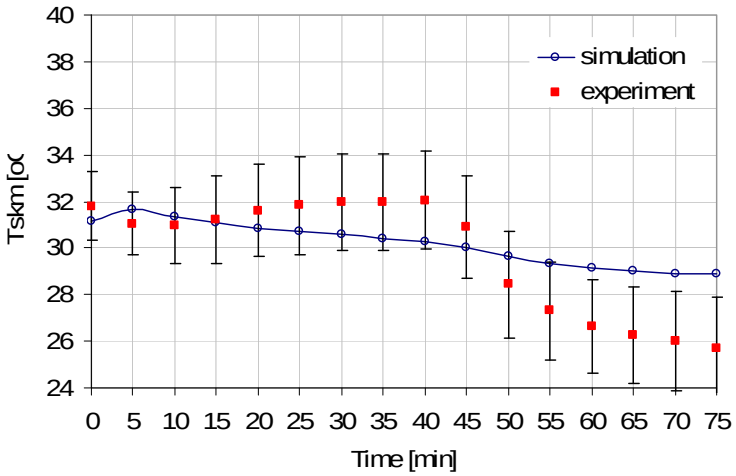

Figure 3.7. Mean skin temperature measured in human subjects and simulated in the iesd-Fiala model (55 in table 3.4). Conditions of exposure: $T_a = T_r = 10$ ºC, RH = 60 %, phase 1 (40 mimutes): $v_a = 0.3$ m/s, MR = 5.2 met; phase 2 (35 minutes): $v_a = 1.0$ m/s, MR = 1.2 met; 12 males exposed 3 times wearing cotton combat suit and long underwear.

Originally, the iesd-Fiala model was validated for an exercising person of an average fitness at activity levels below 8 met. Although the model accepts metabolic rates up to 12 met, the predictions for activities higher than 7 met are based on an extrapolation. During this validation course, the model performed well for free-time sportsmen exercising at 9.2 met (exposure 42 in table 3.4), as indicated by the good fit of measured and simulated core temperatures for this experiment (figure 3.8). Hence, the range of metabolic rate, for which the iesd-Fiala model is validated, was extended.

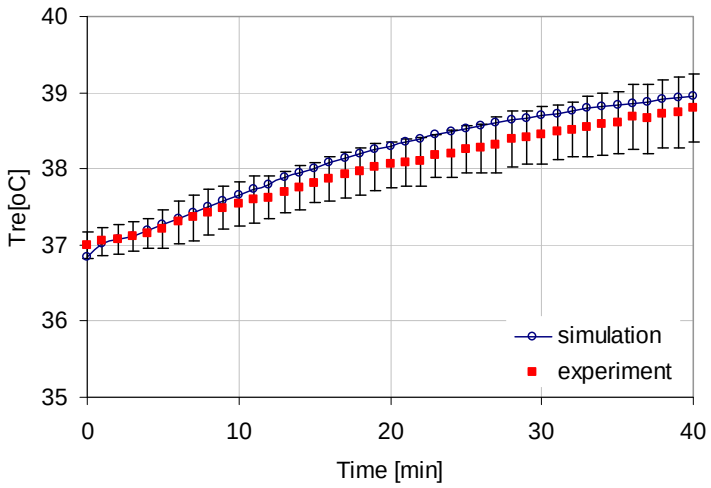

Figure 3.8. Rectal temperature measured in human subjects and simulated in the iesd-Fiala model (42 in table 3.3). Conditions of exposure: $T_a = T_r = 28$ ºC, RH = 50 %, v_a = 3.3 m/s, MR = 9.2 met, 7 males wearing thin polyester-cotton running suits.

In the experiment 41 in table 3.4, professional sportsmen ran on a treadmill at high ambient temperature with the metabolic rate of 12.1 met, which exceeded the upper limit of metabolic rate acceptable for the iesd-Fiala model. This fact and the better vasomotor and sweat response of professional sportsmen are possible reasons for the discrepancies in core temperature observed (figure 3.9). A few other independent experiments seem to confirm this observation, for example, experiments 56-58 in table 3.4, in which the iesd-Fiala model overestimated the core temperature by up to 0.6°C for well-trained individuals rowing in the heat. These examples demonstrated the limitation of the iesd-Fiala model to predict the response of a well-trained exercising person.

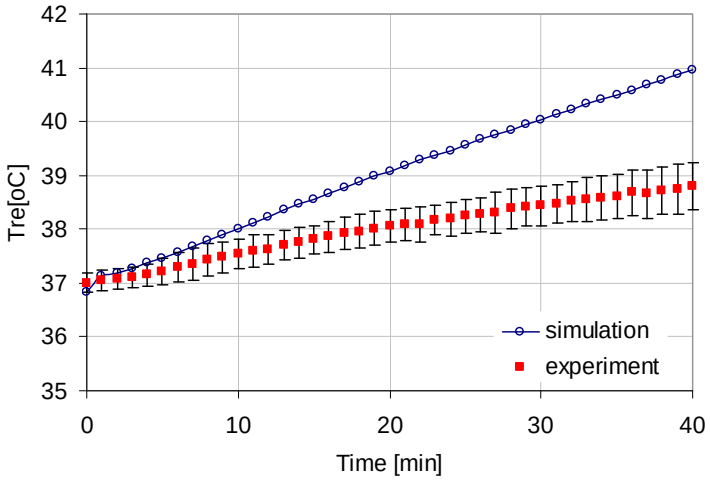

Figure 3.9. Rectal temperature measured in human subjects and simulated in the iesd-Fiala model (41 in table 3.4). Conditions of exposure: $T_a = T_r = 28$ ºC, RH = 50 %, v_a = 3.3 m/s, MR = 12.0 met, 6 males wearing thin polyester-cotton running suit.

Experiments involving well-trained sportsmen (41, 43 and 56-58 in table 3.4) were removed from the database used for statistical analysis, as the iesd-Fiala model was designed to simulate average humans rather than such sportsmen. The mean rmsds for mean skin and core temperatures are somewhat higher that typical standard deviation of experimental data, which were 0.5-1.0°C and 0.2-0.4°C respectively. Nonetheless, in both cases the medians are smaller and fall well within these ranges. Furthermore, using rmsds for assessment of goodness of fit has its drawbacks as it does not consider the quality of the experimental data (i.e. the magnitude of standard deviation). If the experimental standard deviation is large, it allows a greater rmsd value for the same goodness of fit.

3.3. Summary

Many physiological models based on the human experimental data have been developed until now. Some have been improved over time by adding additional experimental data and up-to-date knowledge. However, apart from the iesd-Fiala model, none of these models have been validated extensively.

This validation study focused predominantly on testing the iesd-Fiala model against rather extreme conditions in terms of environmental conditions (ranging from cold and

windy to very hot climates), activity level (hiking with a heavy load, heavy exercising on a bike ergometer) and clothing (ranging from bare face exposed to cold wind to impermeable chemical protection suit worn during exercise in heat). The model proved its ability to predict adequately the human physiological response for the variety of extreme conditions represented in COST 730 database. The mean skin and the core temperatures were predicted with average root-mean-square deviations of 1.31 ± 0.88 °C and 0.35 ± 0.24 °C respectively. The validation work also proved an extended range of activity levels up to possible to 9.1 met, which can be simulated by the iesd-Fiala model. Some limitations of the model were demonstrated, such as inability to simulate the thermophysiological responses of well-trained individuals, a simple static clothing model interfering adversely with the simulation of thermophysiological responses, and a simplified direct radiation model. However, most of these limitations concern the definition of the boundary conditions at the skin surface. As discussed in the section 2.4 of the literature summary, the future human simulators should be able to measure directly the detailed heat exchange between the body parts and the environment. Thus, the limitations related to the boundary-conditions of the iesd-Fiala model could then be neglected in such future applications.

4. Development and validation of the single-sector Thermophysiological Human Simulator (THS)

As discussed previously in section 2.4, there is a great need for advanced thermal devices controlled by physiological models. This project aims at taking a significant step towards the development of such intelligent devices using the iesd-Fiala model of human physiology and thermal comfort and a thermal sweating cylinder of the Swiss Federal Laboratories for Materials Testing (Empa).

4.1. The Torso device

The hardware is a heated sweating cylinder named 'Torso', which is used to measure the environmental heat exchange (Zimmerli and Weder 1996). It consists of a multi-layered cylinder and two heated aluminium guards, which help to minimize lateral heat losses (figure 4.1). The main cylinder of Torso has a diameter of 30 cm and a height of 46 cm, which approximates the size of the adult male trunk. The aluminium cylinder is heated on its inner surface, and is coated on the outer side with a 7 mm thick polyethylene layer. Torso is equipped with temperature sensors embedded within the layers and 54 sweat outlets distributed evenly over the surface of the main cylinder, which are connected to internal, separately-controlled valves. These outlets and a tight-fitting textile 'skin' distribute water, which is used to simulate sweating over the surface of the main cylinder. An external water tank, which supplies the sweat outlets with water, is positioned on a precision balance to determine the mass of the liquid sweated.

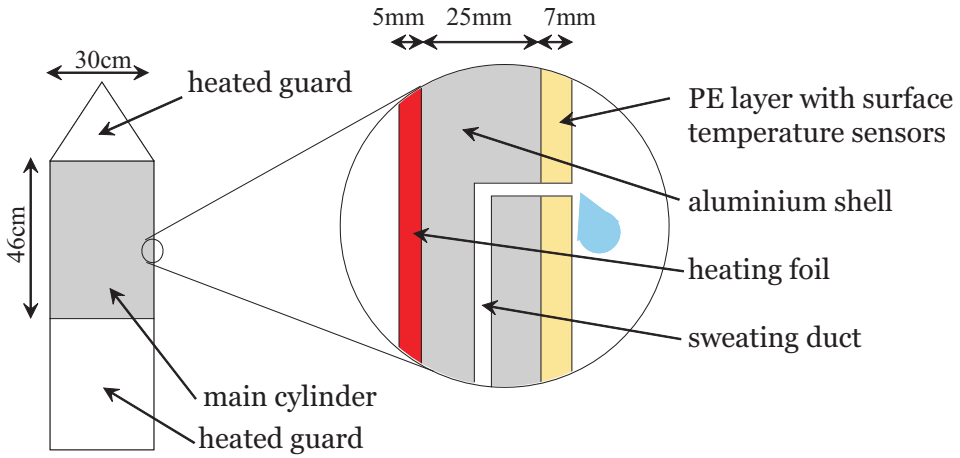

Figure 4.1. Torso with a cross-section illustrating the construction details of the layers.

4.2. Calibration of the Torso

There are 13 temperature sensors located within Torso - on the surface, within the layers, at the guards and inside Torso (figure 4.2). Most of these sensors (11) are PT 100 type class B (EN 60751) embedded in made hollows within the aluminium shells of main cylinder and guards and plastered using a thermoconductive glue. Two Ni surface sensors are resistance nickel wires deployed evenly on the surface of main cylinder in-between the sweating outlets and fixed using a thermoconductive glue and a thin Teflon foil for mechanical protection.

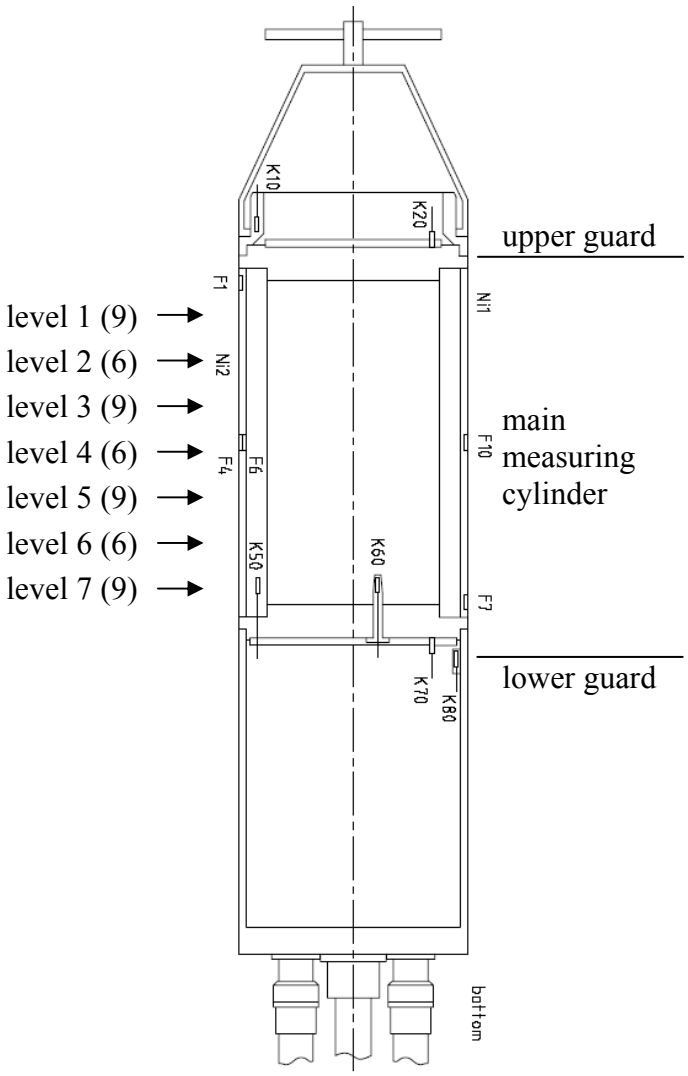

Figure 4.2. Cross-section through Torso device showing the locations of 13 temperature sensors and the stratified system of sweating outlets (numbers in brackets indicate the number of outlets per level). K and F indicate the Pt100 temperature sensors; Ni1 and Ni2 indicate the nickel resistance wire surface sensors.

To be able to simulate human physiological responses properly, the temperature measurement system required precise calibration. For this purpose, Torso was filled with water, which was maintained at constant temperature using an external temperature bath with circulating water through Torso. The temperature of the water within Torso was measured using Kelvimat type 4342-V600 with sensor Pt100 to an accuracy of ±0.015°C. The whole device was encapsulated in a thick-walled insulating box (polystyrene, minimal thickness of 5cm) in the climatic chamber at the same temperature as the water within Torso in order to minimise the influence of

environmental conditions on the distribution of temperature within the Torso. Such a setup was left for a period of time for the stabilisation of temperature (typically 5 hours). Subsequently, the voltages measured from the Torso sensors and calibrating sensor were read. This routine was repeated three times for each calibration point. The calibration points were chosen at regular intervals within the limits of mean temperature of the human skin (15°C, 20°C, 25°C, 30°C, 35°C, 40°C and 45°C). The linear dependence between voltage and temperature was found according to the equation:

$$T_{sensor} = A \cdot V + B, \tag{4.1}$$

where:

T_{sensor} – temperature read on the sensor, (°C);

A – slope of the calibration line, (°C /mV);

B – interception of the calibration line, (°C);

V – voltage measured by the sensor electronics, (mV).

The slope and interception values for the sensors used to control the heated guards (K10 and K80) and the main cylinder (Ni1 and Ni2) are listed in table 4.1. Examples of calibration lines obtained are shown in figure 4.3. Squared Pearson's coefficients shown in table 4.1 indicate a good correlation between the voltage and the temperature.

Table 4.1. Coefficients of the calibration lines and Pearson's coefficients for the sensors used in control of Torso.

Sensor	**Ni1**	**Ni2**	**K50**	**K10**	**K80**
A (slope)	12.99	12.96	8.49	8.54	8.34
B (intercept)	9.56	6.41	8.30	8.08	9.34
R^2	0.9999	0.9999	1.0000	0.9992	0.9914

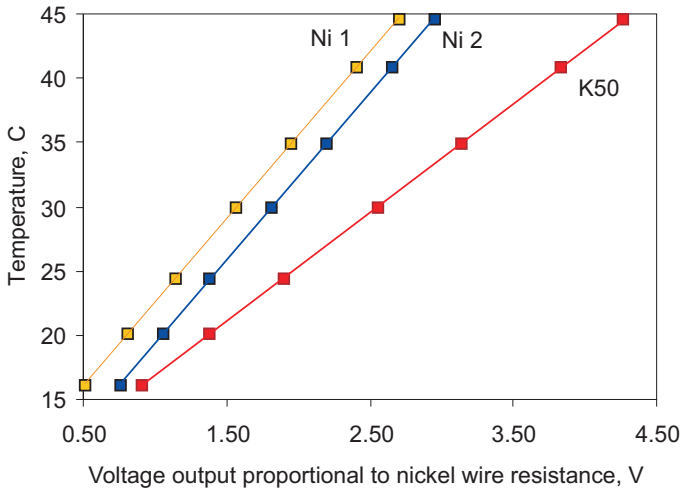

Figure 4.3. Calibration chart of temperature sensors such as nickel resistance wires on the surface of Torso (Ni1 in the front, Ni2 in the back), and Pt100 sensor K50 embedded within the aluminium shell (see figure 4.2).

Sweating is another parameter of human physiological response, which can be simulated by Torso. The sweating system of Torso device consists of a supply tank positioned on a scale, a connecting insulated duct and a valve for each of 54 sweating outlets. The driving force of this system is the hydrostatic pressure from the difference of height between the supply tank and the sweating outlets. From the calibration work of predecessors of the Torso, which used the same sweating system, it has been shown that:

- single droplets are released from each sweat outlet when a constant open time of 250 ms is used;
- the sweat rate is inversely proportional to the time interval between single droplets (figure 4.4).

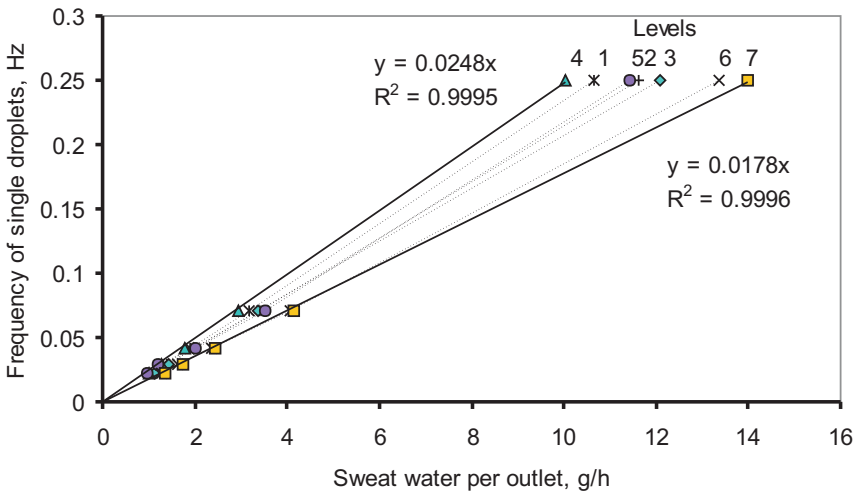

Figure 4.4. Previous calibration chart of sweating outlets for an identical Torso device in a vertical position.

This inverse proportionality enabled a reduced number of calibration points (2 points) to be measured for each level of sweating outlets (figure 4.2). The amount of sweated liquid released for a given time interval between single droplets varied with the height of each sweat outlet level (figure 4.5), mainly due to the different hydrostatic pressures. Therefore, the time intervals between openings of valves (single droplets) used for each layer was calculated from the calibration gradients in order to obtain an even distribution of sweat excreted over the main cylinder.

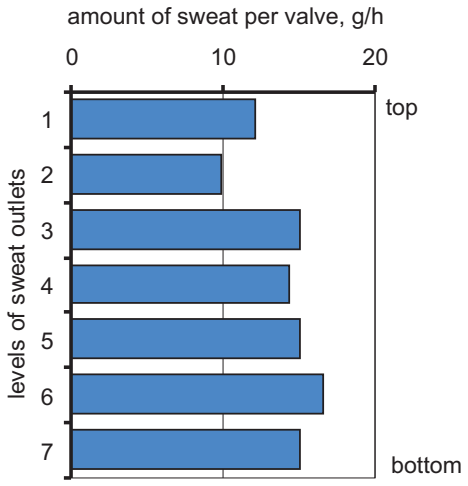

Figure 4.5. Uncompensated distribution of sweat over levels of sweat outlets using a time interval between droplets of 4.0s.

4.3. Regulation of climatic chamber

The climatic chamber is a crucial part of a measurement set-up. Its stability and accuracy in terms of regulating the required climatic conditions (temperatures, humidity, air movement, etc.) is of great importance for the accuracy of the entire system.

The climatic chamber was tested for the optimal position of the measuring device. The relatively small size of the chamber (figure 4.6 a, b) prohibited manipulation of the air streams. Therefore, the air velocity was measured across the volume of the chamber in order to locate an optimal position of the device providing the most homogenous profile of air movement. This optimal position of Torso with regards to all set intensities of circulatory flow (20%, 30%, 50% and 80% of the maximal fan flow) was found to be at a distance of 2.2m from the inlet grid and in the middle of the narrow side of the chamber (figure 4.6 a, b).

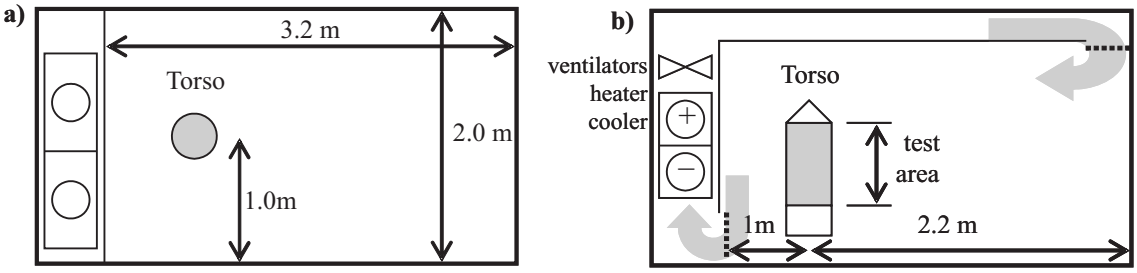

Figure 4.6. Projection (a) and cross-section (b) of Torso climatic chamber.

The regulation curve was determined for this chosen location (figure 4.7) in order to adjust systematically the climatic chamber to the required air movement conditions. Changes in the ambient air velocities (bars in figure 4.7) were observed only up to 50% of the maximal circulatory flow. For higher flow rates the air velocity and its fluctuation remained the same as for 50% of the maximal circulatory flow in tested area. The ambient temperature in the climatic chamber was maintained with an accuracy of ±1°C and relative humidity with an accuracy of ±5%. However below 5°C, no control of relative humidity is possible.

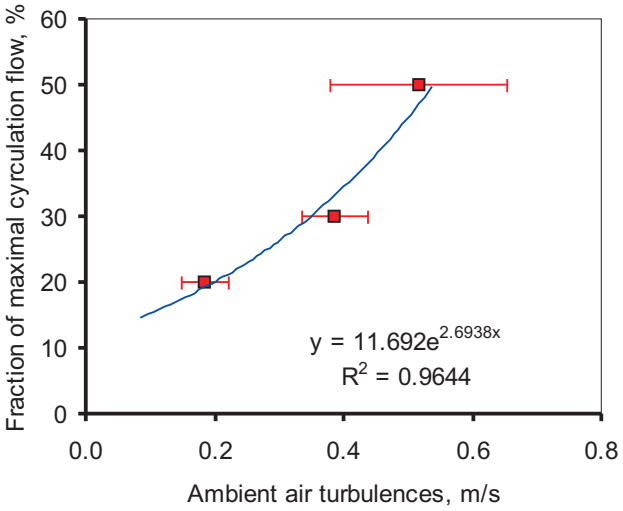

Figure 4.7. The regulation curve – dependency of ambient air velocity on the rate of circulatory flow.

4.4. Coupling method

In order to simulate the overall physiological response, Torso was taken to represent the entire human body (trunk, head and extremities). The coupling method was based on real-time iterative exchange of the relevant data between Torso and the iesd-Fiala model (figure 4.8). Area-weighted averages of the local skin temperatures and the local sweat rates from the physiological model were used as control parameters for Torso. The average heat flux from the cylinder surface of Torso was then used as the feedback signal, which represented the mean amount of heat exchanged with the environment for the clothing worn during a set time interval. Other physiological and perceptual parameters, such as core temperature, skin blood flow, heart rate, and thermal sensation, were calculated by the physiological model and stored in data files for post-processing.

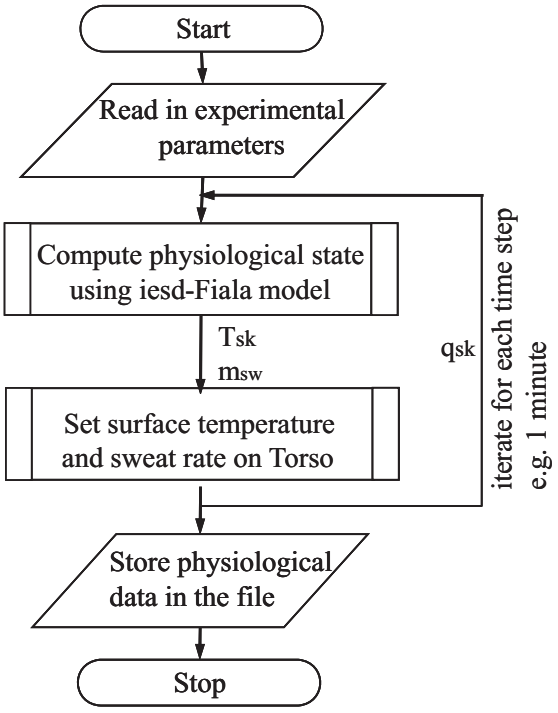

Figure 4.8. Scheme of the data exchange in the thermophysiological human simulator.

The iesd-Fiala model was originally developed for use with environmental boundary conditions, such as ambient air and radiant temperatures, relative humidity, wind speed, activity level, and clothing to predict the resultant heat exchange with the environment. For the human simulator, this model was modified to use a single integral input value of the measured surface heat flux, which was used as the boundary condition at the body's skin surface in the model.

4.5. Use of homogenous heat flux

Since Torso is a single-sector device, the feedback heat flux consists of a single average value, which is then applied to all body parts of the physiological model. This, however, has consequences, as the true physiological state of a person is associated with diverse local skin temperatures and sensitivity coefficients for different body parts. To quantify the effect of the use of homogeneous heat flux for a nude person, various exposures were simulated using the original iesd-Fiala model and the results were compared with predictions of the modified model, which used the average skin heat flux as a boundary

condition at the skin. However, instead of using the heat flux measured by Torso, the average skin heat flux predicted by the original iesd-Fiala model was used as input, so that the results of the original and modified models could be compared directly.

The outputs of both versions of the iesd-Fiala model were compared for all environmental conditions and metabolic rates analysed. Comparisons of steady-state responses for T_a = 15 ºC, 25 ºC and 35 ºC, MR = 1.5 met, 5 met and 10 met with RH = 50 %, v_{air} = 0.1 m/s and $T_r = T_a$ showed the following minor differences in prediction of physiological reactions:

- the skin temperature predicted by the modified model (used in the human simulator) was the same for warm conditions as, and up to 0.5 ºC higher for cold conditions than, that of the original model, regardless of the metabolic rate of the subject;

- the core temperature predicted by both versions of the iesd-Fiala model differed by a maximum of 0.2 ºC, with the largest underestimation occurring for high metabolic rates;

- the predicted sweat rates showed a good agreement (below 1 % difference) for combinations of low to moderate metabolic rates and cool to warm environments. Even for high activity levels (above 7 met), the difference observed was below 25 %.

Simulations of transient exposures with step changes in ambient temperature showed, that the use of a homogenous heat flux would result in the skin temperature being overestimated by a maximum of 1.4 ºC (for a large step change from neutral to cold conditions of 15 ºC) and the core temperature being underestimated by a maximum of 0.4 ºC (for the highest metabolic rate of 10 met studied) before steady-state body temperatures were reached.

Based on the above observations, it was concluded that using a single homogenous heat flux for all body parts in the model; it is possible to simulate the overall human thermal response with acceptable accuracy for steady-state and transient conditions, albeit with decreasing accuracy for strongly transient and extreme conditions.

4.6. Measurement of heat flux

The central cylinder of Torso is heated by heating foils with embedded copper elements. The current is supplied from a regulated power supply adaptor. The magnitude of the current and voltage are dictated by a PID controller and it depends on the difference between the mean surface temperature measured by nickel wire sensors (Ni) and the set value for surface temperature in the software. The heat flux required as an input for the iesd-Fiala model, can be calculated from the power supplied to the central cylinder of Torso divided by its surface area. However, the power measured directly across the copper heating foils by the power supply (determined from the measured current and voltage), fluctuated markedly (by up to 30% of the average value) as a result of rapid adjustments by the PID controller (direct power in figure 4.9). Due to the relatively slow response of the power supply when interrogated by the Torso software using the IEEE interface, only ten power measurements were possible every minute. These were averaged, which reduced the measured power fluctuations only partially. The iesd-Fiala model linked to Torso accepted this highly fluctuating heat flux, and surface temperature of Torso followed closely the skin temperature predicted by the iesd-Fiala model. Nevertheless, the mean skin temperature predicted by the coupled system did not agree with the prediction of the iesd-Fiala model run separately, which is used here as a reference (figure 4.9).

A new method to determine the heat flux from the central Torso cylinder was, therefore, derived. The heat flux from the surface of Torso was measured using the temperature sensors placed within the shell of the main cylinder. The average surface heat flux of the cylinder is calculated using:

$$q_{Torso} = \left(T_{K50} - T_{Ni}\right) \cdot \frac{1}{R_{Torso}}, \qquad (4.2)$$

where:

$R_{Torso} = 0.0185 \pm 0.0005$ m^2°C/W,

and T_{K50} is the temperature measured by the PT100 sensor K50 (°C) positioned in the middle of the aluminium shell of the main cylinder, T_{Ni} (°C) is the mean temperature of

Torso surface measured using two nickel resistance wires deployed evenly over each half of the main cylinder surface, and R_{Torso} ($m^2°C/W$) is the thermal resistance of the aluminium/polyethylene layers between sensors K50 and Ni. R_{Torso} was determined experimentally for various fixed environmental conditions and Torso surface temperatures, and was found to remain constant over the range of conditions analysed (within 2% of average value).

The chosen method provides a measurement of heat flux close to the surface of the cylinder and is considered to be more accurate than the one based on instantaneous power measured by the power supply (heat flux K50-Ni in figure 4.9). Consequently, the mean skin temperature simulated by coupled system agreed with the prediction of the iesd-Fiala model used as the reference. The reason for this is because the heating power delivered to the main cylinder was found not to be equal to its surface heat loss; neither during steady-state nor transient conditions. Due to differences in construction, the main cylinder and guards have different characteristics of cooling and heating, so that internal heat exchange occurs between these elements. The magnitude of this internal heat exchange is constant and dependent on the magnitude of the heat loss during steady-state conditions but changes under transient conditions. Ideally, the surface heat flux should be measured without any significant component of internal heat flux and provided as an input for the physiological model.

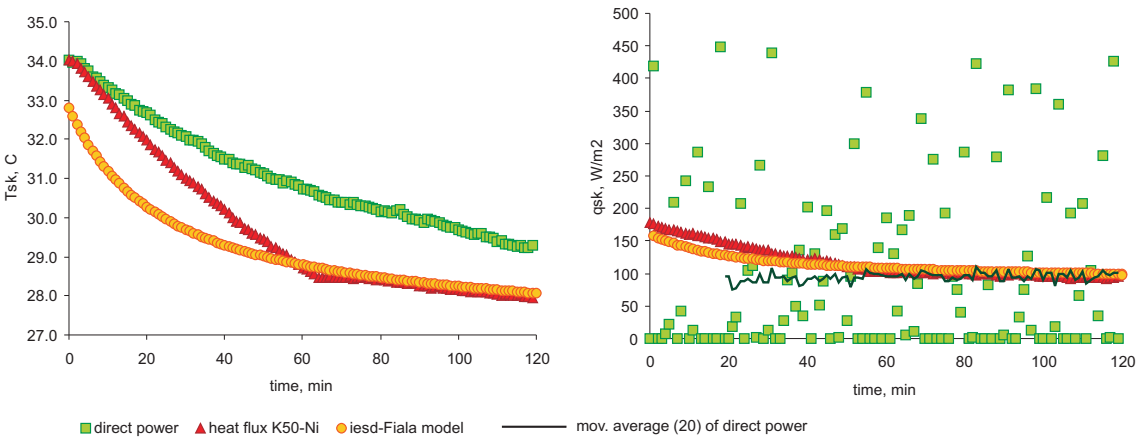

Figure 4.9. Mean skin temperatures and surface heat fluxes predicted by the iesd-Fiala model and measured on Torso as a part of the coupled system, which were based on different heat flux calculation methods. Experiment conditions: T_a = 20 °C, RH = 50 %, v_a = 0.25 m/s, MR = 1 met, nude person.

4.7. Sensitivity of iesd-Fiala model to measurement error

It should be noted, that an error in the measurement of the heat flux will influence the predictions of the physiological model. It was impossible to separate an inherent error of the hardware from fluctuations of the conditions in the climatic chamber (±1 °C for the air and wall temperatures, ±5 % for relative humidity and ±0.04 m/s for ambient air turbulences). Thus, the total mean relative error of the heat flux was measured on Torso heated to a constant temperature of 34°C at various ambient air temperatures (table 4.2).

Table 4.2. Variation in heat flux measurement at various ambient temperatures, with the Torso surface temperature set to 34°C.

Ambient temp.	Mean heat flux	Stand dev	Stand dev/ Mean heat flux
°C	W/m^2	W/m^2	%
10	230	5	2.1%
15	180	4	2.2%
20	132	2	1.8%
	Mean		2.0%

The mean relative error of heat flux measured on Torso was found to be 2% of the measured value. The set of simulations for various heat fluxes was done and compared to results for the same heat fluxes decreased or increased by 2% in order to determine the sensitivity of iesd-Fiala model to inaccuracies in the heat flux measurement. Two examples of cold and hot exposure (large and small heat flux values respectively) are shown in figure 4.10.

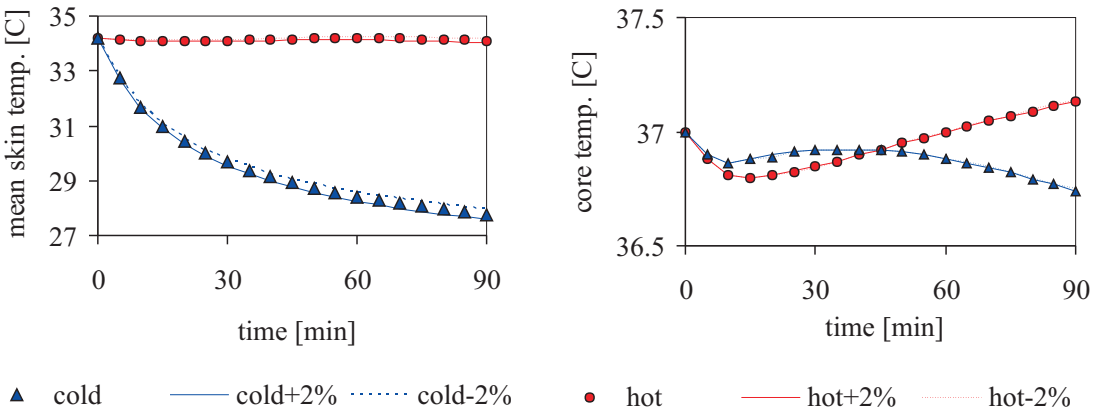

Figure 4.10. Effect of the 2% inaccuracy in measured heat flux on prediction of the iesd-Fiala model for two different climates. Environmental conditions: T_{acold} = 15 °C, T_{ahot} = 33 °C, RH = 50 %, v_a = 0.1 m/s, MR = 1.5 met, nude person.

The predicted core temperature and mean skin temperature varied by less than ±0.01 ºC and ±0.18 ºC respectively, due to the uncertainty in the heat flux measurement. These deviations in prediction are very small compared to typical deviations of measured data from human subject tests. Therefore, the influence of the heat flux measurement error on the iesd-Fiala model was considered to be negligible.

4.8. Dynamics of the system

The majority of real-life situations and human trials represent exposures to time-varying environmental and/or personal conditions, e.g. moving between indoors and outdoors, drifts in air temperatures in air-conditioned buildings, changing clothing, and temporal variations in activity level. Therefore, the ability to simulate transient conditions has to be considered for the practical use of the new device.

Torso consists of materials with defined thermal properties (aluminium and plastic shell parts) and is equipped with dynamic heating and sweating systems, which influence the overall thermal dynamics of the device. The effects of these factors might interfere with

the simulated dynamic responses of the human body. Thus, to determine possible limitations regarding transient simulations, the maximal rates of cooling and heating of Torso were tested against the dynamic predictions of the iesd-Fiala model for temporally decreasing and increasing skin surface temperatures respectively. The fastest cooling of the human skin occurs when nude subjects are exposed to a sudden drop in environmental temperature, while remaining at rest. These conditions were simulated using the original model for step changes of 5, 10, 15 and 20 ºC from comfortable to lower temperatures with RH = 50 %, v_{air} = 0.13 m/s and MR = 0.8 met for a nude person. After being heated initially to 35 ºC and exposed to the respective environmental conditions, the heating power of Torso was switched off and the device was allowed to cool down to the environmental temperature passively. Subsequently, the predicted rates of mean skin temperature decrease were compared to the cooling rate of the Torso. The fastest increase in skin temperature occurs, when the ambient temperature increases suddenly for a human already having a high metabolic rate for a certain period of time (skin wettedness 100 %). A variety of scenarios were simulated, in which pre-cooled subjects (at 10 ºC) moved from comfortable to hot environments (at 30-45 ºC) at metabolic rates of 1-10 met. The predicted rates of change of mean skin temperature were compared to the rate of increase of surface temperature at the maximal available heating power of the Torso. The results are shown in figure 4.11 as application zones, for which the inertia of the Torso device was found not to pose any limitations on the simulation of transient conditions. In other words, for simulations within the application zones, the human simulator hardware would respond fast enough to allow regulation of the surface temperature according to the mean skin temperature predicted by the physiological model.

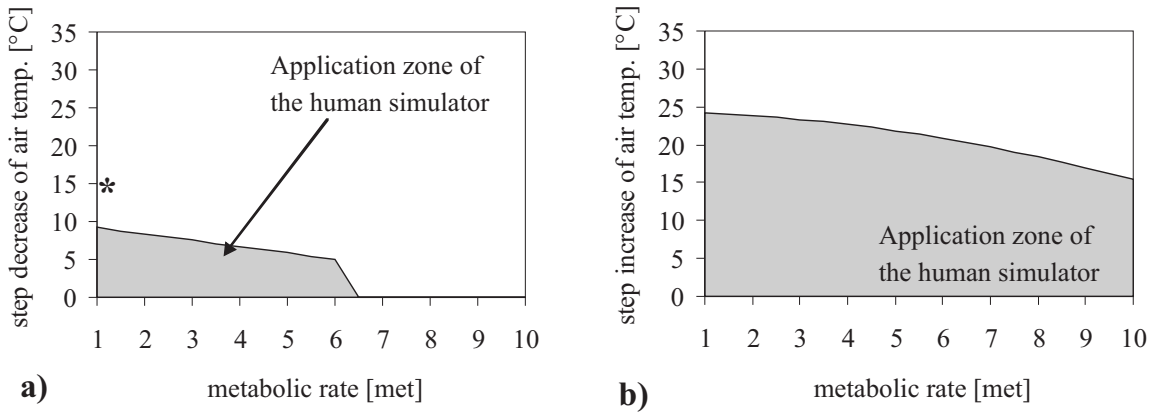

Figure 4.11. Application zones of the thermophysiological human simulator during a step decrease (a) or increase (b) of the air temperature for various metabolic rates. (*) indicates the example described in the text.

As Torso's cooling rate was relatively small, it enabled simulation of only small step decreases in air temperature (of up to 10 ºC) at low-to-moderate metabolic rates. A sudden increase in air temperature exceeded the heating capability of the Torso, when larger temperature steps of 15 °C to 25 °C at respective metabolic rates were simulated. Outside of the application zone, a divergence between the skin temperature predicted by the coupled system and the actual surface temperature measured on Torso was observed. This effect of insufficient cooling or heating occurred temporarily following the step change. For example, for a sudden decrease of ambient temperature of 15 °C from a comfortable temperature with MR = 1 met, the time needed to converge again was approximated 42 minutes (see location of this example in figure 4.11a marked as a star). In contrast to step changes in the environmental temperature, a sudden increase of metabolic rate with constant ambient temperature produced only a small change in skin temperature and did not exceed the cooling/heating capability of Torso. Moreover, a combination of simultaneous step changes in metabolic rate and air temperature had a very small effect on the skin temperature compared to situations when only step changes in air temperature were applied.

4.9. Sweat correction

Torso simulates sweating using water supplied to sweat outlets on the main cylinder surface. These sweat outlets are little nozzles supplied from an external water reservoir via thin plastic tubes and dedicated micro valves. The amount of water supplied is controlled by valves positioned within the lower guard of Torso. The valves operate only in two positions – open or closed - and the regulation of sweat rate is accomplished by regulating the number of sweat drops over time. The optimal open time for each valve is about 250 milliseconds, which permits one droplet to be excreted, where the capillary forces in the duct prevent a drop from coming out of the cylinder any faster than this. Consequently, the sweat regulation is achieved by adjusting the length of the time closed between each drop for a given valve. This execution of sweating caused some initial problems. At low sweat rates (e.g. 1 droplet per 4 minutes), the interval needed between sweat drops is longer than the interval time between the iterations of the experiment (standard setting was 1 min). The new sweat rate is set at every time cycle (if sweating is predicted) and, therefore, a droplet is released at this moment regardless of the previous timing used (i.e. a droplet comes out every minute instead of every 4 minutes). Consequently, the sweat rate might be higher than predicted, due to a faster release of drops than required (Torso before in figure 4.12).

To avoid this increase in sweating, the time step needed to be adjusted for a given sweat rate. This was done by implementing a new algorithm controlling sweating in Torso's software, which was based on a feedback loop. The algorithm compares the actual amount of sweat released with the required amount of sweat and adjusts the time between drops accordingly. The cumulative sum of the sweat released on Torso is measured as a loss of mass of the sweating water tank. The cumulative sum of sweat predicted by the iesd-Fiala model is a result of adding up the predicted sweat amounts per iteration over the elapsed time of the experiment. This algorithm also compensates for inaccuracies in open and close times of the valves caused by timing inaccuracy of the Windows operating system (±30ms). In general, the algorithm used to control sweating is more accurate than the previous one (labelled 'Torso after' in figure 4.12) and it covers the whole range of sweat rates required for simulating human thermo-physiological responses.

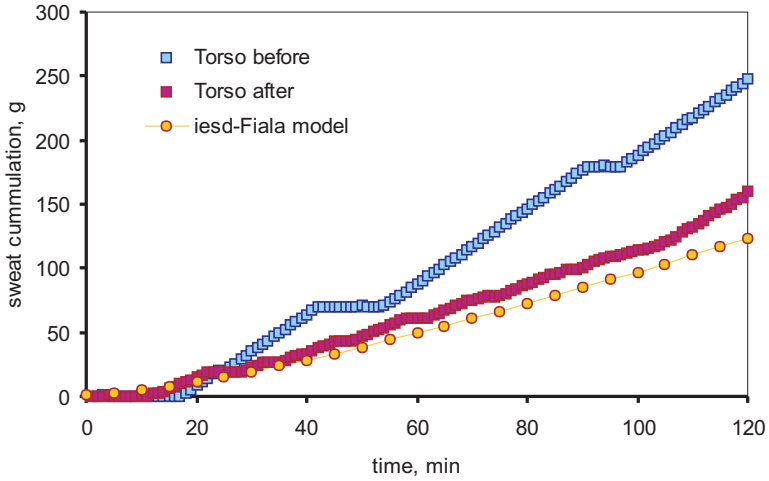

Figure 4.12. Sweat build-up predicted by the iesd-Fiala model and induced on Torso run as a coupled system before and after implementation of the new sweating algorithm. Experiment conditions: T_a = 33 °C, RH = 34 %, v_a = 0.1 m/s, MR = 1 met, clothing = 0.216 clo.

4.10. Validation

The new coupled system was validated by comparison with results of human subject tests. Five experiments were selected, which represent cold, cool, neutral, warm and hot exposures (see table 4.3).

Table 4.3. Experimental conditions analysed in the validation tests.

exposure	T_a [°C]	RH [%]	v_{air} [m/s]	MR [met]	n	rep	clothing [clo]	data source
cold	15.0	40	0.08	0.9	20	1	0.216	(Wagner and Horvath 1985)
cool	20.0	40	0.10	0.9	20	1		(Wagner and Horvath 1985)
neutral	28.0	31	0.10	1.0	3	3-6		(Wagner and Horvath 1985)
warm	33.3	34	0.10	1.0	3	3-6		(Stolwijk and Hardy 1966)
hot	37.5	33	0.10	1.0	3	3-6		(Stolwijk and Hardy 1966)

All experiments involved semi-nude male subjects (wearing only underpants), who reached a physiological quasi-steady-state during the exposure. In most cases, the initial

phase of the exposure represented transient conditions, as the subjects were transferred suddenly from a thermally comfortable pre-test chamber into the chosen experimental conditions.

The validation results are shown in figure 4.13. The core temperature (triangles T_{core}), being one of the most important physiological variables, and the mean skin temperature (squares T_{sk}), which is a useful indicator of thermal comfort sensation and of the overall condition of the body, were chosen as the relevant physiological parameters for validation of the single-sector thermophysiological human simulator.

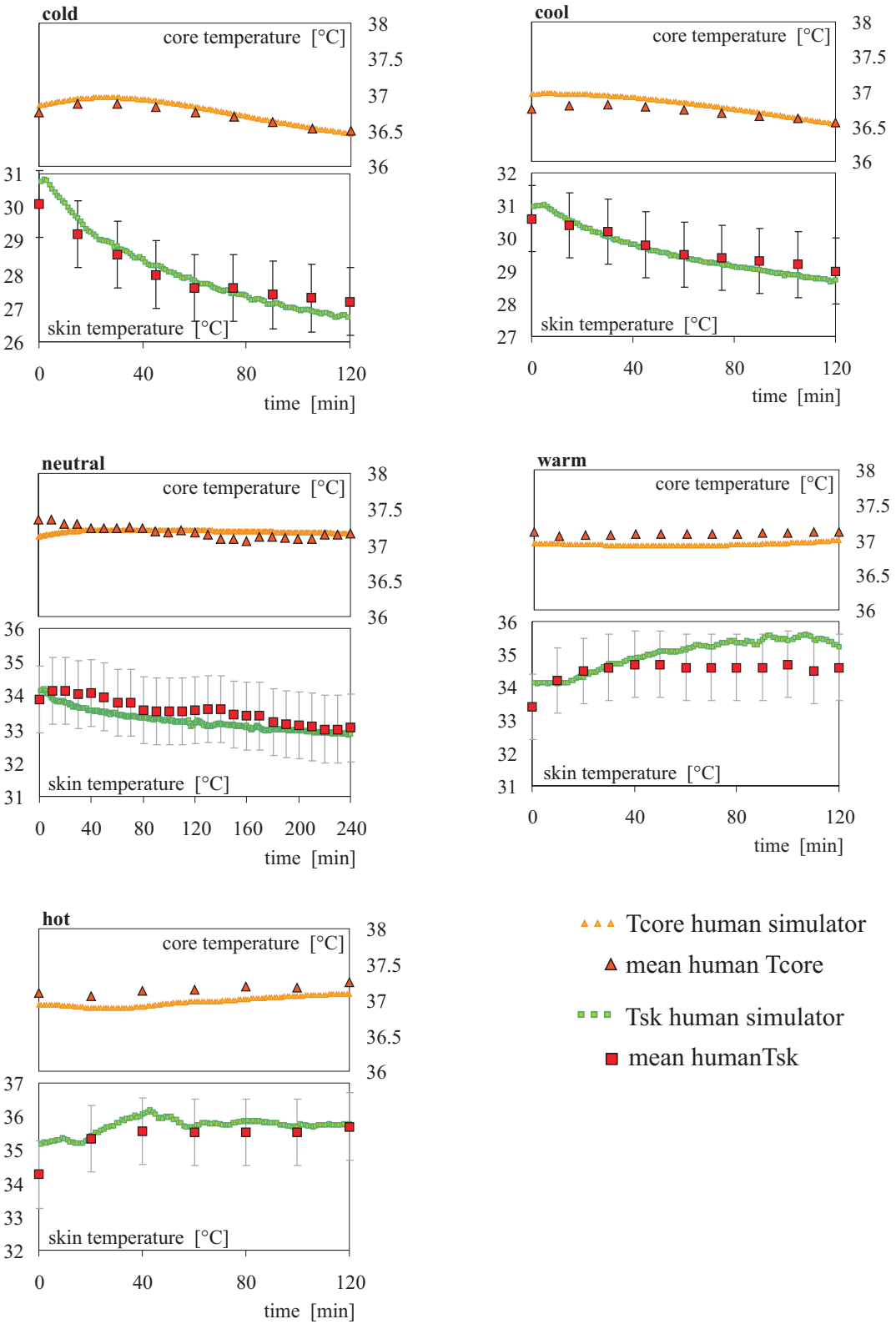

Figure 4.13. Mean skin temperatures and body core temperatures of the test subjects and those predicted by the single-sector thermophysiological human simulator for cold to hot exposures. The experimental conditions and sources of experimental data are given in table 4.3.

Statistical data (standard deviations) for the human test skin temperature in the human tests were only available for the exposures to cold and cool environments (Wagner and Horvath 1985). For the other three experiments (Stolwijk and Hardy 1966), a typical standard deviation of 1 °C due to inter-individual differences was assumed. The root-mean-square deviations (rmsd) (Barlow 1989) listed in table 4.4 indicate the average differences between the simulations and the corresponding human experiments.

Table 4.4. Root-mean-square deviations of core and mean skin temperatures for the exposures analysed.

exposure	rmsd T_{sk} [°C]	rmsd T_{core} [°C]
cold	0.37	0.07
cool	0.24	0.12
neutral	0.18	0.24
warm	0.62	0.16
hot	0.45	0.17

4.11. Discussion

In all the cases studied, the single-sector thermophysiological human simulator closely reproduced the body core temperature observed for human subjects both when approaching quasi-steady-states and during the initial transient period of the exposure (rmsd < 0.24 °C).

During cold, cool and neutral exposures, the skin temperatures also showed good agreement with those measured in human subject experiments (rmsd < 0.37 °C). The beginning of the cold and cool exposures represented typical transient conditions, as the ambient temperature between the pre-test and the test chamber differed notably (subjects were exposed to a room temperature of ~25 °C). However, these transient conditions lay within the application zone shown in figure 4.13 and were accurately simulated using the human simulator.

Prior to each exposure, the simulator remained in the climatic chamber set at the respective ambient temperature. The human simulator was not cooled during this time under warm and hot environmental conditions. Hence, the surface temperature of the

main cylinder was higher at the beginning of test than the skin temperature of human subjects being prepared in the thermo-neutral climatic chamber. This effect could have been avoided if the simulator had been moved quickly from one climate to another as was the case for the human tests. Unfortunately, this was not possible for this study for practical resons. At cold, cool and neutral environmental conditions, it was possible to regulate the surface temperature of the simulator by heating; thus, for these conditions, the simulation began at the correct initial surface temperature.

During the course of the exposure to the warm environment, the surface temperature of the human simulator differed by a rmsd of 0.62 °C from the skin temperature observed in human tests when they reached a quasi-steady-state. The simulated skin temperature tended to be somewhat higher than the one measured in subject testing (although within the assumed range of experimental error). The most plausible explanation for this is insufficient cooling by sweating. The sweating liquid was distributed over the surface of the simulator by an array of sweat outlets and by a hydrophilic textile. The cooling effect was then recorded by the Ni surface temperature sensors (resistance wire wound evenly over the cylinder surface between and around the sweating outlets). However, at very low sweat rates, the moisture released did not spread out from each outlet sufficiently to reach the neighbouring sensor and, consequently, no cooling was detected. The heat flux value measured was, therefore, smaller than the true value. It was observed that the smaller heat flux measured induced some increase in sweating, which was still not sufficient to cool the nearest surface temperature sensor winding.

A similar effect was observed during the hot exposure. Sweating commenced gradually, and, at the beginning, the small quantity of water released did not cool the surface temperature sensor sufficiently. Subsequently, the amount of sweat predicted increased. Finally, after 40 minutes exposure, the moisture had spread out sufficiently wide for the cooling to be detected by the surface temperature sensor. As a result, the surface temperature decreased and followed the skin temperature measured in human subjects more closely.

The validation tests conducted as a part of this study focused on semi-nude subjects. In principle, however, the application range of the human simulator can easily be extended to scenarios, for which clothing is worn. The clothing worn then forms a part of the

environment, which influences the human physiological reactions. In future, it is intended to use the simulator for detailed analysis of the thermal properties of clothing under realistic conditions as well as the overall thermophysiological human response.

4.12. Data management system

In practice, the link needed to be structured and programmed using the Delphi programming language based on Borland Pascal as it was the operational software of both Torso and the iesd-Fiala. The coupled programs were organised into a modular structure (see figure 4.14).

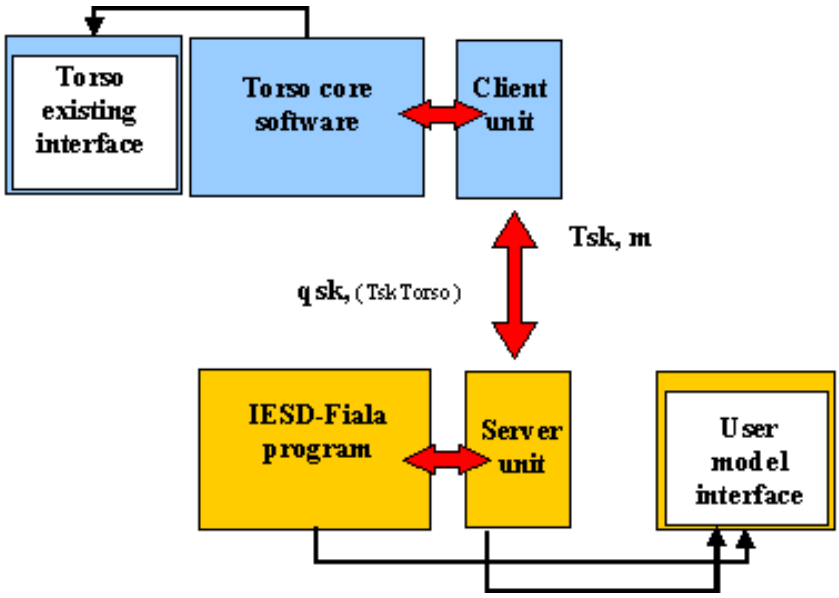

Figure 4.14. The structure of the link between the iesd-Fiala model and Torso software.

Data is exchanged between the two systems using a client-server connection, which was implemented as separate units in the code of both programs. The physiological model serves as a server computing the data required for the client, which is Torso software. An additional module attached to the server serves as a simple user interface of the model, where the analysed data is managed, displayed and saved. The interface consists of a main window providing certain general data (time, exposure conditions) and subordinate child-windows, where particular data sets are displayed graphically on the right as well as within the outline of human body using a colour scale on the left (see

figure 4.15). The data can either be displayed and continously updated during the course of an experiment or loaded from a file for analysis following the completion of an experiment.

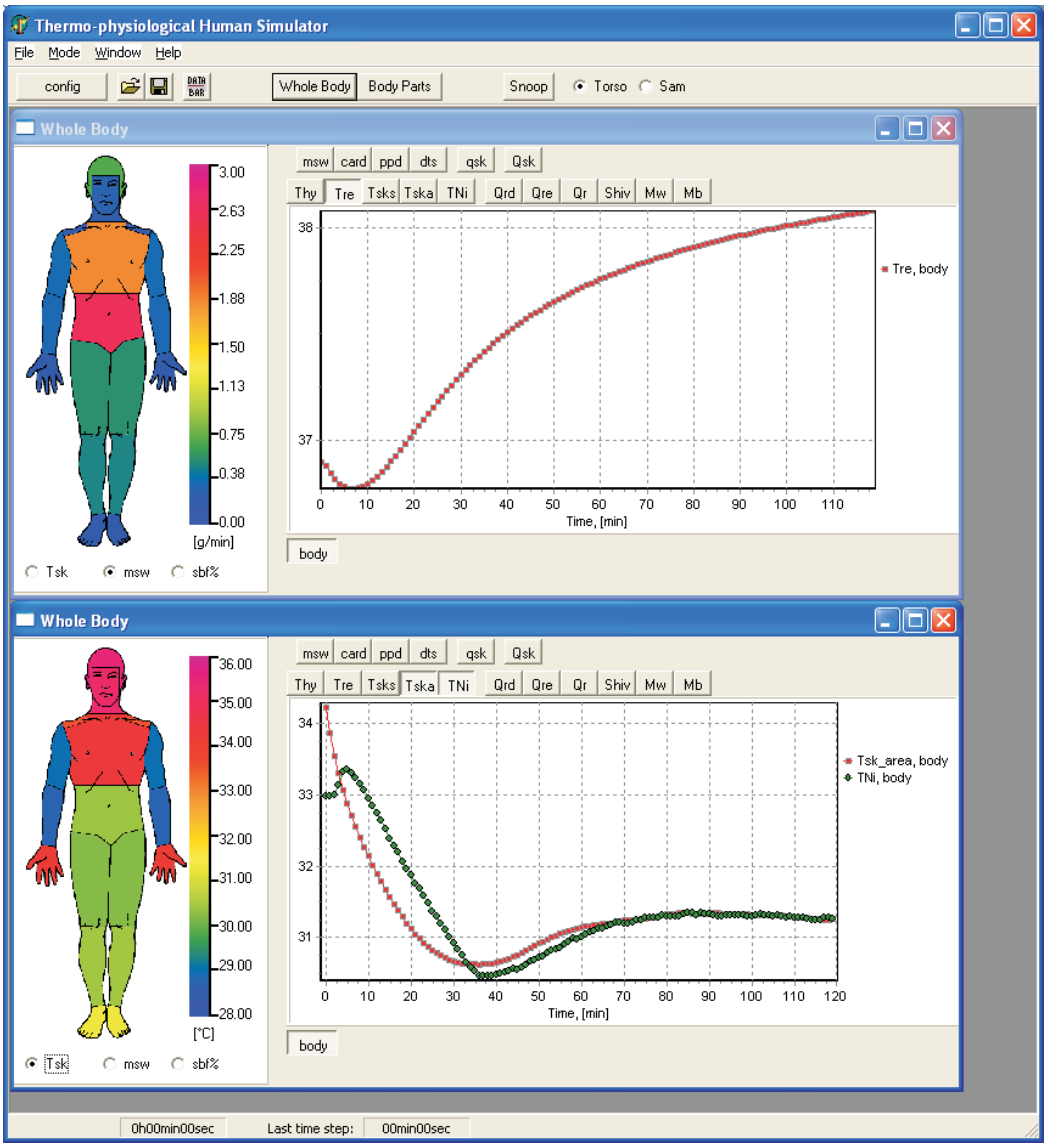

Figure 4.15. The screenshot of the interface to the single-sector thermophysiological human simulator with data displayed on diagrams.

4.13. Summary

This chapter describes the development and the validation of the new single-sector thermophysiological human simulator. The necessary preparatory work included the calibration of Torso's temperature sensors and the sweating excretion, the correction of

the sweating algorithm, the calibration of the climatic chamber in which the coupled system was located, the analysis of drawbacks of using the homogenous heat flux for the whole body, the analysis of the influence of the heat flux measurement error on the performance of the coupled system, and analysis of the dynamics of the coupled system. Finally, the single-sector device was shown to be able to simulate the overall human thermophysiological responses for steady-state conditions with acceptable accuracy. This was confirmed by accurate prediction of core (rmsd < 0.24°C) and mean skin (rmsd < 0.62°C) temperatures compared to human subject results for environmental conditions ranging between 15.0 °C and 37.5 °C (for semi-nude subjects). Within the range of defined application zones, this robust and relatively simple device has also been shown to be capable of accurately simulating the overall dynamic thermal behaviour of the human body.

5. Multi-sector thermophysiological human simulator.

The vision of a new generation of devices that can adequately simulate human beings is challenging. Coupling Torso with the iesd-Fiala model has proven to be successful (see chapter 4) and formed a good basis for developing an 'artificial human'. This 'artificial human' shall consist of a multi-segmental device rather than the single segment device coupled to the physiological iesd-Fiala model. The multi-segmental approach is necessary to simulate the essential human thermo-physiological behaviour, which includes the role of extremities in the human thermoregulation and accurate reproduction of the thermal dynamic behaviour of the human body. Therefore, the multi-segmental device should incorporate a local control for individual body parts. Furthermore, the system needs to be validated by comparison to human data.

5.1. Thermal manikin

Sweating Agile thermal Manikin (SAM) is a multi-segmental and anatomically-formed thermal manikin (see figure 5.1) (Richards and Mattle 2001). It consists of a stainless steel skeleton with movable joints at the hips, knees, shoulders and elbows, and shell parts made of thin-walled polyethylene-aluminium composite. The external movable drive units, which are computer controlled, enables SAM to perform realistic body movements representing different activities including walking, climbing or running. The manikin is equipped with 22 shell-parts, which are separately heated on their inner surface. The temperature of each shell-part is measured at its outer surface using nickel resistance wire deployed evenly over the shall-part. 125 sweat outlets distributed evenly over the manikin's surface allow simulation of variable sweat rates. The sweat liquid excretion is controlled by valves using hydrostatic pressure as the driving force. Due to space limitation inside the manikin, either four, three or just two outlets are attached to one valve within the same shell-part and controlled simultaneously. In addition, a thin hydrophilic textile is used to spread the moisture from the sweat outlets more evenly over the manikin surface.

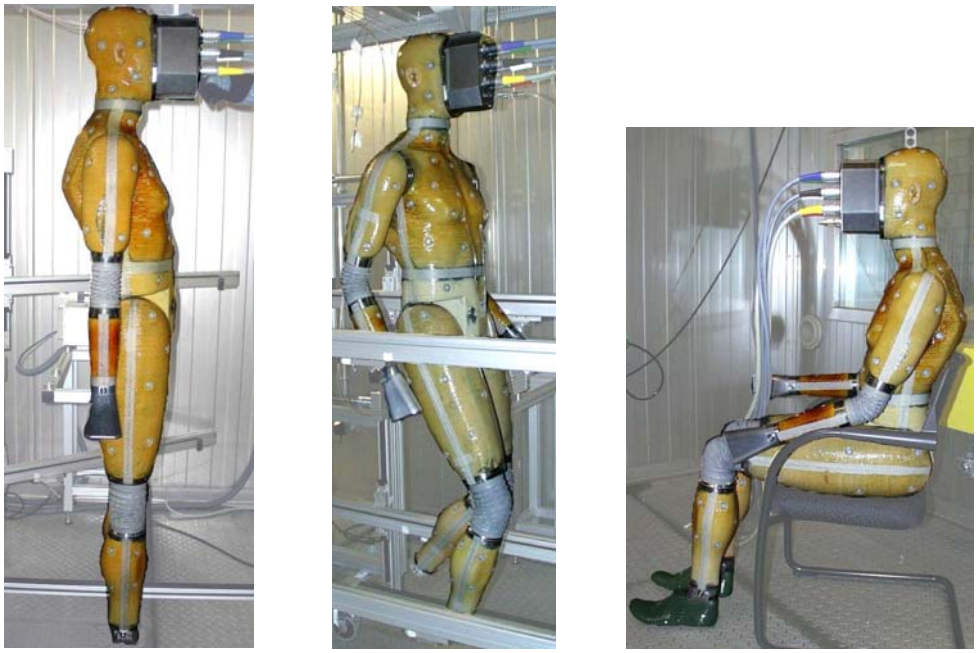

Figure 5.1. Sweating Agile thermal Manikin (SAM) in available testing positions such as standing, walking and sitting (Richards and Mattle 2001).

The face of SAM is substituted by a block of electronic connections of heating foils, temperature sensors, valves and the water delivery duct to sweating outlets. Hands and feet are simplified by leaving out the discrimination of fingers and toes. These parts together with the elbows, the knees and the face block serve as guards rather than body shell-parts. Each guards is equipped with two Pt100 type B sensors. The guards can be set either to follow the temperature of the neighbouring shell parts or to keep a constant set temperature.

5.2. Calibration of SAM

In order to prepare the thermal manikin for coupling with the mathematical model, the calibration of surface temperature sensors and guard sensors was carried out. Such calibration is necessary to be done intermittently to ensure correct conversion of resistance into temperature.

A calibration for six temperatures between 15 °C and 40 °C (steps of 5°C) was conducted. SAM was disconnected from the power supply and the measuring equipment and placed in a climatic chamber at set ambient temperature. It was left there for several hours until the shell parts and the guards reached the same temperature as the ambient air. To avoid non-homogeneity of the air temperature and to accelerate the temperature stabilisation of the manikin, four fans were used to mix air around SAM at low velocity. The temperature of the ambient air at the chest surface of the manikin was measured using a Kelvimat type 4342-V600 with Pt100 sensor to a precision of ±0.015°C. When the temperatures levelled up, the electronic connections were plugged in again and the voltage on the surface temperature sensors and the guard sensors was measured as an average value of 10 minutes measurement. This procedure was repeated for every calibration point.

Subsequently, the voltage was correlated with the temperature and the trend was found to be linear within the above range giving the equation:

$$T_{sec\,tor} = A \cdot V + B, \tag{5.1}$$

where:

A – slope of the calibration line (K/mV),

B – interception of the calibration line (°C),

V – voltage (mV) output from either a surface sensor of the shell-part or a guard

The slope and the interception values are collected in appendix 1 and examples of calibration lines shown in figure 5.2. Squared Pearson's coefficients shown in appendix 1 indicate an excellent correlation of the dependence between voltage and temperature by a straight line.

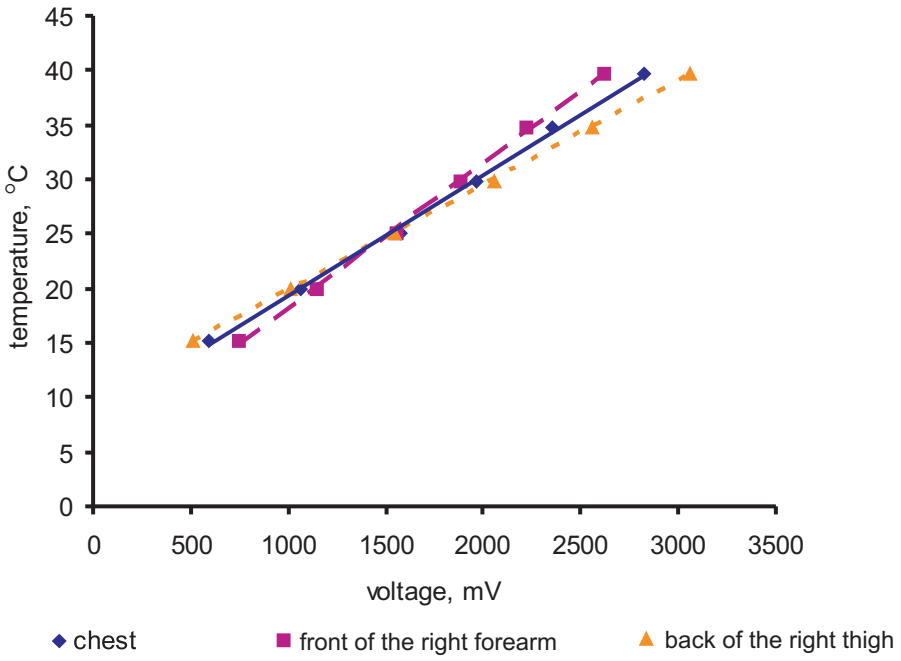

Figure 5.2. Examples of the calibration lines of SAM's shell-parts, namely chest, front of the right forearm and back of the right thigh.

5.3. Regulation of the climatic chamber

A climatic chamber has an important input to the precision and accuracy of the thermal device. The chamber, where SAM was placed, maintains the ambient temperature to within ±1 °C and relative humidity within ±5 %. However, below 5 °C, no control of relative humidity is possible. Initial measurements of the ambient air movement showed a spatial variations of air velocities of up to 28 % of the average value in the cross-section in front of the manikin. The average air velocity depended on the air blow rate in the climatic chamber. At a low air blow (10% of the maximal air blow), the average air velocity in front of the manikin was 0.23 ±0.06 m/s, 0.43±0.08 m/s at 30% and 0.67±0.19 m/s at 50%. Thus, it was not possible to simulate typical indoor climatic conditions with air velocities of less than 0.15 m/s in this climatic chamber. In addition, at higher air blow rates, for example above 30% of the maximum the efficiency of the climatic chamber is better.

Since SAM had a fixed position in the climatic chamber, the problem of too high air velocities had to be solved structurally. The relatively large size of the chamber allowed a manipulation of air streams using additional structures, namely the false ceiling and the back partition (see figure 5.3).

The climatic chamber of SAM was originally designed with a mixing air-conditioning system. In the internal circulation process, the ambient air is taken up from the chamber through the grid at floor level in the back of the chamber to the conditioning unit. Then the temperature and the humidity of the air are adjusted and the air is introduced back to the chamber at ceiling level in the back of the chamber. This configuration of supply and exhaust of air created vortices due to the relatively high speed of air supplied, impinging effect at the supply, reflection from the opposite wall, hence, air movement round manikin was highly turbulent and inhomogenous across its body (see figures 5.3, top and 5.6, top). Adding additional structures to the climatic chamber, namely, the false ceiling and the back partition, aimed at changing the air circulation system from a mixing to a quasi piston flow system, which is known to give a homogenous velocity field and low turbulence level (see figure 5.3, bottom). Due to relatively small size of the air-conditioned space, a full scale model was chosen as the fastest and most reliable method to parameterize and assess the additional structures. The full scale models of false ceiling at various lengths (see figure 5.4, left) and back partition at various heights (see figure 5.5, left) were built and the velocity profiles were measured in the vinicity of SAM. Various configurations were evaluated and the permanent structures were constructed for the solution, which provided the most uniform air flow around SAM (see figures 5.4 and 5.5, right).

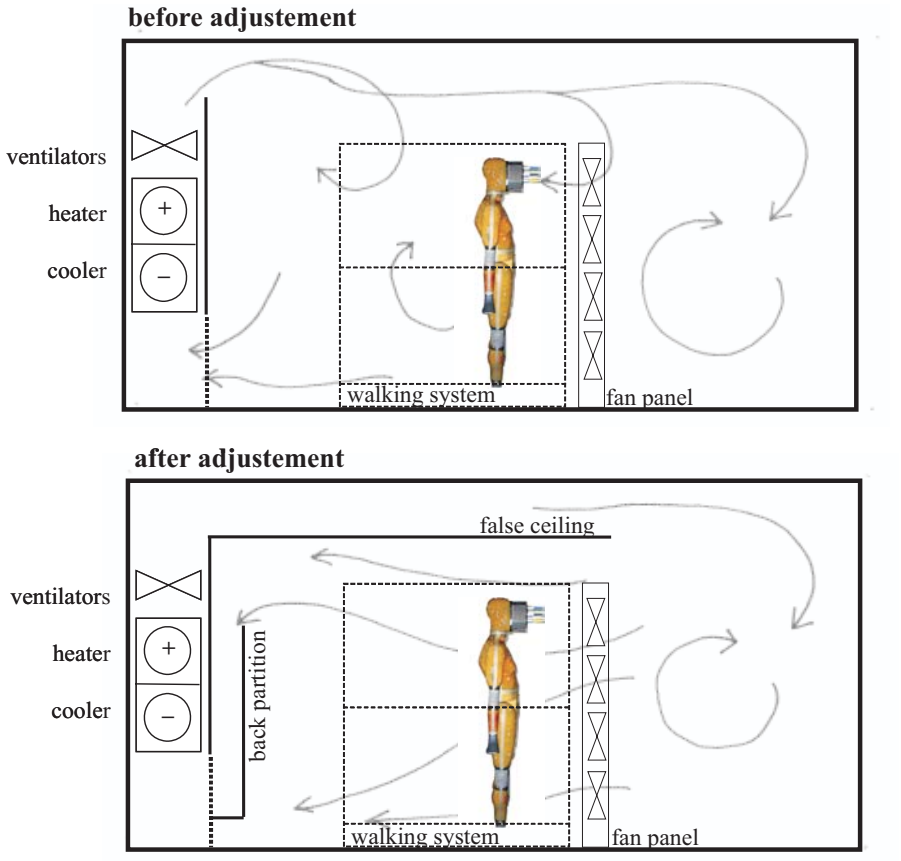

Figure 5.3. The cross-section along the climatic chamber of SAM with the indicated air-conditioning unit, walking system and fan panel as well as additional structures optimising the air flow around the manikin. The arrows indicate approximated directions of air movement in the chamber.

Figure 5.4. The construction of the false ceiling: full scale model (left) and implemented false ceiling (right).

Figure 5.5. The construction of the back partition for homogenous air flow around SAM: full scale model (left) and implemented partition (right).

The quasi piston flow system showed a very good performance reducing the air velocity and its variability in the manikin's location significantly. Figure 5.6 shows the air velocity profiles measured in front of the manikin (without the manikin being present) before and after introduction of the air flow-optimising measures.

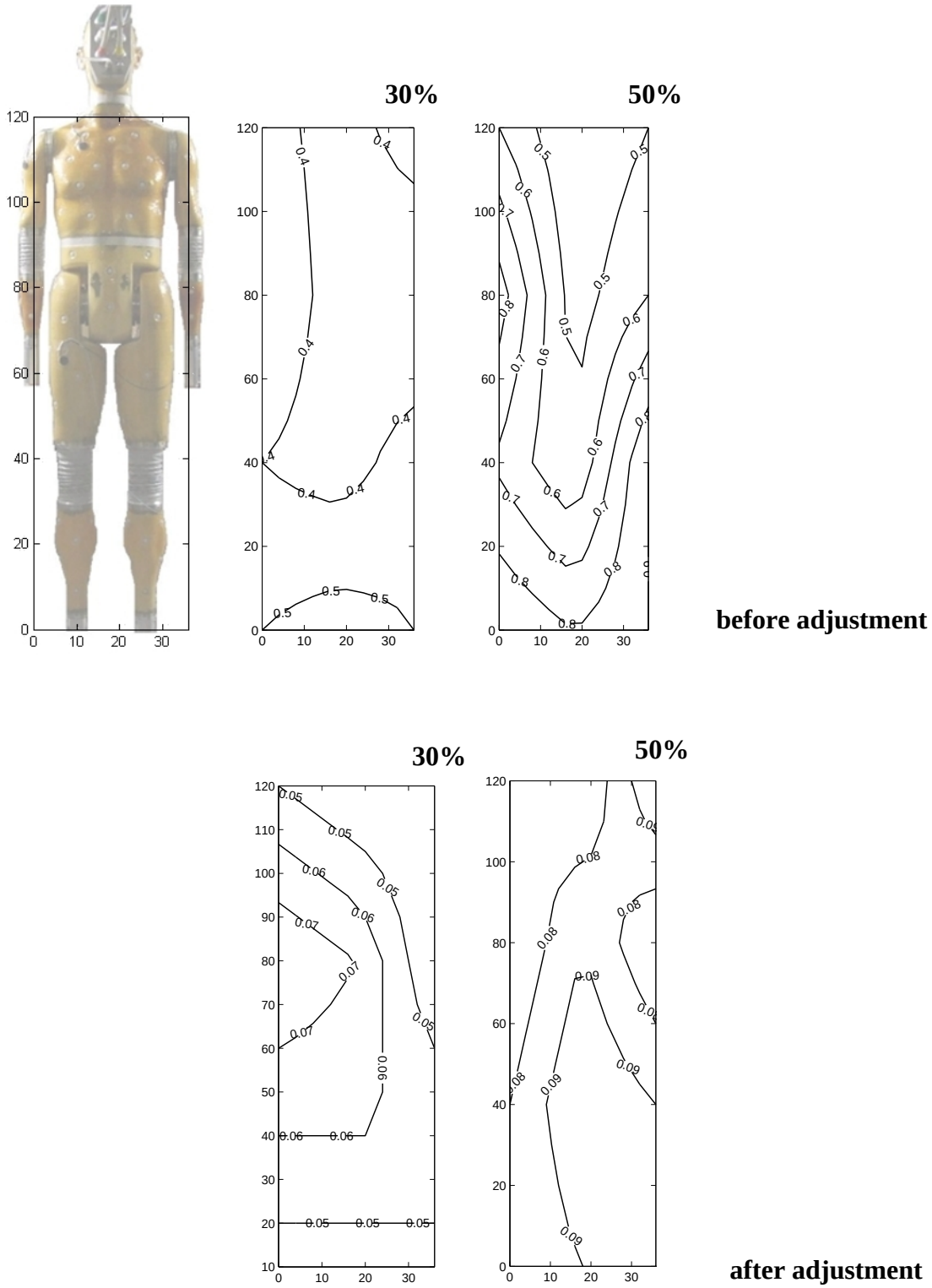

Figure 5.6. The distribution of the air velocity at SAM's location before and after adjustment of SAM's climatic chamber at 30 % and 50 % of internal air circulation flow. The axes represent dimensions of the measurement profile (cm) and isolines show air velocities (m/s).

5.4. Amendment of the PID control with anti-windup algorithm

The PID control system of SAM was originally programmed and tuned for maintaining constant temperature of each shell part. This was due to the intended use of this manikin for standardised steady-state measurements. However, the PID control system, when working in the coupled system, was subjected to step disturbances (step changes of set point temperature, i.e. shell part surface temperature) at every time interval of the experiment (typically 1 minute). These frequent disturbances prevented the manikin from following the desired, physiologically-changing temperature of shell part surfaces with these PID parameters.

To investigate this problem, a simple test of two disturbances was carried out, such as 1°C increase of surface temperature followed by 1 °C decrease of surface temperature after 40 minutes. From this test, it was diagnosed that the PID control algorithm needed to be amended to include an anti-windup procedure (Astrom and Hagglund 1995) to prevent saturation of the integral term. The control variable is the heating power delivered to each shell-part of the manikin, which is limited by the maximum capacity of the respective heater, i.e. actuator. No cooling system is provided for the manikin, thus, the minimum value of the control variable is zero. The PID control predicts dynamically the required power to reach the set point temperature. When a disturbance is applied to the controlled system, such as step increase of the set point temperature, the heating power predicted by the PID controller may exceed the maximal heating power available. For a step decrease of the set point temperature, the power predicted may be negative, though a cooling system is not available in the manikin. When such a situation occurs, the feedback loop is broken and the system runs as an open loop. In other words, the power supply remains at its limit of maximal or minimal power regardless of the process output, which is the shell part surface temperature. If a controller with integrating action is used in this situation, the error will continue to be integrated. This means that the integral term may become very large, and it is then required, that the error has an opposite sign for a long period before the system can return to the feedback loop. Consequently, the controller with integral action gives large transients when the actuator saturates. To overcome this problem an anti-windup

algorithm needs to be implemented, which enforces limits on the control signal as follows:

$$u(t) = \begin{cases} u_{\min} & if \quad u(t) < u_{\min} \\ u(t) & if \quad u_{\min} < u(t) < u_{\max} \\ u_{\max} & if \quad u(t) > u_{\max} \end{cases}, \tag{5.2}$$

where:

u(t) – heating power predicted by the PID controller,

u_{min} – minimal heating power available, u_{min} = 0W,

u_{max} – maximal heating power available, where u_{max} varies with shell part size.

The increase of the set point temperature of shell part by 1°C induced the onset of heating with the maximal power for a short period of time followed by reduced heating required to reach and maintain temperature of 33°C. The actuator did not saturate in this time, because the temperature increase was relatively small as compared to the heating capacity of the shell part of 2.7°C/min when the maximal power is used. Therefore, the transition from 32°C temperature phase to 33°C temperature phase is nearly instantaneous and smooth (see figure 5.7).

The decrease of the set point temperature in the second stage of the experiment resulted in predicting cooling (negative power), which was not available for the shell part. In this case the actuator saturated (at heating power of 0W) and the integral part kept building up its negative value. Finally, the shell part reached the required temperature being cooled passively and the PID control predicted positive values of heating power again. However, it took up to 5 minutes to compensate for the negative integral part, which built up during actuator saturation. Effectively, the temperature of the shell part dropped significantly during this time until the heating was set on again (see figure 5.7, dotted line). Implementation of the anti-windup algorithm prevented the integral part from building up when the actuator saturated. Therefore, the required temperature of the shell part could be maintained instantly after it reached the required value during passive cooling (see figure 5.7, continuous line).

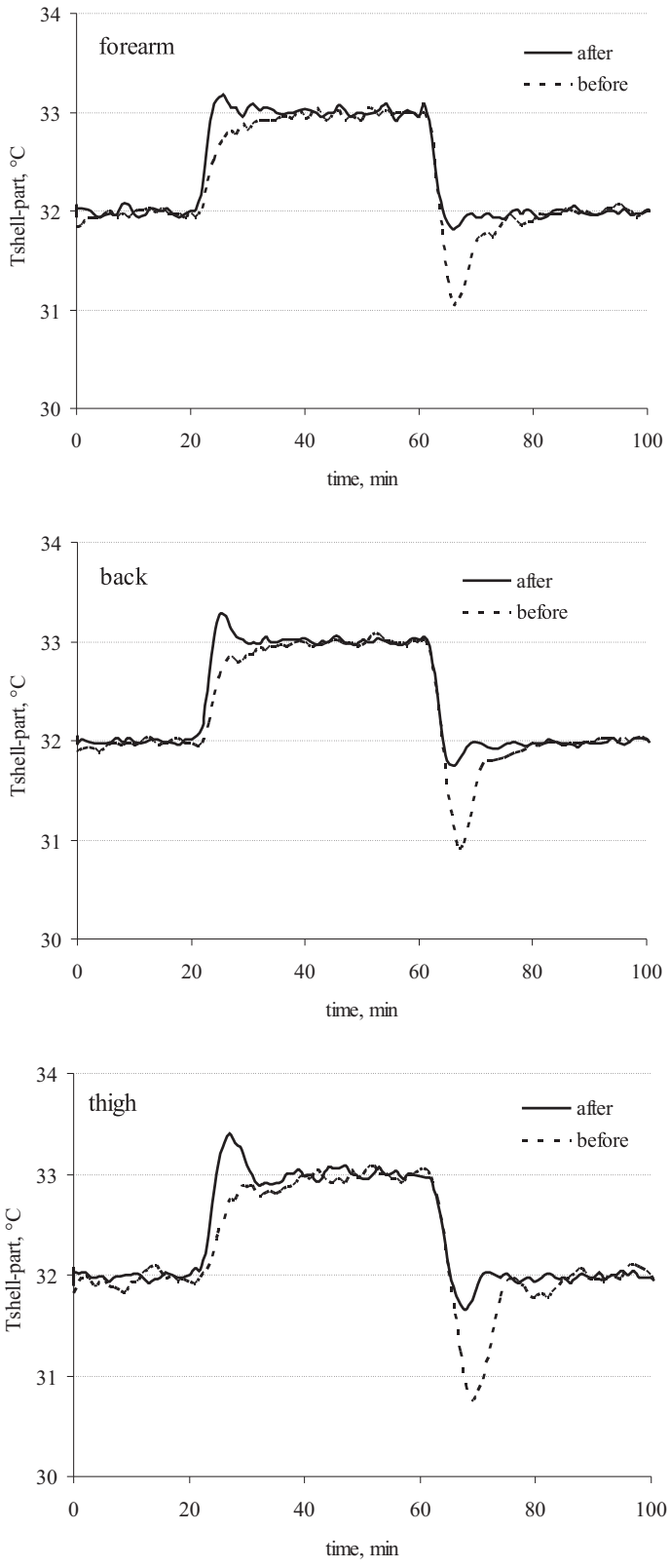

Figure 5.7. Examples of measurements with a step change of shell part temperature (for the first 20 minutes $T_{shell\ set}$ = 32°C, for the next 40 minutes $T_{shell\ set}$ = 33°C, and for the last 40 minutes $T_{shell\ set}$ = 32°C) before and after implementation of the anti-windup algorithm.

5.5. Coupling of SAM and the iesd-Fiala model

The coupling method developed for the single-sector thermophysiological human simulator was the basis for developing the coupling procedure for the multi-segmental thermal manikin. For this purpose, the adjusted iesd-Fiala model described in section 4.4. was used. In order to understand better how a more complex system would respond, the coupling process was accomplished in two stages. At first, the thermal manikin was set up to produce a homogenous surface temperature and sweat rate over the entire body, though changing in time. The area-weighted averages of the local skin temperatures and the local sweat rates predicted by the physiological model were used as input parameters to the manikin control system for each shell part. The feedback signal from the manikin was the average heat flux from all shell parts.

In the second stage of the coupling process, the manikin was set up to produce heterogeneous surface temperatures and sweat rates on individual shell parts. The iterative exchange of the data between the manikin and the iesd-Fiala model included local values of skin temperature and sweat rate for each shell part. The feedback signals from the manikin were local heat fluxes from individual shell parts representing the amount of heat exchanged with the actual environment and clothing worn during a set time interval.

The spatial division of the manikin into the shell parts did not correspond exactly to the body division into sectors of the physiological model. Therefore, this issue had to be addressed in the software. In general, the human body of the iesd-Fiala model consists of a sphere for the head and cylinders for the face, neck, thorax, abdomen, upper arms, forearms, thighs and lower legs, which have surface areas comparable to the surface areas of the human body parts. In contrast, SAM is a more realistic 3D-geometry of the main parts of the human body (without hands, feet and face). In the iesd-Fiala model, hands and feet were modelled as single cylinders. Furthermore, the physiological model includes more body subdivisions than SAM does. Despite of these differences, the subdivision into body parts in the physiological model was a good match to the manikin special subdivision. Most of the cylindrical body parts such as arms, legs and the trunk were divided into four sectors in the iesd-Fiala model, which was not the case for SAM. These include: anterior sectors in front of the body, posterior sectors in the rear of the

body, exterior sectors on the sides of the body parts, and inferior sectors (wherever two body parts are directly opposite each other, e.g. inner sides of the legs). The area weighted averages of skin temperature and sweat rate were calculated for each body part from the corresponding spatial body sectors of the physiological model and applied to the respective shell parts of the manikin. Another difficulty arose from the missing body parts in the manikin. SAM has a connection block instead of a face, and its hands and feet are residual and act as heated guards rather than shell parts used for measurement. Since these missing body parts constituted only 12% of the total area of the human body when compared to the physiological model, they were assumed to be a part of the neighbouring body parts such as head, forearms and lower legs respectively. Effectively, skin temperatures and sweat rates of hands, feet and face predicted by the iesd-Fiala model were included as area-weighted averages in the respective surface temperatures and sweat rates of adjoining shell parts.

5.6. Heat flux measurement

The heating system of SAM consists of a resistance wire winding, a power supply and a PID control for each sector. The heating wires are evenly wound on the inner side of each shell part. The power supply delivers electrical power in square-wave pulses, which are adjusted every second by a dedicated PID control algorithm. Due to very fast rise and fall times of the square-wave pulses, such a system provides a precise determination of the power delivered (sum of the pulses during a given period of time) and it allows immediate adjustment of supplied power by PID control for better accuracy of the entire system. Each shell part of this thermal manikin incorporates the surface temperature sensor, which is a resistance wire deployed evenly on the outer surface of the shell part. With this setup, the heat flux of the shell part can only be estimated using the power delivered to it, divided by its surface area (rather than additionally from measured surface temperature gradient, as for Torso).

Although the measurement of the power delivered is accurate, the actual heat flux flowing out of the shell part may not be estimated correctly by this method. In other words, the heat delivered to the shell part may not be equal to the heat released from its

outer surface to the environment. Each shell part is fixed to the internal steal skeleton by metal screws, which can conduct heat between the skeleton and the shell part. Moreover, shells contact each other at the edges, which creates additional thermal bridges for heat conduction. The electronic components inside the manikin, which operate the temperature sensors and the sweat excretion system also generate a relatively small amount of residual heat, which then may be transferred via free convection and conduction to the skeleton and the shell parts. In order to understand better the heat transfer phenomena within the thermal manikin, a couple of simple tests were carried out.

5.6.1. Variability amongst similar shell parts

The variability of the heat flux from the shell parts was investigated during steady-state conditions (constant temperature of the manikin surface maintained at 34°C) at various ambient temperatures. The shell parts, which are symmetric or of similar shape and kept in the same position (e.g. vertical), were grouped together. Only heat fluxes from shell parts within each group were compared, as the heat transfer coefficients depend on the shape and position of the surface, where the heat exchange occurs. The smaller variation within each group would be, the better accuracy of the thermal manikin.

The shell parts groups were defined as follows:

- head – two symmetric shell parts;
- arms – four symmetric shell parts (front and back shell parts are of similar shape and both upper arms are symmetric);
- forearms - four symmetric shell parts (front and back shell parts are of similar shape and both lower arms are symmetric);
- chest and back are of similar shape;
- abdomen and buttocks are of similar shape;
- thighs – four symmetric shell parts;
- shins – two symmetric shell parts;

- calves – two symmetric shell parts.

The air movement profile described in figure 5.6 (after adjustment, circulation 50%), which was used in this experiment, was homogenous with average air velocity of 0.09±0.01m/s. The variability of the heat flux within each group was determined as a maximum heat flux residual within the group over the average heat flux in this group. The percentage ratios indicating its variability for three given ambient temperatures are plotted in figure 5.8. The average values of heat flux are listed in appendix 2.

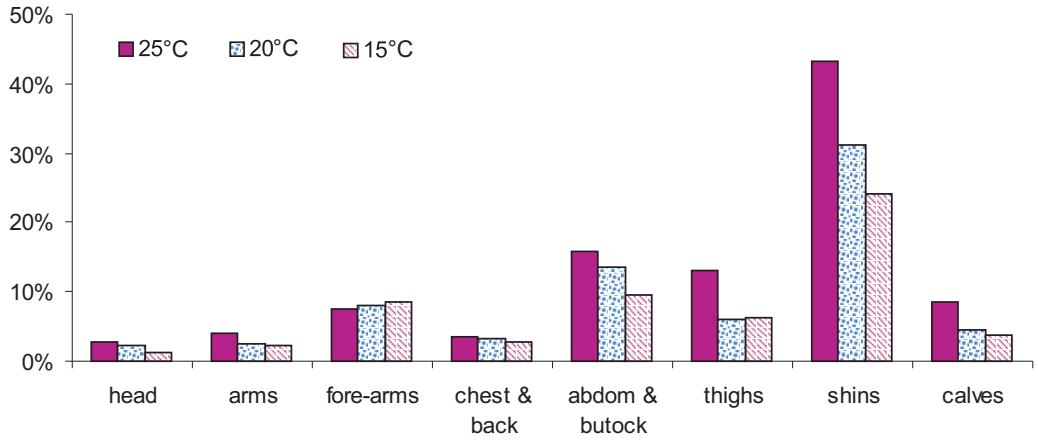

Figure 5.8. The average values of heat flux and the ratios of maximum heat flux residual within the group over the average heat flux in this group for given ambient temperatures.

This simple comparison showed a variability of the surface heat fluxes within groups of similar-shape shell parts. The thermal plume, which was created around the manikin, was not entrained by the low air flow speed in the climatic chamber (chamber air flow 0.09m/s was lower than boundary air velocity needed to entrain the thermal plume of the manikin, which is 0.20m/s (Melikov 2007)). Thus, the changes in thickness of boundary air layer of thermal plume could not influence the heat exchange on the manikin surface. In addition, transitory random eddies, which could have affected the thickness of this layer instantaneously, would equilibrate their effect on shell parts during long time measurement of four hours. A plausible explanation of the variability amongst shell parts can be an internal heat flow between shell parts and other structural

elements. For example, heated guards are equipped with temperature sensors, which measure the temperature only at the position, where they are mounted. Such measurement may not be representative for the mean temperature of the heated guard; hence, the guard might be a heat sink or a heat source for the adjoining shell parts. Guards, such as joints, hands, feet and face connection block are part of the steel skeleton, which are exposed directly to the environment and could be direct sources or sinks of heat. As the heated guards are set to follow the average temperature of the adjoining shell parts, the imperfect temperature measurement at the guards could result in an asymmetric variability of heat flux between shell parts.

5.6.2. Convective heat flow inside the manikin

In order to estimate the share of the internal convection in the heat dissipation within the manikin, the cavities inside the manikin were loosely filled with low-density bubble foil. This filler minimised any air circulation within the joined cavities of the manikin with minimal increase of the conductive heat exchange. Effectively, change in the measured heat flux was observed only for the trunk and the head shell parts for various ambient air temperatures. However, these changes were small (on average less than 2% of the power delivered to these shell parts).

5.6.3. Verification using external heat flux sensor

The next method used to verify the reliability of the heat flux measurement was to compare the measurements from the shell parts provided by the manikin software with those obtained from an external heat flux sensor. This sensor measured the heat flux actually released from the shell part surface to the environment, whereas the manikin measured the heat delivered to the shell part but not necessarily released from its outer surface. The external heat flux sensor PU22T Hukseflux consists of many differential temperature sensors, incorporated in a medium of constant thermal properties (PU) and a thickness of 1 mm. The generated output of the sensor is proportional to the local heat flux perpendicular to the sensor surface. The diameter of the sensing area is 30mm and it is surrounded by a guard of 10 mm width, which minimises a collateral heat flow. The expected accuracy ensured by the producer is ±5 % of the measured value. The limited flexibility of this sensor, with a minimum bending radius of 25mm, allowed it to be

used on only some of the shell part areas where the surface curvature was sufficiently small, such as on the chest, back, upper arm, buttock and thigh. The heat flux sensor was mounted on the shell part using the thin foil medical patches with special care being taken to avoid air layers or bubbles between the surface of the sensor and the shell part. In subsequent tests, different methods of fixing the heat flux sensor to the surface were evaluated. As a result, these foil patches, proved to have a negligible influence on the dry heat transfer. The results of the parallel measurement of the heat flux using the manikin and the heat flux sensor at various ambient temperatures are given in appendix 3. The residuals of heat fluxes measured in parallel by the manikin and the heat flux sensor referred to the measurement on the manikin are plotted in figure 5.9.

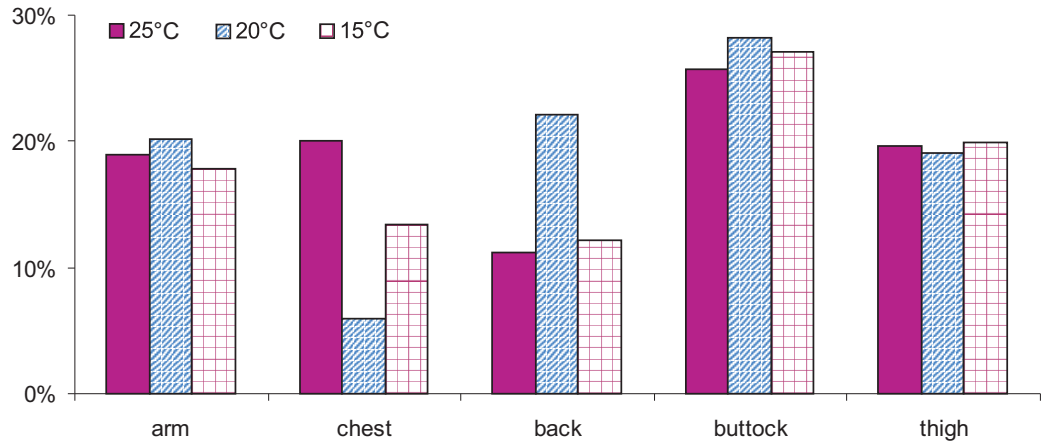

Figure 5.9. The residuals of heat fluxes measured in parallel by the manikin and the heat flux sensor at the various ambient temperatures and the air movement of 0.09±0.01m/s referred to the measurement on the manikin.

These two different methods of measuring the heat flux from the shell parts showed significant variability at all locations measured. On average, the external heat flux sensor measured 17% less heat flow than the manikin (see figure 5.9). Due to the curvature of most shell part surfaces, it was difficult to conduct measurements at many different locations on a single shell part. Nonetheless, such measurements for the thigh at two different locations (upper and lower part) showed that the heat was dissipated homogenously over the shell part (less than 4% difference between locations). Assuming that this was the case for all shell parts, being produced using the same

technology, the point measurements of heat flux were taken to be representative for respective shell parts. Nonetheless, the topology of the shell part surface could influence the external heat flux sensor readings. The resistance wires for temperature sensor, which are wound densely but intermittently on the shell part surface, are only covered with a thin layer of epoxy resin and create raised convex surface structures of up to 1mm. Thus, the sensor was only in direct contact with the shell part at the peaks of these structures and a layer of air was trapped between these peaks.

5.6.4. Comparison of global and local dry heat transfer coefficients

In order to verify the heat flux measurements, the total and local dry heat transfer coefficients calculated from data measured on SAM were compared with data available in the literature. Since it was not possible to split up the measured surface heat transfer coefficients into convective and radiative coefficients in this study, the overall coefficients for literature studies were calculated and compared with those measured on SAM.

The total dry heat transfer coefficient depends on many factors, such as ambient air temperature, manikin surface temperature and shape, effective air movement, temperature of surrounding surfaces, emission coefficients of the manikin and surrounding surfaces. Thus, in order to compare these coefficients from various studies, they had to be derived for the identical environmental conditions, which were as follows:

- temperature gradient between manikin surface and the ambient air of 12 °C;
- ambient air movement below 0.1 m/s (only natural convection occurred);
- temperature of surrounding surfaces equal to ambient air temperature;
- similar anatomical shape of the body parts of manikins;
- emission coefficients of the manikin surface similar to this of human skin ($\varepsilon_{surface} = 0.95$);
- comparable emission coefficients of the surrounding surfaces.

The total dry heat transfer coefficients measured on the manikin were calculated using the following formulae:

$$h = h_r + h_c \tag{5.3}$$

$$q = h \cdot \left(T_{surface} - T_o\right) \tag{5.4}$$

where h, h_r and h_c (W/m^2K) are total, radiative and convective heat transfer coefficients of the shell part respectively, q (W/m^2) is the heat flux measured on the manikin's shell part, $T_{surface}$ (°C) is the temperature of the shell part surface, and T_o (°C) is the operative temperature of the climatic chamber (both ambient and radiative temperatures were equal operative temperature in these measurements). The total heat transfer coefficients for several shell parts of SAM calculated for the heat flux measured using manikin as well as the external heat flux sensor are shown in figures 5.10 (SAM and sensor) and 5.11.

De Dear (deDear, Arens et al. 1997) and Quintela (Quintela, Gaspar et al. 2004) performed an extensive study on convective and radiative heat transfer coefficients for individual body segments using an anatomically-shaped manikin in a wind tunnel. The construction of this manikin is based on the concept of using a single resistance wire on the outer surface of manikin parts for both heating and for measuring the surface temperature alternatively in a sequential routine. The calculations were performed assuming that, under steady-state conditions, the heat supplied to heating wire of each body part was equal to the amount of heat lost from skin to the environment. Although the manikin had a very small time constant, its surface temperature was not uniform (Tanabe, Arens et al. 1994). To enable a comparison, the natural convective and radiative heat transfer coefficients for the environmental conditions described above were selected, summed up and plotted for individual body parts in figure 5.10 and for the whole body in figure 5.11. These were compared to literature values.

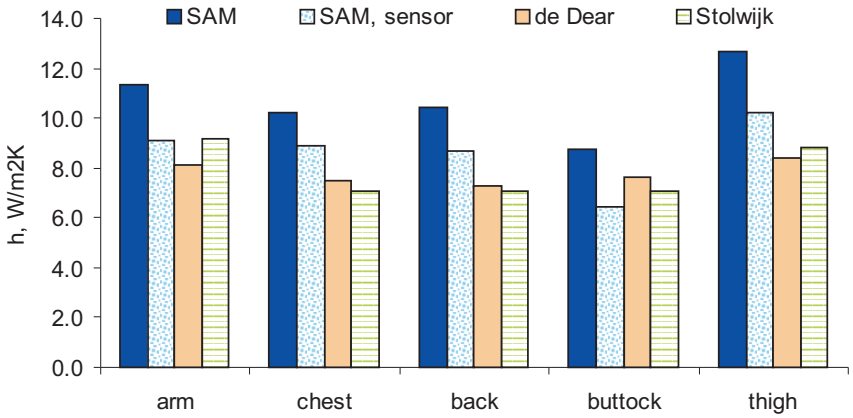

Figure 5.10. Total dry heat coefficients for respective body parts calculated from: the measurements using the manikin (SAM) and the separate heat flux sensor (SAM, sensor), and those given in the literature for anatomical shape manikin obtained by de Dear (deDear, Arens et al. 1997), and for body parts simplified to cylinders and spheres by Stolwijk in de Dear (deDear, Arens et al. 1997).

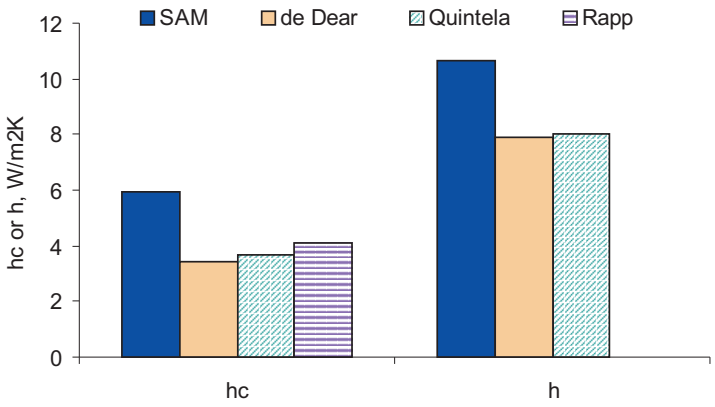

Figure 5.11. Total (h) and convective (h_c) surface heat transfer coefficients for the whole body calculated from: measurements on the manikin (SAM), and those given in the literature for the anatomical shape manikin by de Dear (deDear, Arens et al. 1997), Quintela (Quintela, Gaspar et al. 2004) and Rapp (Rapp 1973).

Both the total and local heat transfer coefficients measured on SAM were significantly higher than those provided in literature (Rapp 1973; deDear, Arens et al. 1997; Quintela, Gaspar et al. 2004). Another approach to estimate heat transfer coefficients

from individual body parts was to use conventional engineering techniques to estimate the radiative and convective heat transfer coefficients from simple approximate geometric representations of human body parts, e.g. cylinder, sphere. Though this method provided only approximate values of coefficients due to simplification of shape, it was free from consideration of internal heat fluxes within a thermal manikin. Stolwijk, in his physiological model, estimated these coefficients for individual body parts (figure 5.10) (deDear, Arens et al. 1997). Effectively, they were similar to those measured on the thermal manikin by de Dear.

5.6.5. Difficulties with accurate measurement of the heat flux on SAM

The investigation of the internal heat flow indicated, that there may be a substantial inaccuracy in measuring the heat flux for individual shell parts. The internal convective currents were proved to have small influence on heat redistribution within the manikin. A more plausible reason could be the conductive heat flow between the metal skeleton, the guards and shell parts being responsible for the uncontrolled heat dissipation within and out of the manikin. Neither the heat redistributed within the manikin structure nor the heat flowing out to the environment through heated guards could be measured by the manikin. Thus, these phenomena could not be quantified within the scope of this project.

Moreover, the comparison of the heat transfer coefficients found in literature showed, that SAM was heated on average by 33% more at the given temperature gradient between its surface and the environment than the other manikins. In an other interlaboratory study by Richards and McCullough (Richards and McCullough 2004), six different manikins were compared and showed variability in dry heat measurement of 22-46% with SAM results comparing favourably with these from other labs. This fact demonstrates the handicap of the present manikins, and poses the limitation for an implementation of the physiological control to existing systems.

5.7. Multi-sector thermophysiological simulator with homogenous heat flux

In the first stage of developing the multi-sector thermophysiological human simulator, the manikin SAM was coupled with the iesd-Fiala model assuming a homogenous average heat flux for the entire manikin. This system was validated by comparison with the results of human subject tests used before for the validation of the single-sector thermophysiological human simulator in section 4.10. Three experiments were selected, which represented cold, cool and neutral exposures (see table 4.3 in section 4.10). The experiments used for validation involved semi-nude male subjects exposed to the respective environmental conditions for two hours, during which they reached a physiological quasi-steady-state.

As in chapter four, the core and the mean skin temperatures were chosen as the relevant physiological parameters for validating of the multi-sector thermophysiological human simulator. The total instantaneous heat fluxes (q manikin in figure 5.12) together with their weighted standard deviations over individual shell parts (dotted lines) were also plotted and compared to the results obtained from the simulation of the respective exposures using the iesd-Fiala model (q iesd-Fiala model in figure 5.12).

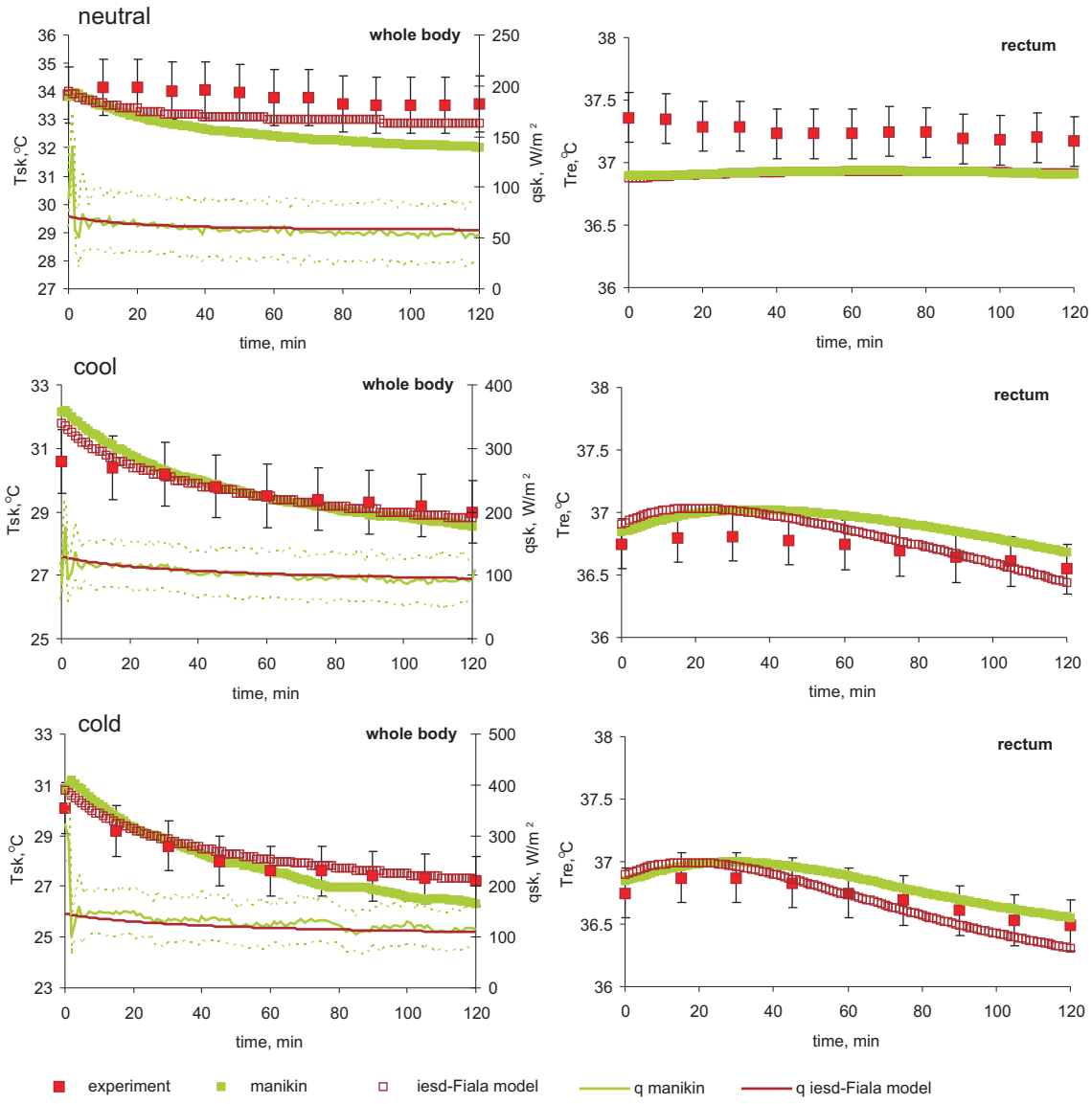

Figure 5.12. The mean skin and the body core temperatures of the test subjects and those predicted by the multi-sector thermophysiological human simulator, and the iesd-Fiala model. In addition, the heat fluxes measured on the multi-sector thermophysiological human simulator with weighted standard deviation between shell parts and those predicted by the iesd-Fiala model. The experimental conditions and sources of experimental data, as given in table 4.3 in section 4.10, are for neutral, cool and cold exposures.

The root-mean-square deviations (rmsd) (Barlow 1989) listed in table 5.1 indicate the average differences between the simulations performed using the multi-sector human simulator and the corresponding human experiments.

Table 5.1. The root-mean-square deviations of the core and the mean skin temperatures for the exposures analysed.

exposure	rmsd T_{sk} [°C]	rmsd T_{core} [°C]
cold	0.56	0.15
cool	0.63	0.19
neutral	1.26	0.33

The mean skin temperatures and the core temperatures predicted by the multi-sector human simulator showed good agreement with experimental data especially at cooler environmental conditions. Given the difficulties with the measurement of the actual heat flux flowing from the shell parts to the environment, which were described in section 5.5., the overall performance of the multi-sector human simulator can be classified as good for the exposures investigated. However, the individual shell parts showed large differences in the measured heat flux with weighted standard deviation of 49% of weighted average heat flux for neutral, 36% for cool and 33% for cold environmental conditions. At the same time, the surface temperature of individual shell parts varied by less than 0.05 °C. This suggests that the internal heat flow between the shell parts and guards exists in such a way, that the heat balance for the entire body of the manikin is maintained, although a local redistribution of the heat takes place. This finding entails considerable limitation with regards to the use of such a system for measurement of clothing with a highly inhomogenous distribution of the thermal insulation. In such a case, the heat may well migrate from warmer (more insulated) parts to cooler (less insulated) parts and affect substantially the accuracy of the whole measurement.

5.8. System run with heterogeneous heat fluxes

In the second stage of the development, the manikin SAM was coupled with the iesd-Fiala model allowing heterogeneous heat fluxes to occur over the manikin. That means, that each shell part was controlled using an individual set point temperature, which corresponded to the respective body part in the iesd-Fiala model. The heat fluxes from the individual shell-parts were then measured after a given time interval and the values

were sent to the iesd-Fiala model as a feedback. The results obtained from the system coupled in this manner are shown in figure 5.13.

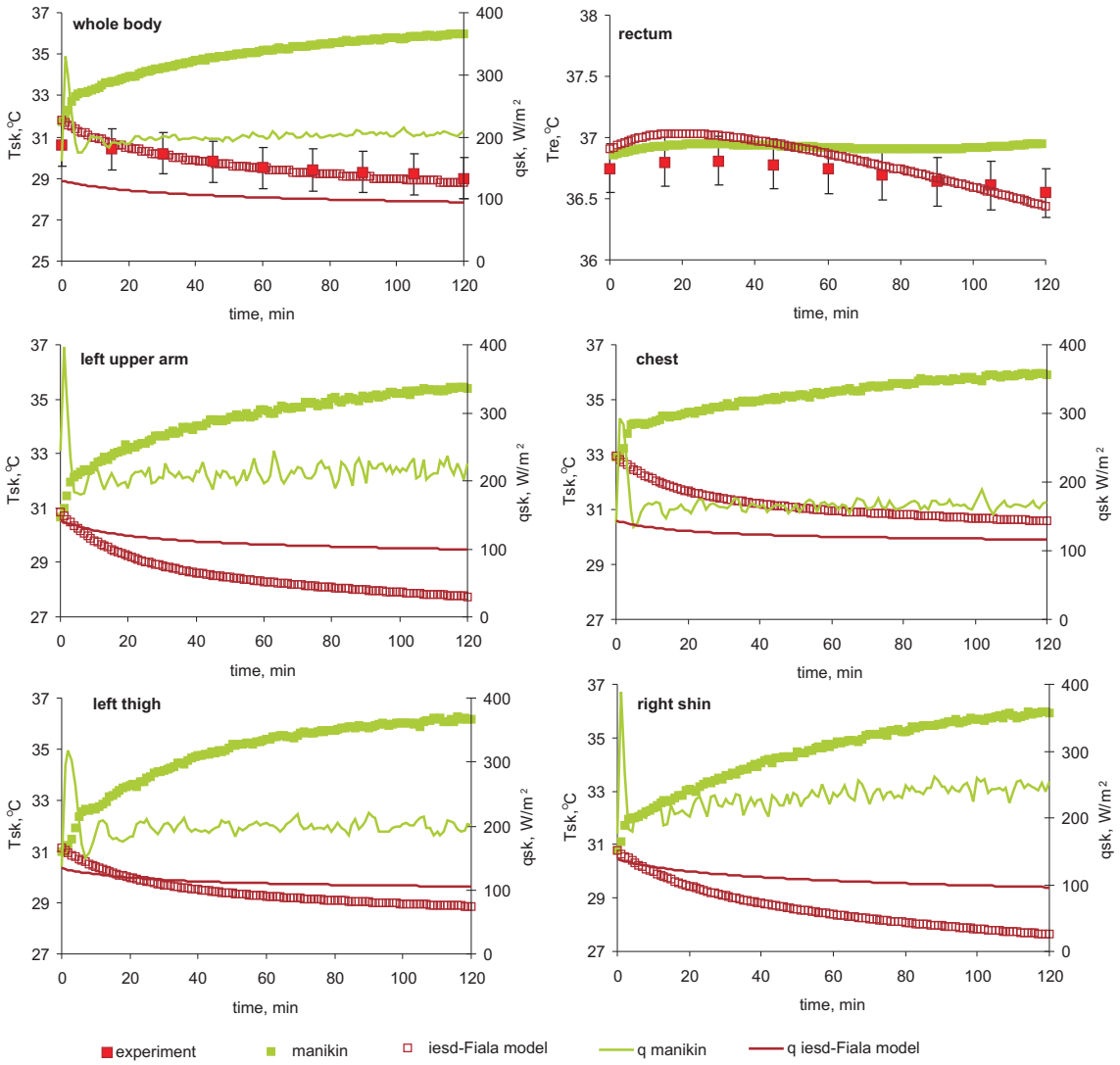

Figure 5.13. The mean and the local skin temperatures and the body core temperature of the test subjects and those predicted by the multi-sector thermophysiological human simulator with heterogenous surface temperature, and the iesd-Fiala model. In addition, the heat fluxes measured on the simulator and those predicted by the iesd-Fiala model. The experimental conditions and sources of experimental data for cool exposure are listed in table 4.3 in section 4.10.

The core and the mean skin temperatures were compared with the human subject data. In addition, the local surface temperatures of upper arm, chest, left thigh and right shin were plotted for further analysis, although the detailed data on local skin temperatures in the human experiments were not available. Since the iesd-Fiala model has been

proven to be an accurate prediction tool for situations, when clothing is not worn, it was used as a reference for the local and global physiological parameters predicted by the multi-sector human simulator with heterogeneous surface temperature (iesd-Fiala model in figure 5.13). The total instantaneous heat fluxes (q manikin in figure 5.13) were also plotted and compared with simulation results obtained using the iesd-Fiala model (q iesd-Fiala model in figure 5.13).

Based on these results, it was concluded that the coupling was not successful, when the system is run with heterogeneous heat fluxes. Though the set point temperatures predicted by the human simulator were attained at the shell-part surfaces, the simulation results differed significantly from the human subject results as well as from the results predicted by the iesd-Fiala model run separately. Because the heat flux measured at the shell parts of the manikin was too high, incorrect skin temperatures were predicted by the coupled physiological model. This effect was observed for cold, cool as well as neutral exposures tested. Summarising, these results suggest that the problem is associated with the method of measuring the heat fluxes on the thermal manikin.

The heat flux measured by the multi-sector human simulator with heterogeneous surface temperature distribution and that predicted by the iesd-Fiala model run separately differ significantly (in average up to 100W/m^2) (figure 5.13). The relative difference (referred to the heat flux measured) for the chest shell part is plotted over time for cold, cool and thermoneutral exposures in figure 5.14. The observed relative differences tended to reach a constant percentage after a short initial period, during which the strongest transient exposure took place. Similar patterns were observed for all shell parts of the thermal manikin. In addition, these percentage differences were independent of the magnitude of the measured heat flux (see figure 5.15).

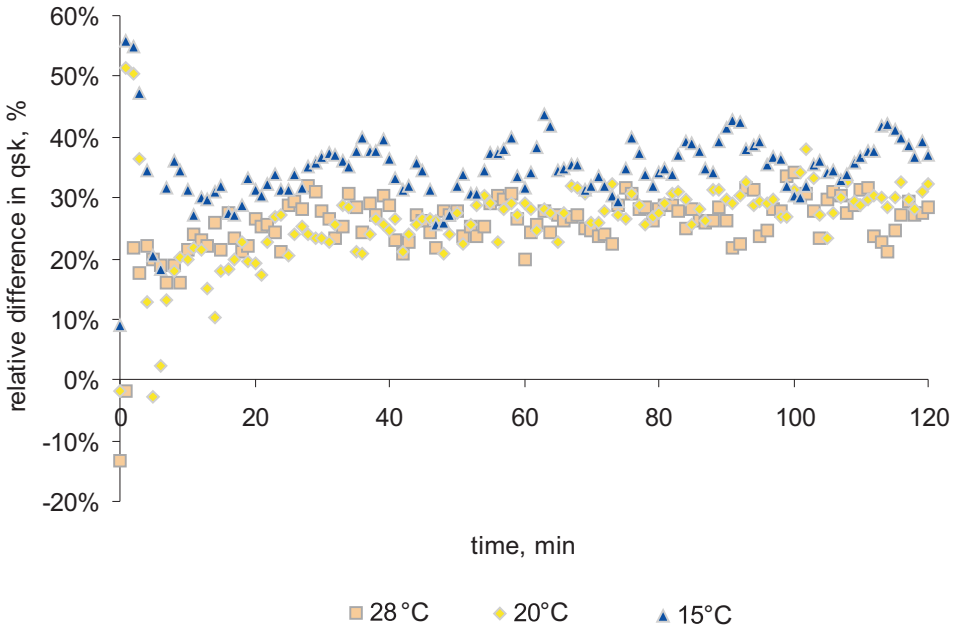

Figure 5.14. Relative differences between the heat fluxes measured using the multi-sector thermophysiological human simulator with heterogeneous surface temperature distribution and those predicted by the iesd-Fiala model for the chest. The difference is referred to the measured value of the heat flux.

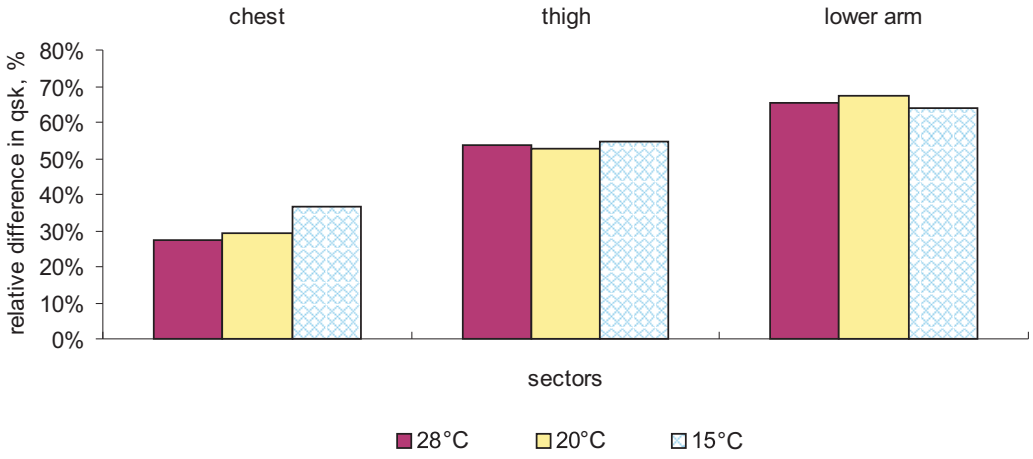

Figure 5.15. Relative differences between the heat fluxes measured on the multi-sector thermophysiological human simulator with heterogeneous surface temperature distribution and those predicted by the iesd-Fiala model for the chest, the thigh and the lower arm as the largest, intermediate and the smallest shell parts respectively. The difference is referred to the measured value of the heat flux and averaged over the last 60 minutes of the exposure.

The method of determining the power delivered to the shell part provided a sum of heating pulses (the current multiplied by the voltage delivered to the shell part at every second) over a time interval. This method produced as much as 5 % of the measurement error. Hence, the difference between the heat flux predicted by the iesd-Fiala model and the heat flux measured by the multi-sector thermophysiological human simulator with heterogeneous surface temperature distribution could not be explained by this error alone.

Another potential source of error could be the simplified determination of the surface area of the shell parts. The entire area of each shell part was measured using a three-dimensional scanning technique. Then, the active area, which participates in the heat exchange with the environment was assumed to constitute of half of the total surface area. In reality, the outer area is larger than the inner one due to the convexity of the anatomically-shaped shell parts. In addition, the lateral surfaces practically do not exchange heat with the environment.

The possible error of the estimation of the surface area of the shell part was evaluated by analysing the difference in surface areas of spherical and cylindrical shell parts of various diameters and the thickness identical with SAM's shell parts. The maximal observed difference between the outer and inner surface area constituted 10% for the spherical shell part with a diameter of 5 cm. Effectively, such an inaccuracy (in the worst case) would have produced an error in the heat flux measurement of 9%, which is still too little to explain the observed differences.

The surface temperature measurements of each shell part were performed using the PT100 temperature sensor of class A with an inaccuracy of 0.015°C. The calibration at five temperatures showed an excellent correlation with Pearson's coefficient of more than 0.99 for all sectors. This relatively small inaccuracy of the temperature sensors could have produced an error of heat flux released from shell parts of the manikin of only up to 3 % of the measured value.

5.9. Summary

This chapter describes two further stages of developing of the 'artificial human'. Firstly, the multi-sector thermophysiological human simulator with homogenous surface temperature distribution was developed and, subsequently, it was advanced to enable heterogeneous distribution of the surface temperature. The simulator with homogenous surface temperature distribution was shown to reproduce the thermal behaviour observed in human subject tests (the core and mean skin temperatures) with good accuracy for cold, cool and thermoneutral conditions. Although the average heat flux measured on this simulator complied with the one predicted by the iesd-Fiala model run separately, the heat fluxes measured on the individual shell parts varied significantly.

An attempt to advance this human simulator to the one with the heterogeneously distributed surface temperature was unsuccessful as the results predicted by the simulator differed greatly from those obtained in human subject tests and those predicted by the iesd-Fiala model run separately. The analysis of potential sources of error, such as inaccuracies in the measurement of the power supplied to the shell part, in the calculation of the surface area of the shell part, and in the measurement of the surface temperature of the shell part, could not adequately explain the behaviour of the advanced simulator with heterogeneous surface temperature.

Further investigations are, therefore, required, which could not be conducted within the time frame of this PhD project. For this reason, the single-sector thermophysiological human simulator was chosen for further validation tests using clothed human subject data and the actual clothing ensembles.

6. Application of single-sector thermophysiological simulator for clothing evaluation

Many human activities in outdoor and indoor spaces often require additional protection (e.g. equipment, clothing, sleeping bag) against adverse effects of the ambient environment. Work with hot and/or polluting industrial processes, work in clean rooms, military activities or work in hot or cold climates are few examples where such protection measures are required. One of the methods to provide an efficient barrier for excessive heat exchange and/or pollution is wearing protective clothing, which properties have to ensure both protection of health and comfort of the wearer.

6.1. Validation of the single-sector thermophysiological simulator in clothing trials

Although the validation tests of the single-sector thermophysiological simulator (Psikuta, Richards et al. 2008) focused on semi-nude subjects, the application range of the human simulator can easily be extended to scenarios, for which clothing is worn. The clothing worn then forms a part of the environment, which influences the human physiological reactions (see figure 6.1). However, additional validation tests using experiments with clothed subjects had to be carried out. The experiments used are listed in table 6.1. For these tests both the actual clothing ensembles and the physiological data were available.

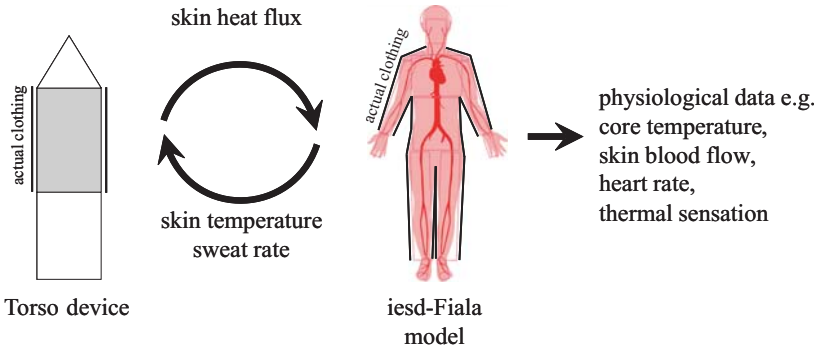

Figure 6.1. Scheme of the data exchange in the single-sector thermophysiological human simulator used in clothing trials.

Table 6.1. List of experiments used for validation of the single -sector thermophysiological simulator in clothing trials.

No.	source of data	time	Ta	RH	va	MR	subjects	clothing	description	rmsd Tsk	rmsd Tre
		min	°C	%	m/s	met	number			°C	°C
1	Camenzind et al.2005	480	-18	-	0.2	0.8	6	sleeping bags	sleeping	-	-
2	Makinen et al. 2000	90	-5	40	0.2	1.4	8	winter clothing	sitting on net chair	0.51	0.15
3	Gonzalez et al. 1997	100	35	50	1	3.75	10	impermeable suit	walking	-	0.12
4	Marszalek 2006	55	40	30	0.2	2	6	impermeable suit	walking	1.02	0.35
5	Marszalek 2006	55	40	30	0.2	2	6	cotton overall	walking	0.6	0.36
6	Jack et al. 2006	40	28	50	3.3	9.2	7	sport suit	running	0.35	0.15

Table 6.1 also contains the root-mean-square deviations (Barlow 1989), which indicate the average differences between the simulations and the corresponding human experiments.

The validation was conducted by comparing the human simulator results with those available from the human subject studies. For the majority of cases, only the mean skin and the core temperatures were available and, hence, could be used for comparison. Although other physiological parameters could not be validated, their plausibility can be derived from the validated parameters. For example, the skin blood flow and the sweat rate should result in the adequate skin temperature or the overall thermal sensation is calculated based on the mean skin and the core temperatures.

6.1.1. Validation for exposures to cold conditions

Two validation tests were performed in cold conditions. The details of exposures and the rmsd's for the core and mean skin temperatures are listed in table 1. Both of these experiments are described below.

The study of Camenzind (2005) was designed to assess the thermal performance of winter sleeping bags. In this experiment, six human subjects slept in a climatic chamber at ambient temperature of -18 °C in the winter sleeping bags wearing long underwear and a pullover. The skin temperature was taken at four locations, i.e. chest, back, toe and finger. Although the core temperature was not measured, it was assumed not to be lower than the average temperature of the chest and the back skin temperatures.

The environmental conditions were reproduced in the climatic chamber. The single-sector human simulator dressed in the experimental clothing was placed in a horizontal position, in the winter sleeping bag before each measurement was started. The results of both the human tests and the simulator predictions are depicted in figure 6.2. Although the single-sector human simulator measured the average heat flux of the human body, the coupled physiological model also predicted local skin temperatures.

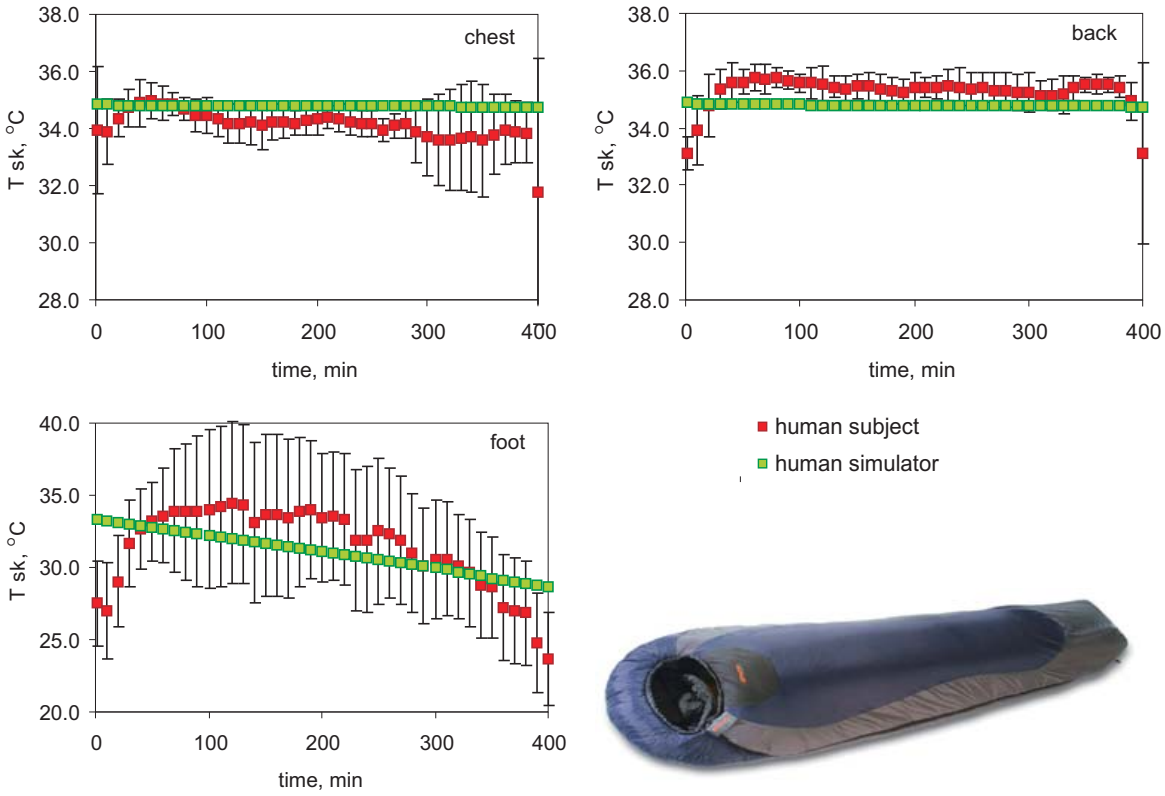

Figure 6.2. Local skin temperatures measured on human subjects in the experiment of Camenzind (Camenzind, Weder et al. 2005) and these predicted by the single-sector human simulator for the identical experimental conditions (see table 6.1).

At the beginning of the experiment the subject's local skin temperatures were lower than these predicted by the simulator due to the fact that the volunteers had to pass through the cold climatic chamber wearing only their long underwear before getting into the sleeping bag, whereas the simulator was prepared and stabilised within the sleeping bag under cold conditions, prior to each experiment.

The chest and the back skin temperatures of the human subjects were predicted by the single-sector human simulator to be mainly within the experimental standard deviation of the human tests rmsds of 0.69 °C and 0.83 °C respectively. The prediction of the instep of the foot was less accurate, i.e. rmsd of 1.92 °C, though still mainly within the standard deviation of the experimental data.

Makinen et al. (2000) studied subjects wearing the Finnish army winter combat suits. In this experiment conducted in a climatic chamber, the subjects were exposed to a cold environment of -5 °C while seated still for one hour. The rectal temperature and the skin temperatures were measured at eighteen locations.

To simulate this experiment, the original clothing was acquired from the authors and fitted to the size of the simulator. Subsequently, the simulator was put into its vertical position and the measurement started. The results of the human tests and the corresponding predictions of the simulator are compared in figure 6.3.

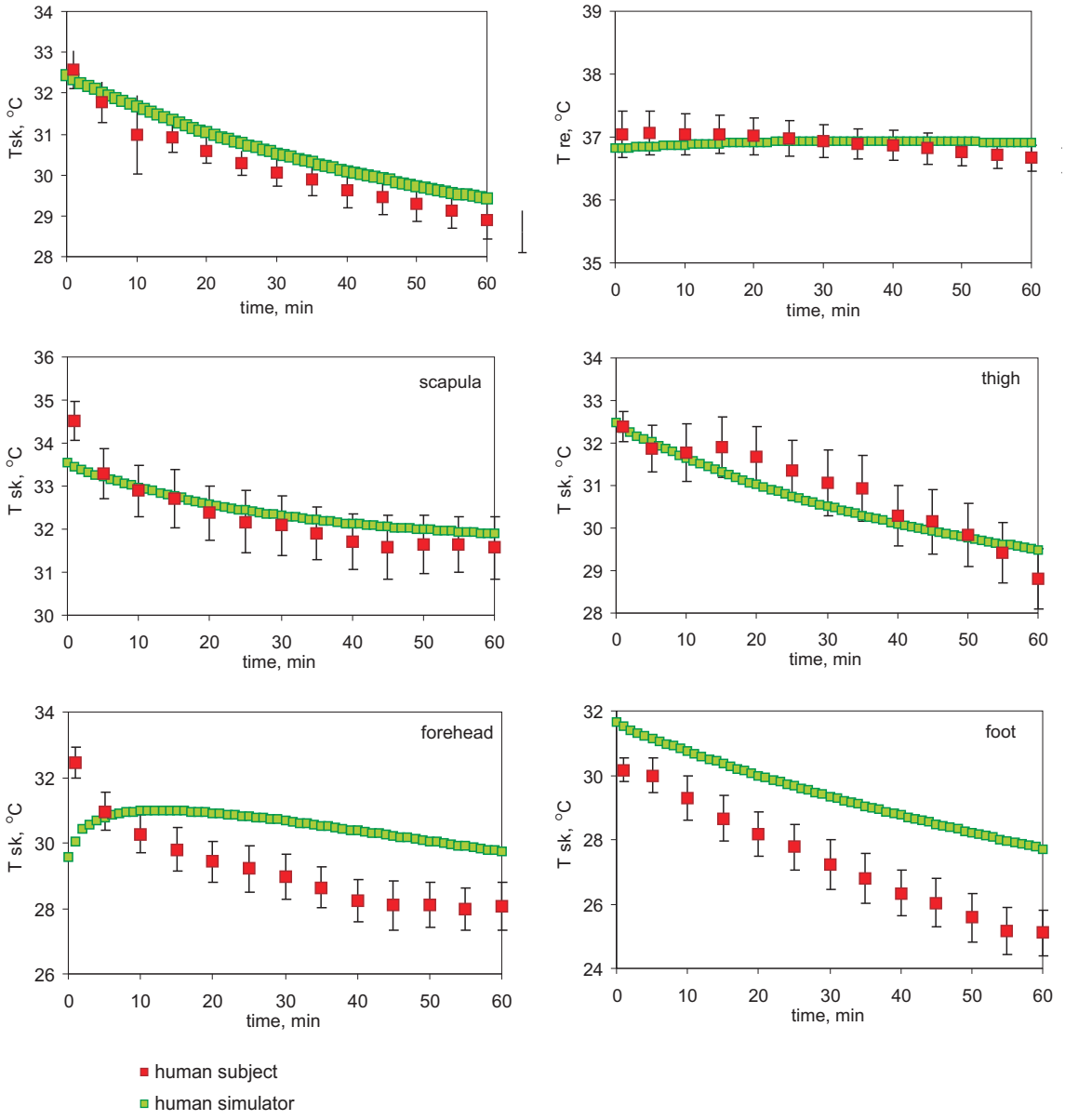

Figure 6.3. The mean and local skin temperatures, and the core temperature measured in human subjects (Makinen, Gavhed et al. 2000) and these predicted by the single-sector human simulator for the identical experimental conditions (see table 6.1).

The mean skin and the core temperatures were predicted close to temperatures measured in the human subjects with rmsds of 0.51 °C and 0.15 °C respectively.

It should be noted, that the surface of the single-sector human simulator was completely covered by clothing as opposed to the test subjects, whose face was completely exposed with thinner insulation covering the head, hands and feet. This caused discrepancies in predictions due to use of the average heat flux input. Therefore, while the predictions for the scapula and thigh skin temperatures were more accurate with rmsds of 0.39 °C and 0.86 °C respectively, the predictions for the uncovered forehead and less insulated foot were less accurate resulting in rmsds of 1.77 °C and 2.12 °C respectively (see figure 6.3).

6.1.2. Validation for exposures to hot conditions

Four validation tests were performed in hot conditions while wearing various type of clothing (impermeable/permeable, thicker multilayered/thinner single layered). The conditions and the rmsd's for the core and mean skin temperatures are listed in table 6.1. These experiments are illustrated below with more details.

In the experiment conducted by Gonzalez at al. (1997), human subjects attempted a 100 minute walk on a levelled treadmill at the pace of 1.34 m/s (until self withdrawal or until their rectal temperature reached 39 ºC) at an ambient temperature of 35 ºC and a relative humidity of 50 %. The volunteers wore completely encapsulating chemical protective ensembles (NBC). Only the rectal temperature was reported for this experiment. Although the clothing tested was not available for simulations, it could be replicated based on information from the literature (Gonzalez, McLellan et al. 1997). Two pieces of textiles corresponding to the tight underwear and the loose impermeable overall were put on the simulator preserving tight and loose fitting accordingly. Then the measurement was carried out on the motionless device. The results are compared in figure 6.4.

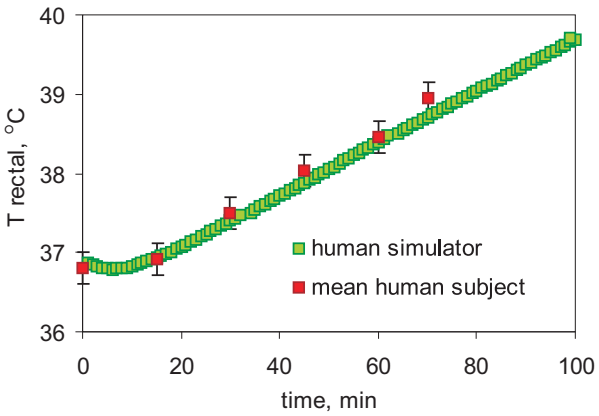

Figure 6.4. The core temperature measured on human subjects in the experiment (Gonzalez, McLellan et al. 1997) and these predicted by the single-sector human simulator for the similar experimental conditions (see table 6.1).

The predictions of core temperature by the single-sector human simulator showed an excellent agreement with the experimental data with an rmsd of 0.12 °C.

In the experiment of Marszlalek (2006), test subjects walked for 55 minutes on a treadmill at a speed of 3 km/h (without fan simulating air movement at the walking speed), an ambient temperature of 40 °C and a relative humidity of 30 % (until self withdrawal or until their rectal temperature exceeded 38 ºC). They wore long thin cotton underwear and either a cotton protective suit or an impermeable coverall without head coverage. The skin temperature was measured at four locations (ISO9886 2004) and the core temperature was taken in the auditory canal. These test conditions were reproduced in the experimental set up and the simulation was conducted on the motionless device without additional wind simulating speed of walking. The suits are presented in figure 6.5 and the results are plotted in figures 6.6 and 6.7.

Figure 6.5. A cotton protective suit (left) or an impermeable coverall without head coverage (right) used in experiment of Marszalek (2006).

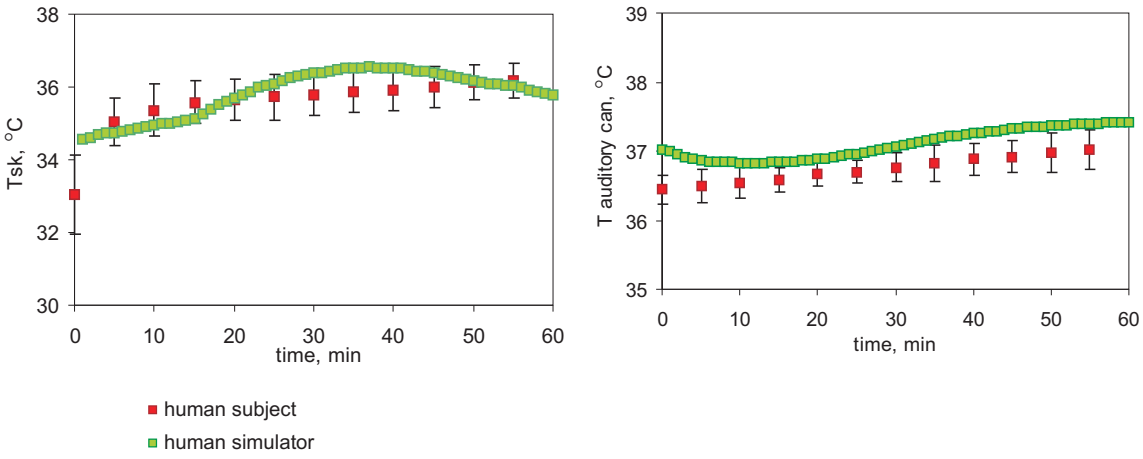

Figure 6.6. The mean skin and the core temperatures measured on human subjects in the experiment (Marszalek 2006) and these predicted by the single-sector human simulator for similar experimental conditions (see table 6.1, cotton).

The body core temperature measured in the auditory canal in the subjects was compared with the head core temperature predicted by the human simulator. The simulator reproduced the mean skin temperature with rmsd of 0.60°C and the core temperature with rmsd of 0.36°C for the test with the cotton suit indicating good overall performance of the single-sector human simulator for this exposure.

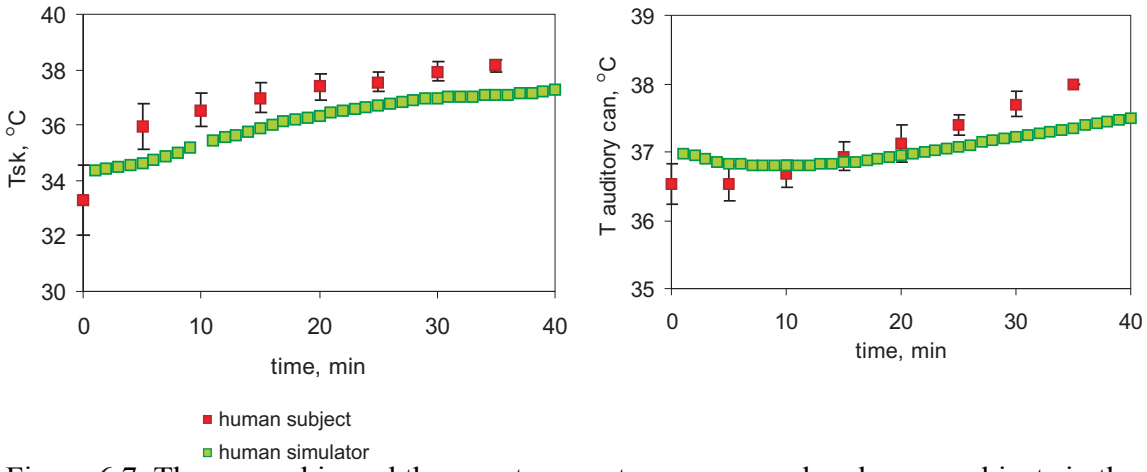

Figure 6.7. The mean skin and the core temperatures measured on human subjects in the experiment (Marszalek 2006) and these predicted by the single-sector human simulator for similar experimental conditions (see table 6.1, impermeable).

The comparison of the results of the test with the impermeable protective suit resulted in rmsd of 1.02 °C for the mean skin temperature and 0.35 °C for the core temperature.

The dataset available from Empa (Jack 2007) represents the experiment, in which seven averagely trained individuals wearing a polyester running suit ran on a treadmill at 9.2met for 40 minutes at the warm environmental conditions (T_a = 28 ºC, RH = 50 % and v_{air} = 3.3 m/s corresponding to the speed of running). Prior to the experiment, subjects were prepared in identical environmental conditions for at least 30 minutes. The rectal temperature and the skin temperatures taken at eight locations according to ISO8996:2004. The results are compared in figure 6.8.

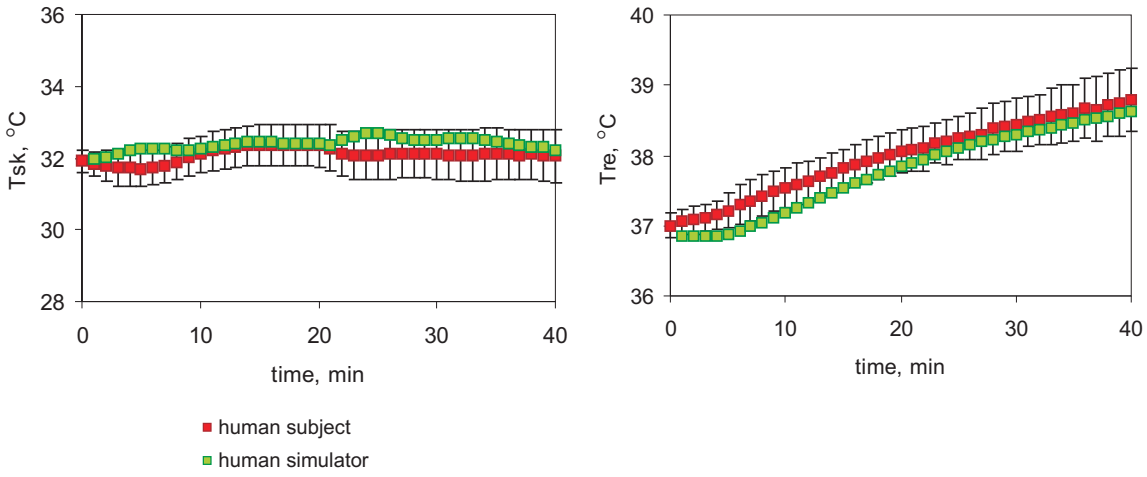

Figure 6.8. The mean skin and the core temperatures measured on human subjects in the experiment (Jack 2007) and these predicted by the single-sector human simulator for the identical experimental conditions (see table 6.1).

The average skin and the rectal temperatures were predicted accurately with rmsd of 0.40 °C and 0.19 °C respectively.

6.1.3. Discussion

In general, the single-sector human simulator predicted accurately the skin and the core temperatures for trials in cold conditions. However, this concerns only instances when clothing with homogenously distributed insulation over the whole body was worn.

Compared to cold conditions, hot exposures are more difficult to simulate. Although the single-sector thermophysiological human simulator performed well in validation trials under hot environmental conditions, special care had to be taken to ensure the proper heat exchange. The simulator did not work properly in hot exposures when there was no or insufficient cooling by induced sweating simulated. This drawback resulted from the difference in heat capacity between the simulator and the average person who can absorb more heat per unit of the surface temperature increase. In the validation tests, this was the case at the beginning of an exposure when a subject at thermo-neutral state entered a hot environment. To simulate such a transient condition, the simulator was exposed at first to the ambient temperature lower than the initial surface temperature predicted for the particular exposure until steady state was reached. After that the temperature in the climatic chamber was increased to the value required in the actual exposure (higher than the initial required surface temperature of the simulator). During

this time (10 minutes per 10°C temperature increase of ambient air) the surface temperature of the simulator increased only somewhat (i.e. 0.04°C/min when temperature gradient approximated 5°C). In addition, the increase of predicted skin temperature at the beginning of hot exposures was faster than this resulted from the passive heating from the ambient air (also for low metabolic rates). Effectively, the required surface temperature of the simulator was maintained by active heating and showed good fit with rmsd's of less than 0.36°C for the core temperature and less than 1.02°C for the mean skin temperature (see table 6.1).

6.2. Summary

The single-sector physiological simulator has been shown to perform well in prediction of the core and mean skin temperatures in the validation tests with use of clothing ensembles. The mean skin temperature was predicted with rmsd below 1 °C and the body core temperature with rmsd below 0.36 °C. In addition, this device was demonstrated to provide complementary data on physiological response of the average person to the tested scenario characterised by environmental conditions, activity level, clothing worn and initial condition prior to the actual exposure. Time saving testing, repeatability of the measurement of the physiological response of an average individual and the ability of testing in conditions unsafe for humans are major advantages of this human simulator. The intended application of this device is to measure thermophysical properties and physiological effects of a broad range of clothing and sleeping systems, including multi-layer ensembles, sleeping bags, mattresses and blankets over a wide range of climatic conditions.

7. Conclusions

The attempt to develop a thermal manikin with physiological components, which adequately simulates the thermal behaviour of the human being, has been successful. The work has been completed in the following stages:

- extended validation of the physiological model;
- development of the single-sector thermophysiological human simulator by coupling the iesd-Fiala model and the thermal sweating cylinder;
- development of the multi sector- thermophysiological simulator by extending the coupling procedures developed previously;
- demonstration of validity and usability of the single-sector human simulator for clothing research.

7.1. Extended validation of the iesd-Fiala model

The iesd-Fiala model has been validated extensively during the course of this PhD work which makes it unique amongst the physiological models based on the human experimental data available until now. The model proved its ability to adequately predict human physiological response for the variety of conditions represented in the extensive database of COST 730. The validation work also verified an extended range of activity levels up to 9.1 met, which can be simulated accurately by the iesd-Fiala model. The limitations of the model that have been revealed concerned mainly definition of the boundary conditions at the skin surface. As human simulators should measure directly and in detail the heat exchange between the body parts and the environment, these limitations are not essential for the application of the model in human simulators.

7.2. Development of the single-sector thermophysiological human simulator

The single-sector thermophysiological simulator has been successfully developed and validated. It was shown to be able to simulate the overall human thermophysiological responses for steady-state conditions with good accuracy for the core (rmsd < 0.24°C) and mean skin (rmsd < 0.62°C) temperatures for environmental conditions ranging

between 15.0 °C and 37.5 °C. Within the range of defined application zones, this robust and relatively simple device has also been shown to be capable of accurately simulating the overall dynamic thermal behaviour of the human body. Initially, this stage of work was supposed to facilitate the understanding of the coupling procedure while using the simpler device. Nonetheless, the single-sector human simulator turned out to be an advanced and accurate tool itself, useful for clothing research and testing.

7.3. Development of the multi sector- thermophysiological simulator

The multi-sector thermophysiological human simulator was developed in two steps. Firstly, the multi-sector simulator with homogenous surface temperature distribution was developed based on experience gained during work on single-sector human simulator. It was shown to reproduce the thermal behaviour observed in human subject tests (the core and mean skin temperatures) with good accuracy for cold, cool and thermoneutral conditions. Although the average heat flux measured on this simulator complied with the physiological data, the heat fluxes measured on the individual shell parts varied significantly.

Secondly, an attempt to advance this human simulator to one with the heterogeneously distributed surface temperatures proved unsuccessful, as the results predicted by the simulator differed greatly from those obtained in human subject tests. The major source of error was the thermal manikin. The analysis of the inaccuracies in the measurement of the power supplied to each shell part, in the calculation of the surface area of the shell part, and in the measurement of the surface temperature of the shell part, could not adequately explain the behaviour of the multi-sector human simulator when operated with heterogeneous surface temperatures. An internal heat exchange between shell parts, guards and environment seemed to unable use of input power as a precise indicator of the heat flux released at the manikin surface. This heat exchange, however, could not be measured with the measurement setup available for the manikin. Thus, additional instrumentation and further investigations are required, which could not be conducted within the time frame of this PhD project.

7.4. Application of the single-sector human simulator

Due to difficulties encountered with the development of the multi-sector human simulator, the single-sector thermophysiological human simulator was chosen for further validation. For these tests clothed human subject data and the actual clothing ensembles worn were used. The single-sector human simulator has been shown to perform well in prediction of the core and mean skin temperatures in the validation tests. The mean skin temperature was predicted with rmsd below 1°C and the body core temperature with rmsd below 0.36°C. In addition, this device was demonstrated to provide complementary data on the physiological response of the average person to the tested scenario characterised by environmental conditions, activity level, clothing worn and initial conditions prior to the actual exposure. Time saving testing, repeatability of the measurement of the physiological response of an average individual and the ability of testing in conditions unsafe for humans are major advantages of this human simulator. The intended application of this device is to measure thermophysical properties and physiological effects of a broad range of clothing and sleeping systems over a wide range of climatic conditions.

7.4. Recommendation for further work

Since the main source of failure was the technical problem of measuring heat flux on the thermal manikin, the concept of the measuring the actual surface heat flux should be revised in the course of further work. First of all, the manikin structure and control system should be checked to trace sources of large lateral heat fluxes, for example, by comparing set and actual temperatures on guards and shell parts using alternative temperature measurement system such as infrared camera. This step could improve accuracy of the entire system and hence estimation of power input as the indicator of the released heat flux. Alternatively, separate heat flux sensors placed on the shell parts and coupled with the measuring system of the thermal manikin could be used to measure the actual heat flux released from the shell part. The drawback of this method is an assumption that the heat flux would be uniform over the entire shell part and equal to the one at the point of measurement. Finally, the optimal improvement could be achieved by using a new type of shell parts that have embedded heat flux sensors on

their surface and thus are able to measure the actual heat flux from the entire shell part surface.

Bibliography

ASHRAE-55 (2004). Thermal environmental conditions for human occupancy.

ASTMD7024-04 (2004). Standard Test Method for Steady State and Dynamic Thermal Performance of Textile Materials.

ASTME96/E96M-05 (2005). Standard Test Methods for Water Vapor Transmission of Materials.

ASTMF1291-05 (2005). Standard Test Method for Measuring the Thermal Insulation of Clothing Using a Heated Manikin.

ASTMF1868-02 (2002). Standard Test Method for Thermal and Evaporative Resistance of Clothing Materials Using a Sweating Hot Plate.

ASTMF2298-03 (2003). Standard Test Methods for Water Vapor Diffusion Resistance and Air Flow Resistance of Clothing Materials Using the Dynamic Moisture Permeation Cell.

ASTMF2370-05 (2005). Standard Test Method for Measuring the Evaporative Resistance of Clothing Using a Sweating Manikin.

Astrom, K. and T. Hagglund (1995). PID controllers: theory, design and tuning, Research Triangle Park, NC : Instrument Society of America (ISA).

Barlow, R. J. (1989). Different definitions of the standard deviation. Statistics. A Guide to the Use of Statistical Methods in the Physical Sciences. D. J. Sandiford, F. Mandl and A. C. Phillips. Chichester, John Wiley & Sons Ltd.**:** 10-12.

Behenke, W. P., A. J. Geshury, et al. (1990). "Thermo-man": Full scale tests on the thermal protective performance of heat resistant fabrics. 4th International Conference on Environmental Ergonomics, Texas, USA.

Bethea, D. and S. Powell (2005). Dehydration Review. H. S. Executive. Buxton, Health & Safety Laboratory.

Bluestein, M. and J. Zecher (1999). "A new approach to an accurate wind chill factor." Bulletin Of The American Meteorological Society **80**(9): 1893-1899.

Bouskill, L. M., G. Havenith, et al. (2002). "Relationship between clothing ventilation and thermal insulation." Aihaj **63**(3): 262-268.

Burke, R. A., F. T. O'Neil, et al. (1994). The development of a heat pipe driven manikin with variable flow irrigated skin. 6th International Conference on Environmental Ergonomics, Montebello, Canada.

Camenzind, M., M. Weder, et al. (2005). Mesurements of sleeping bags at very low temperatures. Part 2 - Human Subject Tests. St Gallen, Empa.

Charles, K. E. (2003). Fanger's Thremal Comfort and Draught Models, National Research Council Canada. Institute for Research in Construction.

Chen, Y. S., J. Fan, et al. (2003). "Clothing thermal insulation during sweating." Textile Research Journal **73**(2): 152-157.

Cheng, X. Y. and J. T. Fan (2004). "Simulation of heat and moisture transfer with phase change and mobile condensates in fibrous insulation." International Journal of Thermal Sciences **43**(7): 665-676.

Cheng, X. Y. and J. T. Fan (2005). "Heat and moisture transfer with sorption and phase change through clothing assemblies part II: theoretical modeling, simulation, and comparison with experimental results." Textile Research Journal **75**(3): 187-196.

deDear, R. J., E. Arens, et al. (1997). "Convective and radiative heat transfer coefficients for individual human body segments." International Journal of Biometeorology **40**(3): 141-156.
Dozen, Y., K. Adachi, et al. (1989). "Studies on the heat and moisture transfer trough clothing using a sweating thermal manikin." Mercer JB Thermal Physiology. Excerpta Medica: 519-524.
Dukes-Dobos, F. and U. Reischl (2003). A simple and inexpensive thermomanikin - development of a prototype. 2nd European Conference on Protective Clothing and NOKOBETEF 7, Montreux, Switzerland.
Elabbassi, E. B., K. Beighazi, et al. (2004). "Dry heat loss in incubator: comparison of two premature newborn sized manikins." European Journal of Applied Physiology **92**(6): 679-682.
EN13537 (2002). Requirements for sleeping bags.
Fan, J. and Y. S. Chen (2002). "Measurement of clothing thermal insulation and moisture vapour resistance using a novel perspiring fabric thermal manikin." Measurement Science & Technology **13**: 1115-1123.
Fan, J. T. and X. Y. Cheng (2005). "Heat and moisture transfer with sorption and phase change through clothing assemblies Part I: Experimental investigation." Textile Research Journal **75**(2): 99-105.
Fanger, P. O. (1970). Thermal Comfort. New York, McGraw-Hill Book Co.
Farrington, R., J. Rugh, et al. (2004). "Use of a Thermal Manikin to Evaluate Human Thermoregulatory Responses in Transient, Non-Uniform, Thermal Environments." Society of Automotive Engineers International **2004-01-2345**.
Fiala, D. (1998). Dynamic simulation of human heat transfer and thermal comfort. Institute of Energy and Sustainable Development. Leicester, De Montfort University. **PhD**.
Fiala, D., K. J. Lomas, et al. (1999). "A computer model of human thermoregulation for a wide range of environmental conditions: the passive system." Journal of Applied Physiology **87**(5): 1957-1972.
Fiala, D., K. J. Lomas, et al. (2001). "Computer prediction of human thermoregulatory and temperature responses to a wide range of environmental conditions." International Journal of Biometeorology **45**(3): 143-159.
Fiala, D., K. J. Lomas, et al. (2003). "First Principles Modelling of Thermal Sensation Responses in Steady-State and Transient Conditions." ASHRAE Transactions **109**: 179-186.
Gagge, A. P., J. A. Stolwijk, et al. (1967). "Comfort and Thermal Sensation and Associated Physiological Responses at Various Ambient Temperatures." Environmental Research **1**: 1-20.
Gagge, A. P., J. A. Stolwijk, et al. (1971). "Effective Temperature Scale, Based on a Simple Model of Human Physiological Regulatory Response " ASHRAE Journal **13**(1): 58-&.
Ghaddar, N., K. Ghali, et al. (2003). "Integrated human-clothing system model for estimating the effect of walking on clothing insulation." International Journal of Thermal Sciences **42**(6): 605-619.
Gisolfi, C. V. and F. Mora (2000). The Hot Brain. Survival, Temperature and the Human Body. London, Massachusetts Institute of Technology.

Gonzalez, R. R., T. M. McLellan, et al. (1997). "Heat strain models applicable for protective clothing systems: comparison of core temperature response." Journal of Applied Physiology **83**(3): 1017-1032.
Graveling, R. A., L. A. Morris, et al. (1988). Working in hot conditions in mining: a literature review. H. S. Executive, Institute of Occupational Medicine.
Havenith, G. (1985). Individual parameters in thermoregulatory control. A review, Institute for perception.
Havenith, G. (2001). "Individualized model of human thermoregulation for the simulation of heat stress response." Journal of Applied Physiology **90**: 1943-1945.
Havenith, G., R. Heus, et al. (1990). "Clothing Ventilation, Vapor Resistance and Permeability Index - Changes Due to Posture, Movement and Wind." Ergonomics **33**(8): 989-1005.
Havenith, G., R. Heus, et al. (1990). "Resultant Clothing Insulation - a Function of Body Movement, Posture, Wind, Clothing Fit and Ensemble Thickness." Ergonomics **33**(1): 67-84.
Havenith, G., I. Holmer, et al. (1999). "Clothing evaporative heat resistance - Proposal for improved representation in standards and models." Annals of Occupational Hygiene **43**(5): 339-346.
Havenith, G. and H. Nilsson (2004). "Correction of clothing insulation for movement and wind effects, a meta-analysis." European Journal of Applied Physiology **92**: 636-640.
Havenith, G., M. G. Richards, et al. (2008). "Apparent latent heat of evaporation from clothing: attenuation and "heat pipe" effects." Journal of Applied Physiology **104**(1): 142-149.
Hensel, H. (1981). Termoreception and Temperature Regulation. London, Academic Press.
Holmer, I. (2004). "Thermal manikin history and applications." European Journal of Applied Physiology **92**(6): 614-618.
Holmer, I., H. Nilsson, et al. (1999). "Clothing convective heat exchange - Proposal for improved prediction in standards and models." Annals of Occupational Hygiene **43**(5): 329-337.
Hoppe, P. R. (1993). "Heat balance modelling." Experientia **49**: 741-746.
Huang, J. H. (2006). "Sweating guarded hot plate test method." Polymer Testing **25**(5): 709-716.
Huizenga, C., Z. Hui, et al. (2001). "A model of human physiology and comfort for assessing complex thermal environments." Building and Environment **36**(6): 691-699.
Hwang, C. L. and S. A. Konz (1977). "Engineering models of human thermoregulatory system - review." IEEE Ttansactions on biomedical engineering **24**(4): 309-325.
ISO9886 (2004). Ergonomics — Evaluation of thermal strain by physiological measurements. Geneva, Switzerland, ISO.
ISO9920 (2007). Ergonomics of the thermal environment -- Estimation of thermal insulation and water vapour resistance of a clothing ensemble.
ISO11079 (2007). Ergonomics of the thermal environment - Determination and interpretation of cold stress when using required clothing insulation (IREQ) and local cooling effects.

ISO11092 (1993). Textiles - Physiological effects - Measurement of thermal and water-vapour resistance under steady-state conditions (sweating guarded-hotplate test).
ISO15831 (2004). Clothing - Physiological effects - Measurement of thermal insulation by means of a thermal manikin. ISO.
Jack, A. (2007). **PhD**.
Jessen, C. (2001). Temperature regulation in humans and other mammals. Berlin, Springer.
Kar, F., J. Fan, et al. (2007). "Comparison of different test methods for the measurement of fabric or garment moisture transfer properties." Measurement Science & Technology **18**(7): 2033-2038.
Keiser, C. (2007). Steam burns moisture management in firefighter protective clothing. PhD Thesis. Department of Mechanical Engineering, ETH Zürich **PhD**.
Kothari, V. K. and K. Bal (2005). "Development of an instrument to study thermal resistance of fabrics." Indian Journal of Fibre & Textile Research **30**(4): 357-362.
Kuklane, K., M. Sandsund, et al. (2004). "Comparison of thermal manikins of different body shapes and size." European Journal of Applied Physiology **92**(6): 683-688.
Li, Y. and B. V. Holcombe (1998). "Mathematical simulation of heat and moisture transfer in a human-clothing-environment system." Textile Research Journal **68**(6): 389-397.
Lichtenbelt, W. D. V., A. J. H. Frijns, et al. (2004). "Effect of individual characteristics on a mathematical model of human thermoregulation." Journal Of Thermal Biology **29**(7-8): 577-581.
Lotens, W. A. (1988). "Comparison of Thermal Predictive Models for Clothed Humans." ASHRAE Transactions **16**: 1321-1340.
Lotens, W. A. (1993). Heat Transfer From Humans Wearing Clothing. Soesterberg, Technical University of Delft.
Lotens, W. A. and G. Havenith (1995). "Effects of Moisture Absorption in Clothing on the Human Heat-Balance." Ergonomics **38**(6): 1092-1113.
Lotens, W. A., F. J. G. Vandelinde, et al. (1995). "Effects of Condensation in Clothing on Heat-Transfer." Ergonomics **38**(6): 1114-1131.
Makinen, T., D. Gavhed, et al. (2000). "Thermal responses to cold wind of thermoneutral and cooled subjects." European Journal of Applied Physiology **81**(5): 397-402.
Malchaire, J. B. M. (2006). "Occupational heat stress assessment by the Predicted Heat Strain model." Industrial Health **44**(3): 380-387.
Marszalek, A. (2006). "Physiological reactions of the human body during work wearing protective clothing in the hot environment." Bezpieczenstwo Pracy **3**(3): 11-15.
McCullough, E. A. (2002). The use of thermal manikins to evaluate clothing and environmental factors. 10th Conference on Environmental Ergonomics, Fukuoka, Japan.
McCullough, E. A., B. Jones, et al. (1985). "A comprehensive database for estimating clothing insulation." ASHRAE Transactions **91**: 29-47.
McCullough, E. A., M. Kwon, et al. (2003). "A comparison of standard methods for measuring water vapour permeability of fabrics." Measurement Science & Technology **14**(8): 1402-1408.
Meinander, H. (1994). "Coppelius - The perspiring thermomanikin." Building Research and Information **22**: 64-65.

Melikov, A. (2004). "Breathing thermal manikins for indoor environment assessment: important characteristics and requirements." European Journal of Applied Physiology **92**(6): 710-713.
Melikov, A. (2007). Climacademy within Euroacademy on Ventilation and Indoor Climate under Marie Curie Actions, Course 2: Individually controlled environment. Pamporovo.- personal communication
Osczevski, R. J. (1995). "The basis of wind chill." Arctic **48**(4): 372-382.
Parsons, K. (2003). Human Thermal Environments. The Effects of Hot, Moderate and Cold Environments on Human Health, Comfort and Performance. London, Taylor & Francis.
Parsons, K. C., G. Havenith, et al. (1999). "The effects of wind and human movement on the heat and vapour transfer properties of clothing." Annals of Occupational Hygiene **43**(5): 347-352.
Pickup, J. and R. De Dear (1999). An Outdoor Thermal Comfort Index (OUT_SET*) - Part I - The Model and its Assumptions. Biometeorology and Urban Climatology at the Turn of the Millenium, Sydney.
Powell, S., A. Davies, et al. (2005). The effects of thermal environments on the risks associated with manual handling. H. S. Executive. Buxton, The Health and Safety Laboratory.
Psikuta, A., M. Richards, et al. (2008). "Single-sector thermophysiological human simulator." Physiological Measurement **29**(2): 181-192.
Quintela, D., A. Gaspar, et al. (2004). "Analysis of sensible heat exchanges from a thermal manikin." European Journal of Applied Physiology **92**(6): 663-668.
Rapp, G. M. (1973). "Convective heat transfer and convective coefficients of nude man, cylinders and spheres at low velocities." ASHRAE Transactions **22**(4): 75-87.
Richards, M. G. M. and D. Fiala (2004). "Modelling fire-fighter responses to exercise and asymmetric infrared radiation using a dynamic multi-mode model of human physiology and results from the Sweating Agile thermal Manikin." European Journal of Applied Physiology **92**(6): 649-653.
Richards, M. G. M. and N. G. Mattle (2001). Development of a sweating agile thermal manikin (SAM). 4th International Meeting on Thermal Manikins, EMPA, St. Gallen, Switzerland.
Richards, M. G. M. and E. A. McCullough (2004). Revised Interlaboratory Study of Sweating Thermal Manikins Including Results from the Sweating Agile Thermal Manikin. Rerformance of Protective Clothing: Global Needs and Emerging Markets, PA USA, ASTM International Standards Worldwide.
Richards, M. G. M., A. Psikuta, et al. (2006). Current development of thermal sweating manikins at Empa. Thermal Manikins and Modelling. J. Fan. Hong Kong, The Hong Kong Polytechnic University**:** 173-179.
Richards, M. G. M., R. Rossi, et al. (2008). "Dry and wet heat transfer through clothing dependent on the clothing properties under cold conditions." International Journal of Occupational Safety and Ergonomics **14**(1): 69-76.
Rugh, J. and D. Bharathan (2005). Predicting Human Thermal Comfort in Automobiles. The Vehicle Thermal Management Systems Conference, Toronto, Canada.
Rugh, J. P. and J. Lustbader (2006). Application of a Sweating Manikin Controlled by a Human Physiological model and Lessons Learned. 6th International Thermal Manikin and Modelling Meeting (6I3M), Hong Kong.

Sanders, P. (2003). A Comparison of the Predictive Accuracy of Human Thermoregulatory Models. Victoria, Australian Department of Defence. Defence Science and Technology Organisation.

Sawka, M. N. and K. B. Pandolf (1990). "Effects of Body Water Loss on physiological Function and Exercise Performance." Perspectives in Exercise Science and Sports Medicine. Fluid Homeostasis During Exercise **3**: 1-38.

Sharpiro, Y., K. B. Pandolf, et al. (1982). "Predicting Sweat Loss Response to Exercise, Environment and Clothing " European Journal of Applied Physiology and Occupational Physiology **48**: 83-96.

Shitzer, A. and R. C. Eberhart (1985). Heat transfer in Medicine and Biology. Analysis and Applications. New York and London, Plenum Press.

Stolwijk, J. A. and J. D. Hardy (1966). "Partitional Calorimetric Studies of Responses of Man to Thermal Transients." Journal of Applied Physiology **21**(3): 967-&.

Stolwijk, J. A., E. R. Nadel, et al. (1973). "Development and Application of a Mathematical - Model of Human Thermoregulation " Archives des Sciences Physiologiques **27**(3): A303-A310.

Takada, S., S. Hokoi, et al. (2007). "Experimental and analytical investigation of moisture movement in clothing." Journal of Building Physics **31**(2): 125-142.

Tanabe, S., E. A. Arens, et al. (1994). "Evaluating Thermal Environments by Using a Thermal Manikin with Controlled Skin Surface Temperature." ASHRAE Transactions **100**: 39-48.

Tanabe, S., K. Kobayashi, et al. (2002). "Evaluation of thermal comfort using combined multi-node thermoregulation (65MN) and radiation models and computational fluid dynamics (CFD)." Energy and Buildings **34**(6): 637-646.

Ueda, H., Y. Inoue, et al. (2006). "Regional microclimate humidity of clothing during light work as a result of the interaction between local sweat production and ventilation." International Journal of Clothing Science and Technology **18**(3-4): 225-234.

Wagner, J. A. and S. M. Horvath (1985). "Influences of Age and Gender on Human Thermoregulatory Responses to Cold Exposures." Journal of Applied Physiology **58**(1): 180-186.

Wexler, R. K. (2002). "Evaluation and treatment of heat-related illnesses." American Family Physician **65**(11): 2307-14.

Wissler, E. H. (1985). Mathematical simulation of human thermal behaviour using whole body models. Heat transfer in Medicine and Biology. Analysis and Applications. A. Shitzer and R. C. Eberhart. New York and London, Plenum Press. **1:** 325-374.

Wyon, D. P. (1989). "Use of Thermal Manikins in Environmental Ergonomics." Scandinavian Journal of Work Environment & Health **15**: 84-94.

Yi, L., F. Z. Li, et al. (2004). "An integrated model for simulating interactive thermal processes in human-clothing system." Journal Of Thermal Biology **29**(7-8): 567-575.

Zhang, H., C. Huizenga, et al. (2001). "Considering individual physiological differences in a human thermal model." Journal Of Thermal Biology **26**(4-5): 401-408.

Zimmerli, T. and M. Weder (1996). Protection and comfort - a sweating Torso for the simultaneous measurement of protective and comfort properties of PPE. 6th International Symposium on Performance of Protective Clothing: Emerging Protection Technologies, Orlando, FL, USA, ASTM STP 1273.

Appendix 1

The coefficients of the calibration lines and Pearson's correlation coefficients for all shell-parts and heated guards of SAM.

	Shell-parts							
Name	head right	head left	upper arm right front	upper arm right back	forearm right front	forearm right back	upper arm left front	upper arm left back
Nr	**1**	**2**	**3**	**4**	**5**	**6**	**7**	**8**
A (Slope)	0.0115	0.0135	0.0133	0.0131	0.0133	0.0131	0.0133	0.0129
B (Intercept)	7.23	4.84	7.00	7.77	4.88	2.52	6.58	4.78
R^2	0.9957	0.9962	0.9980	0.9986	0.9990	0.9990	0.9989	0.9987

	Shell-parts							
Name	forearm left front	forearm left back	chest	back	abdomen	buttocks	thigh right front	thigh right back
Nr	**9**	**10**	**13**	**14**	**15**	**16**	**17**	**18**
A (Slope)	0.0135	0.0133	0.0112	0.0115	0.0124	0.0123	0.0111	0.0096
B (Intercept)	5.82	6.96	8.12	5.66	9.17	6.74	8.28	10.20
R^2	0.9992	0.9992	0.9985	0.9977	0.9999	0.9998	0.9984	0.9999

	Shell-parts					
Name	calf right front	calf right back	thigh left front	thigh left back	calf left front	calf left back
Nr	**19**	**20**	**21**	**22**	**23**	**24**
A (Slope)	0.0124	0.0125	0.0116	0.0114	0.0124	0.0126
B (Intercept)	5.54	7.13	6.83	7.62	5.26	6.43
R^2	0.9998	0.9998	0.9986	0.9987	0.9997	0.9995

	heated guards							
Name	right hand	left hand	right foot	left foot	right elbow	left elbow	right knee	left knee
Nr	**11**	**12**	**25**	**26**	**27**	**28**	**29**	**30**
A (Slope)	0.0101	0.0102	0.0101	0.0103	0.0121	0.0106	0.0105	0.0106
B (Intercept)	8.85	8.55	8.44	6.85	-5.77	8.04	5.98	7.05
R^2	1.0000	1.0000	0.9999	0.9999	0.9890	1.0000	0.9999	0.9999

Appendix 2

The average values of heat flux and the ratios of maximum heat flux residual within the group over the average heat flux in this group for given ambient temperatures.

		head	arms	fore-arms	chest & back	abdom & but-tock	thighs	shins	calves
	number of shell parts	2	4	4	2	2	4	2	2
Ta = 25°C	mean heat flux, W/m^2	122	106	126	98	103	116	176	101
	max differ-ence	3%	4%	8%	4%	16%	13%	43%	9%
Ta = 20°C	mean heat flux, W/m^2	177	165	205	138	151	175	247	169
	max differ-ence	2%	3%	8%	3%	14%	6%	31%	4%
Ta = 15°C	mean heat flux, W/m^2	235	222	278	184	214	232	319	231
	max differ-ence	1%	2%	9%	3%	10%	6%	24%	4%

Appendix 3

The heat fluxes measured in parallel by the manikin (SAM) and the heat flux sensor (sens) at the various ambient temperatures and the air movement of 0.09 ± 0.01m/s.

		arm		chest		back		buttock		thigh	
	method	SAM	sens	SAM	sens	SAM	sens	SAM	sens	SAM	sens
Ta = 25°C	mean heat flux, W/m^2	102	82	99	79	96	85	75	56	118	95
	difference, W/m^2,	19		20		11		19		23	
	% of SAM	19%		20%		11%		26%		20%	
Ta = 20°C	mean heat flux, W/m^2	159	127	134	126	143	111	130	93	172	139
	difference, W/m^2,	32		8		32		37		33	
	% of SAM	20%		6%		22%		28%		19%	
Ta = 15°C	mean heat flux, W/m^2	212	174	177	154	189	166	192	140	234	188
	difference, W/m^2,	38		24		23		52		46	
	% of SAM	18%		13%		12%		27%		20%	